On the measurement of a weak classical force coupled to a harmonic oscillator: experimental progress

Mark F. Bocko

Department of Electrical Engineering, University of Rochester, Rochester, New York 14627

Roberto Onofrio

Dipartimento di Fisica 'Galileo Galilei', Università di Padova, I-35131 Padova, Italy

Several high-precision physics experiments are approaching a level of sensitivity at which the intrinsic quantum nature of the experimental apparatus is the dominant source of fluctuations limiting the sensitivity of the measurements. This quantum limit is embodied by the Heisenberg uncertainty principle, which prohibits arbitrarily precise simultaneous measurements of two conjugate observables of a system but allows one-time measurements of a single observable with any precision. The dynamical evolution of a system immediately following a measurement limits the class of observables that may be measured repeatedly with arbitrary precision, with the influence of the measurement apparatus on the system being confined strictly to the conjugate observables. Observables having this feature, and the corresponding measurements performed on them, have been named quantum nondemolition or back-action evasion observables. In a previous review (Caves *et al.*, 1980, Rev. Mod. Phys. **52**, 341) a quantum-mechanical analysis of quantum nondemolition measurements of a harmonic oscillator was presented. The present review summarizes the experimental progress on quantum nondemolition measurements and the classical models developed to describe and guide the development of practical implementations of quantum nondemolition measurements. The relationship between the classical and quantum theoretical models is also reviewed. The concept of quantum nondemolition and back-action evasion measurements originated in the context of measurements on a macroscopic mechanical harmonic oscillator, though these techniques may be useful in other experimental contexts as well, as is discussed in the last part of this review. [S0034-6861(96)00103-1]

CONTENTS

Our interpretation of the experimental material rests essentially on the classical concepts

Niels Bohr, 1927

I. INTRODUCTION

The first discussions of repeated measurements on a quantum system date back to nearly the beginning of quantum theory (Landau and Peierls, 1931). Two consecutive measurements of the position of a free particle were considered and it was shown that the accuracy with which an initial measurement was performed affected the position uncertainty of a subsequent measurement. This started a debate on the measurability of physical quantities in quantum field theory (Bohr and Rosenfeld, 1933, 1950) and on the validity of the energy-time uncertainty relationship (Aharonov and Bohm, 1961, 1964; Fock, 1962, 1965; Aharonov and Petersen, 1971; Vorontsov, 1981). Elsasser (1937) introduced a concept

of nonperturbing measurements in connection with the understanding of the role of the uncertainty principle in the foundations of statistical quantum mechanics. The idea of a noninvasive measurement on a quantum system also appeared in the monograph on quantum mechanics by Bohm (1951), but probably due to a lack of experimental accessibility these ideas were not pursued further. Interest in a quantum theory of repeated measurements on a system returned with the development of MASERS that made quantum phenomena apparent on a macroscopic scale (Louisell *et al.*, 1961). Soon thereafter the quantum-mechanical lower bound to the noise figure of a general linear amplifier was predicted (Heffner, 1962; Haus and Mullen, 1962). By making a very general argument, their conclusion was that any system that provides gain must add noise to a received signal. This led to investigations of the quantum-noise limits of generalized quantum receivers and eventually resulted in the development of a theory of optimal quantum-mechanical measurements (Helstrom, 1976). This elegant mathematical theory assumed that precise measurements of one observable or another in a system could be performed, but it did not address the practical issue of how to realize such measurements. Experimental practice had not yet demanded that this issue be confronted.

Experiments designed to test the predictions of general relativity, and in particular the search for gravitational radiation, call for incredibly precise measurements of the minute displacements of macroscopic objects such as multiton gravitational wave antennae (Braginsky, 1970; Misner, Thorne, and Wheeler, 1973; Amaldi and Pizzella, 1979; Douglass and Braginsky, 1979; Thorne, 1980). This application pushed a number of experimentalists and practical-minded theorists to try to understand the quantum-mechanically imposed limitations of the sensitivity of measurements made on a harmonic oscillator serving as a model of a gravitational wave antenna. Braginsky and his collaborators first discussed this problem and identified the quantum limit for the sensitivity of gravitational wave antennae (Braginsky, 1967; Braginsky and Nazarenko, 1969). An independent semiclassical analysis (Giffard, 1976) showed that the precision of a measurement of the force acting on a gravitational wave antenna is limited by the unavoidable quantum noise of the amplifier used in the measurement. Braginsky *et al.* (1975) showed that this so-called ''standard quantum limit'' arises because conventional measurement techniques demand information about two conjugate observables of the gravitational wave antenna, the amplitude and the phase of one of the antenna's normal modes of vibration. Braginsky also recognized that the quantity of fundamental interest, in this case the weak force acting on a gravitational wave antenna, sometimes may be measured more accurately by monitoring harmonic-oscillator observables other than position. This was the introduction of the idea of a quantum nondemolition (QND) measurement. The QND idea was extended and several new schemes for monitoring a harmonic oscillator were suggested by Caves *et al.* (1980). They also refined the insight that optimal QND measurements require the observable of interest to be decoupled from its conjugate observable during the system's free evolution. This is because during a measurement of an observable the conjugate observable is unavoidably disturbed; if the uncertainty in the conjugate observable feeds back to contaminate the observable of interest a sequence of precise measurements is impossible. These special observables are called quantum nondemolition observables. A familiar counterexample of a QND observable is the position of a harmonic oscillator, x. If one precisely measures x then the conjugate observable, the oscillator momentum p, becomes uncertain according to the Heisenberg relation, $\Delta x \Delta p \geq \hbar/2$, and during the subsequent evolution of the oscillator the momentum uncertainty forces the future values of the position to become correspondingly uncertain.

One QND measurement proposed by Braginsky and Vorontsov was to monitor the number of phonons in a harmonic oscillator (Braginsky and Voronstsov, 1974). The harmonic-oscillator observable conjugate to the number of phonons, which is equivalent to the oscillator energy, is the phase of the oscillator. Even if the phase were completely unknown at the expense of a precise measurement of energy, the small energy uncertainty would be maintained since energy is a constant in the free evolution of the oscillator. Unfortunately it is impractical to directly measure the energy of a mechanical oscillator at acoustic frequencies since it would require an interaction Hamiltonian quadratic in the displacement of the harmonic oscillator, and there do not appear to be sufficiently strong nonlinear effects to achieve such coupling. Subsequently, proposals for the measurement of QND observables that are linear in the displacement of the harmonic oscillator were made (Thorne, Drever, *et al.*, 1978; Thorne, Caves, *et al.*, 1979). In particular, the continuous back-action evasion (BAE) measurement of one component of a harmonic oscillator's complex amplitude was proposed and this appeared to be more practically realizable than earlier proposals. Classical analyses of apparatuses capable of measuring an oscillator's complex amplitude showed that such schemes avoid the fluctuating back-action force of the measuring apparatus on the measured component of the mechanical oscillator's complex amplitude. Moreover, it was demonstrated that the idea proposed by Thorne, *et al.* (1979) was a special case in the family of the already known electromechanical parametric transducers (Johnson and Bocko, 1981; Bocko and Johnson, 1982). Demonstration of the operating principles of a parametric transducer capable of BAE measurements has been accomplished by several groups, and the continuous refinement of BAE transducers has brought them close to implementation on second- and third-generation gravitational wave antennae (Cinquegrana *et al.*, 1994; Bonifazi *et al.*, 1996).

Aside from the application to gravitational wave antennae, the back-action evasion measurement idea has also been investigated during the last decade for its utility in other areas, particularly in quantum optics, in su-

perconducting microwave mixers, and for dedicated experiments to examine repeated quantum measurements on macroscopic objects. Back-action evasion measurements of an optical field have been reported (Levenson *et al.*, 1986; Bachor *et al.*, 1988; La Porta *et al.*, 1989; Grangier *et al.*, 1991; Friberg *et al.*, 1992; for a review of the experimental results see Roch *et al.*, 1992). The ideas underlying the generation of squeezed states of optical and microwave electromagnetic fields, a topic of considerable recent activity, are related to the concepts of quantum nondemolition measurements (Grishchuk and Sazhin, 1975; Walls, 1983; Giacobino and Fabre, 1992; Drummond *et al.*, 1993). A QND measurement of a harmonic oscillator's complex amplitude leaves the harmonic oscillator in a squeezed state, that is to say, a quantum state in which the fluctuations of the two quadrature phases of the oscillator complex amplitude are unequal. The squeezed-state experiments prepare a traveling mode of an electromagnetic field in a state in which the fluctuations of one phase of the field are reduced at the expense of increased fluctuations in the quadrature phase; then the squeezed electromagnetic field propagates to a detector which destroys the field in a single measurement. In the squeezed-state experiments, the state preparation and the state measurement functions are separate, whereas in a QND measurement both functions are performed by the same apparatus. The most significant distinction from the point of view of quantum measurement theory is that, in performing a QND measurement, one continuously monitors the same quantum system, which makes central the question of the effect of the measurement apparatus on the system being measured.

Also, in the mechanical QND measurements, the intended application has been the detection of impulsive forces with a broadband spectrum. In this context it is convenient to express the advantage of a back-action evasion measurement scheme in terms of an integrated noise measure, the noise temperature, independent of the shape of the signal spectrum. By contrast, in the optical case various characterizations of the degree of improvement of a QND measurement have been proposed (Holland *et al.*, 1990; Grangier *et al.*; 1992; for a review see Poizat, Roch, and Grangier, 1994), which depend on the correlation functions and the corresponding spectral densities of more general classes of the input signals. Moreover, we point out that the continuous QND measurement of the complex amplitude of a harmonic oscillator and the QND measurement of the energy of an oscillator or waveguide require distinctly different techniques; the latter will not be described here (for overviews on this subject see, for instance, Braginsky, 1989; Brune *et al.*, 1990, 1992; Haroche, 1992; Braginsky and Khalili, 1996). Another related subject not covered here is the discussion of high-precision measurements of the position of single atoms, an important topic in atomic optics, for which detailed overviews have already appeared (Wallis, 1995; Thomas and Wang, 1995).

Making repeated quantum measurements on a single quantum system is outside of the familiar applications of quantum mechanics in fields such as condensed matter, quantum optics, atomic, nuclear, and elementary-particle physics. In those contexts, measurements are considered to be performed on an ensemble of identically prepared microscopic objects, and one does not inquire about the state of the measured system after the measurement process is complete. Neither the formalism nor the interpretation of ordinary quantum mechanics seem suitable for describing repeated or continuous measurements on single, isolated quantum systems, so dedicated experiments to investigate the effect of a measurement on a single macroscopic quantum system will yield interesting insights into the quantum nature of isolated macroscopic objects consisting of large numbers of microscopic components—and in particular into the interaction of such systems with measuring apparatuses and the classical world. Recently, attempts to include the measurement process in a unified dynamics succeeded in describing the behavior of a single quantum particle under continuous observation in terms of a stochastic Schrödinger equation (for a review see Belavkin, Hirota, and Hudson, 1995), although we are still far from having understood the consequences of this dynamics in several aspects, including the possibility to describe intrinsically complex objects as macroscopic quantum systems. Perhaps the most intriguing possibility for a departure from our conventional understanding of such systems has been outlined by Leggett (1986) when he suggested "we would then have to take seriously the possibility that the physics of complex macroscopic objects cannot be deduced in all respects from that of their constituents—a conclusion that would clearly run totally counter to the 'reductionist' wisdom of the science of the last two hundred years, but might in the end have a liberating effect that outruns our present imagination." Unfortunately, QND measurements on macroscopic mechanical systems have yet to be performed; however, experimentalists are well on their way to exploring this fascinating regime.

This review article emphasizes the experimental progress toward performing quantum measurements on macroscopic harmonic oscillators, in the spirit of giving both an introduction to the subject and a summary of the progress made so far. In Sec. II we provide a summary of the quantum-mechanical description of measurements, both conventional and QND, on a harmonic oscillator acted upon by a weak force. We begin Sec. III with a discussion of the framework for classical models of systems acted upon by weak signals plus noise. The systems of interest can be described by classical random variables, and the key measured quantities, such as autocorrelation functions of these variables or their power spectra, can be directly predicted by time averages of the variables, which are equivalent to ensemble averages according to the ergodic hypothesis. The classical approach is extended to a semiclassical treatment by introducing noise sources, which account for the quantum fluctuations; however, we still use our essentially classi-

cal descriptive tools. The outcome of this section is the development of classical models of systems capable of performing quantum nondemolition measurements and the prediction of their sensitivity in the presence of classical sources of noise. This forms the basis for understanding and guiding the experimental work on quantum nondemolition measurements described in Sec. IV. The description of these instrumental efforts carried out so far is complemented, in Sec. V, by a discussion of the applications of QND measurement techniques to high-precision experiments. Sec. VI contains the conclusions and critical comments on the status of this area of research.

II. THE STANDARD QUANTUM LIMIT AND QUANTUM NONDEMOLITION MEASUREMENT STRATEGIES

A. Statistical mechanics of a quantum harmonic oscillator

We begin this section with a cautionary statement on the difficulty of isolating the classical limit of quantum mechanics, which is necessary for the consistent physical interpretation of quantum theory. The classical limit is usually considered to be obtainable simply by taking the limit as Planck's constant approaches zero or by allowing some parameter of the system under study to become very large, for example the mass of a free particle. In either instance the quantum effects become negligibly small. It would be more consistent to establish whether a system is in the quantum or the classical regime by including in the quantum-mechanical description of the system under study the system's interaction with the environment. Thereby one would assert that the classical regime is obtained when the effect of the fluctuations associated with the degrees of freedom of the system's environment dominates the noise arising from the measurement process, i.e., due to the interaction of the system with the ''noiseless'' measuring apparatus. Models able to describe the time evolution of an observable of a generic quantum system immersed in a generic statistical reservoir have not yet been developed, although the goal seems within the scope of existing theoretical physics and is known as the study of open quantum systems (Davies, 1976; Gorini *et al.*, 1976; Lindblad, 1976). Despite this, progress has been achieved by reaching a general understanding of the absence of superposition states in a measurement apparatus (Zurek, 1981, 1982) and in macroscopic systems (Ghirardi, Rimini, and Weber, 1986; Diosi, 1989). Less ambitious but more concrete approaches have focused attention on systems and environments for which the dynamics can be explicitly solved. For instance, a quantum-mechanical harmonic oscillator immersed in a heat bath is a simple example of an open quantum system due to the linear nature of the oscillator and the simple statistics obeyed by a thermal bath. There has been considerable interest in this problem and many different formalisms have been created to deal with it. Until now, three main approaches to quantization have been proposed, namely the canonical approach, which dates back to the original attempts to introduce a consistent quantum theory, the path-integral approach due to Feynman (Feynman, 1948; Feynman and Hibbs, 1965), and the stochastic approach (Nelson, 1980, 1985; Guerra, 1981).

In the canonical formalism, two avenues have been pursued to take into account the effect of a reservoir (Louisell, 1973). One can model the reservoir as an infinite number of quantized harmonic oscillators with linear coupling to the system's harmonic oscillator and with specific properties that enforce the statistics of the thermal bath. Alternatively, one can introduce a noise source, which represents the effect of the oscillators in the thermal bath by introducing an effective force noise and a damping factor that arise from the coupling to the bath similar to the familiar Langevin approach to statistical mechanics. In the path-integral formalism, the harmonic oscillator is considered as a subsystem in a larger system with an infinite number of degrees of freedom. The path integral of the subsystem averages over all other degrees of freedom to give the path of the single harmonic oscillator in which the usual weight is multiplied by a factor, called the influence functional, that expresses the averaged influence of the reservoir (Feynman and Vernon, 1963; Caldeira and Leggett, 1983a, 1983b; Exner, 1985). Finally, in the finite-temperature version of stochastic quantization, the quantum uncertainties and the statistical-mechanics uncertainties are expressed in the same language, namely the theory of stochastic processes (Ruggiero and Zannetti, 1985). The existence of an equivalent to Newton's law for the system dynamics—a stochastic Newton's law—assures a formalism in which the effect of dissipative forces can be naturally included, unlike the case of canonical (Hamiltonian-based) or path-integral (Lagrangian-based) formalisms.

In all three formalisms the effect of the thermal reservoir on the quantum harmonic oscillator is describable by a Fokker-Planck equation for the time evolution of the oscillator observables. The dependence of the system observables upon the reservoir degrees of freedom is embodied in a relaxation time; furthermore, all three formalisms predict that the relaxation time of system observables in the quantum limit is the same as it is in the classical regime. The relaxation time is critical because it determines the rate at which energy is exchanged between the reservoir and the system. To determine if a system is in the quantum or the classical regime, the amount of energy exchanged between the system and the thermal bath should be compared to the energy introduced by the measuring apparatus during the process of measurement. The energy ΔE exchanged in a time Δt between the system, with a relaxation time τ, and the reservoir at temperature T is

$$\Delta E = k_B T \frac{\Delta t}{\tau}, \tag{2.1}$$

where k_B is Boltzmann's constant. The exchange of energy between the oscillator and the reservoir results in a random walk of the oscillator with zero average displacement and a root-mean-square displacement value

$$\Delta x_{rms} \cong \left(\frac{2k_B T}{m\omega^2} \frac{\Delta t}{\tau} \right)^{1/2}, \tag{2.2}$$

where m is the mass and ω is the resonant angular frequency of the oscillator. In a simple model one can view the measurement as the exchange of one quantum of energy between the measuring apparatus and the measured system during their interaction. Thus the condition for the noise from the thermal bath to be small compared to the noise associated with the measurement, expressed as a quantum of the energy of the measured system, is

$$k_B T \frac{\Delta t}{\tau} \ll \hbar\omega. \tag{2.3}$$

This inequality, introduced by Braginsky and Vorontsov (1974), was later derived in a more formal manner in a functional approach to quantum Brownian motion (Escobar *et al.*, 1994) by using the decoherence time scale (Unruh and Zurek, 1989; Zurek, Habib, and Paz, 1993; Zurek and Paz, 1995), a measure of how long a system maintains its quantum features when coupled to a thermal bath at temperature T, and by imposing a decoherence time much larger than the measurement time. As was pointed out for the first time by Braginsky (1967), realistic values of the temperature, relaxation times, and the nearly quantum-limited amplifiers used for gravitational wave antennas will allow us to experimentally reach the quantum regime, in other words to satisfy condition (2.3). A gravitational wave antenna can be accurately represented as a macroscopic harmonic oscillator that is continuously monitored for the influence of a weak force exerted by a passing gravitational wave, so in the quantum regime this system can be treated as a single quantized harmonic oscillator, isolated from its environment save for a measurement apparatus that subjects the system to a sequence of measurements. Because of the statistical nature of the usual interpretation of quantum mechanics, it is not possible to predict, in a deterministic way, the state evolution of a single isolated system subjected to continuous measurement. Therefore, it is especially interesting to pursue this class of measurements that constitutes a natural environment for analyzing a single degree of freedom under repeated monitoring in the quantum regime.

B. Quantum theory of repeated measurements on a single object

1. The standard quantum limit

In the usual approach to quantum mechanics, the free evolution of a quantum system is treated separately from the process of measurement. During its free evolution the quantum state of the system evolves unitarily. During a quantum measurement, the unitary evolution no longer applies and the state of the quantum system is projected onto one of the basis states defined by the measurement apparatus, the outcome of the state projection process being described only in a probabilistic sense. Strictly speaking then, quantum mechanics as it is usually applied does not apply to a single system undergoing a continuous measurement. The usual way out of this quandary is to identify the statistical information, which in the Copenhagen interpretation of quantum mechanics applies to a set of identical measurements on an ensemble of identically prepared systems, with the variance of a number of repeated measurements on a single quantum system. This is clearly not a realistic description of a sequence of measurements on a single system for the fundamental reason that it overlooks the effect of early measurements in the sequence on those that occur later in the sequence, that is, it overlooks the back action of the measurement apparatus. This problem, after considerable progress through the introduction of a semigroup master equation for the density matrix describing a system subjected to continuous measurements (Barchielli, Lanz, and Prosperi, 1982; Barchielli, 1983; Ludwig, 1985; Barchielli, 1986), also applied to the specific case of a gravitational wave antenna (Barchielli, 1985), has been solved recently with the introduction of a stochastic Schrödinger equation (Gisin, 1984a, 1984b; Pearle, 1986; Diosi, 1988a, 1988b; Belavkin, 1989; Belavkin and Staszewski, 1989) describing the stochastic dynamics of a pure state in the presence of a measurement. This was later recognized as a particular case of the quantum-state diffusion equation for open systems and was connected to various formalisms previously developed (Gisin and Percival, 1992a, 1992b; Percival, 1994; Breuer and Petruccione, 1995; Presilla, Onofrio, and Tambini, 1996), giving rise to a nucleus of a new theory still under development, the so-called measurement quantum mechanics. Since we think that this will continue to be a subject of great theoretical debate in the forthcoming years, our attention in this review is focused on identifying the regime in which, experimentally, one will be able to explore the physics of repeated or continuous measurements on single macroscopic quantum systems, as has been done recently for single microscopic systems in quantum optics (Carmichael, 1993). One hopes that the experiments will lead the way to confirm the predictions of measurement quantum mechanics on macroscopic single systems or alternatively to a firmer theoretical foundation.

In order to proceed, we will overlook the fundamental issue regarding the applicability of quantum mechanics to a continuous measurement on an isolated quantum system and we will adopt the approach described above to theoretically investigate the question: ''What is the limit imposed by quantum mechanics on the precision of a measurement on a quantum oscillator?'' Identifying the statistical predictions of conventional quantum theory with the variances for a sequence of measurements of an observable of a single quantum system, we ask the question. What is the smallest disturbance acting on a harmonic oscillator that may be detected in the presence of quantum noise?

This question was first posed in the context of linear amplifiers by Heffner (1962), and by Haus and Mullen (1962), in which the measurement of a radiation field,

formally equivalent to the determination of the state of a harmonic oscillator, was discussed. The conclusion in both analyses was that the measurement process unavoidably adds noise to the measured quantity. In the radio-engineering language of Haus and Mullen, the amplifier noise figure, defined as the signal-to-noise ratio at the output of the amplifier, has a minimum value of 2, in other words, the amplifier must add at least half a quantum of energy per unit measurement time to an incoming signal.

In the 1970's, the worldwide effort to detect gravitational waves from astrophysical sources motivated the investigation of the quantum limits of gravitational wave detection (Misner, Thorne, and Wheeler 1973; Amaldi and Pizzella, 1979; Douglass and Braginsky, 1979; Thorne, 1980). A gravitational wave detector under the influence of a passing gravitational wave can be modeled as a quantum oscillator acted upon by a weak force, so determination of the weakest detectable gravitational wave was examined in the context of optimal measurement strategies for a quantum oscillator. The early work by Braginsky *et al.* on this topic was later reexamined, summarized and extended by Unruh (1978, 1979), Hollenhorst (1979), Dodonov, Man'ko, and Rudenko (1980), and Caves *et al.* (1980). One of the outcomes of this work was the identification of the so-called "standard quantum limit" for the detection of a weak force acting on a harmonic oscillator. It was found that if the quantum oscillator were prepared in a quantum-mechanical minimum-uncertainty state, that is, a coherent state, then the best sensitivity one could attain for a measurement of the oscillator position would be

$$\Delta x = \sqrt{\hbar/(2m\omega)}, \tag{2.4}$$

where m is the mass and ω is the angular resonant frequency of the mechanical oscillator. This limit is analogous to that found by Heffner, Haus, and Mullen for a linear amplifier, the common feature being that a linear measurement of the amplitude and phase of a quantum oscillator, or mode of a radiation field, is carried out. Other measurement strategies for determining the energy, momentum, or complex amplitude of the oscillator were examined and it was found that the standard quantum limit could be exceeded in principle by a variety of measurement techniques but, with the exception of one proposal to measure the oscillator complex amplitude, there were no practical measurement schemes proposed. The issue of the quantum limit and alternative oscillator measurement schemes was fully explored in the review by Caves *et al.* (1980). In the following we include a short summary of the theoretical basis for quantum nondemolition measurements to complement the more experimentally oriented discussions in Sec. III of this review.

2. Quantum nondemolition strategies: general definition

The sensitivity limit for measurements of the amplitude and phase of the displacement of a harmonic oscillator is determined by the properties of quantum-mechanical coherent states that are the minimum-uncertainty states with equal variances of the position and momentum. Nonrelativistic quantum mechanics allows measurement of any observable to arbitrary precision; however, the uncertainty principle imposes a limit on the precision of the simultaneous measurement of two conjugate observables. If one monitors a harmonic oscillator to measure a weak classical force acting upon it, a single high-precision measurement is insufficient, rather it is necessary to make a sequence of precise measurements. The deviation of the measured position of the harmonic oscillator from the predicted position, inferred from earlier measurements, signals the presence or the absence of a force. The basic principle of a quantum nondemolition measurement is to perform a sequence of measurements of an observable of a single quantum system in such a way that the act of measurement does not diminish the predictability of the results of subsequent measurements of the same observable. To realize a quantum nondemolition measurement the instants of time at which the measurements are performed and the interaction Hamiltonian governing the interaction of the system with the measuring apparatus should all be carefully chosen for a given dynamical system. For instance, an initial high-precision measurement of the position of a free particle implies a large dispersion in the possible values of succeeding measurements of the momentum, according to the uncertainty principle. Following the first position measurement, a second measurement of position may have a large dispersion, depending upon the instant at which the measurement is made. This is because the future position of the oscillator depends upon the initial momentum, thus an initially large dispersion in the momentum leads to a large dispersion of the position at later times. Thus for a free particle, the position cannot be monitored in a QND way even in principle, unless the momentum dispersion were reduced by an ancillary method, an issue that resulted in a debate on the possibility of preparing the initial state to beat the standard quantum limit (Yuen, 1983; Caves, 1985; Ozawa, 1988, 1989). On the other hand, if a measurement of momentum could be made, a sequence of measurements would give the same result since the momentum is conserved for a free particle. Thus, the momentum of a free particle can be monitored in a QND fashion and detailed schemes have been proposed making use of this concept (Braginsky and Khalili, 1990).

To specify the general conditions sufficient to perform a QND measurement, let us consider an arbitrary quantum-mechanical system described by the free-system Hamiltonian $\hat{H}_0$ (see Bohm, 1951, for further details). The goal is to measure a system observable $\hat{A}$ with a measuring apparatus that will be described by a Hamiltonian $\hat{H}_M$. A measurement is an interaction between the measured system and a measuring apparatus in which information from the system is transferred from the system to the apparatus, producing some change in the dynamical variables of the apparatus. This interaction process is described by an interaction Hamil-

tonian, $\hat{H}_I$, which depends upon the observables both of the measured system and of the apparatus, acting only during the measurement time. The total Hamiltonian for the system plus apparatus, in the absence of external forces, is therefore

$$\hat{H}=\hat{H}_0+\hat{H}_I+\hat{H}_M . \tag{2.5}$$

A QND measurement of an observable $\hat{A}$ of a system is defined as a sequence of measurements of $\hat{A}$ performed in such a way that the outcomes of each measurement are predictable from the result of the initial state-preparing measurement. The loss of predictability of the later measurements in a sequence can be attributed to either the influence of the measuring apparatus or to the influence of the conjugate observables on the free evolution. It turns out that once an observable has been identified that is unaffected by the conjugate observables, an interaction Hamiltonian suitable for QND measurements is, at least in principle, easily found. Therefore we will first concentrate on identifying the requirements an observable must satisfy to be protected from the influence of conjugate observables during the system's free evolution. This analysis is simplest in the Heisenberg picture.

Let the first measurement be performed at time t_0. The normalized eigenstates of $\hat{A}(t_0)$ are denoted by $|A,\alpha\rangle$, where α labels the states in any degenerate subspaces of $\hat{A}(t_0)$. According to the projection postulate, after the first measurement the system state will collapse into an eigenstate of $\hat{A}(t_0)$ with the corresponding eigenvalue for the expectation value of the observable:

$$|\psi(t_0)\rangle=\sum_{\alpha} c_{\alpha}|A_0,\alpha\rangle. \tag{2.6}$$

In the Heisenberg picture, the state of the system does not change during its free evolution, $|\psi(t)\rangle=|\psi(t_0)\rangle$, so if we demand that a second measurement will give a predictable result, the states $|A_0,\alpha\rangle$ must also be eigenstates of $\hat{A}(t_1)$, but not necessarily with the same eigenvalue. This means that the result of the second and all successive measurements is a deterministic function of the first measurement

$$\hat{A}(t_1)|A_0,\alpha\rangle=f_1(A_0)|A_0,\alpha\rangle, \tag{2.7}$$

where f_1 is an arbitrary real-valued function. This implies the operator equation for a measurement at the general time t_k,

$$\hat{A}(t_k)=f_k[\hat{A}(t_0)]. \tag{2.8}$$

Very often the equivalent condition is used,

$$[\hat{A}(t_i),\hat{A}(t_k)]=0, \tag{2.9}$$

which can be derived from Eq. (2.8) through a Taylor expansion of the function f in terms of the derivatives of the observable.

If the condition in Eq. (2.9) holds only at discrete instants of time, then the observable is called a stroboscopic QND observable, otherwise if Eq. (2.9) is satisfied at all times it is called a continuous QND observable. A particular case of a continuous QND observable is a quantity that is conserved in the absence of external forces during the time evolution of the system, provided that the interaction Hamiltonian is suitably chosen, as we will see later. This condition can be stated in terms of the free Hamiltonian operator as

$$\frac{d\hat{A}}{dt}=\frac{\partial\hat{A}}{\partial t}-\frac{i}{\hbar}[\hat{A},\hat{H}_0]=0. \tag{2.10}$$

For instance, the free Hamiltonian itself is a continuous QND observable provided that it is time independent. In the following sections we will also encounter examples of continuous QND observables that are nonconserved quantities. Furthermore, not all observables satisfying Eq. (2.10) will reflect the influence of a force acting on the system. For a QND observable to yield information about a force acting on a system, one should be able to make repeated measurements of the observable at arbitrarily closely spaced instants of time in such a way that the result of a measurement is determined by the result of the most recent previous measurement and the force $F(t)$ acting on the oscillator; furthermore, the force dependence should be such that one can unequivocally infer $F(t)$. This leads to the introduction of the concept of a QNDF observable (QND in the presence of an external force), which corresponds to the following condition, in addition to Eq. (2.10), for the evolution in the Heisenberg picture of the observable $\hat{A}$:

$$\hat{A}(t)=f[\hat{A}(t_0);F(t');t,t_0], \tag{2.11}$$

with the provision that the dependence of the observable upon the force acting between the time interval $[t_0,t]$ $(t_0<t'<t)$ is an invertible functional.

We have identified the conditions that must exist in a free quantum system so that a sequence of measurements is possible in which the first measurement of an observable will allow one to predict the outcome of successive measurements of that observable. We now specify the condition that must be fulfilled by the interaction Hamiltonian to allow a sequence of predictable measurements. It is natural to assume that the measurement of an observable is possible only if the interaction Hamiltonian depends upon that observable. Moreover, if the interaction Hamiltonian is chosen so that it commutes with the observable to be measured then the observable will not change its value during the measurement. Note that during the interaction with the measurement apparatus, the Hamiltonian that enters into Eq. (2.10) is the one that describes the system, the measuring apparatus, and the interaction term. A QND observable of the free system remains a QND observable of the system even when coupled to the apparatus if the following condition is satisfied:

$$[\hat{A}_I(t),\hat{H}_I(t')]=0, \tag{2.12}$$

where $\hat{A}_I(t)$ and $\hat{H}_I(t')$ are the interaction-picture forms of the observable and the interaction Hamiltonian, namely

$$\hat{A}_I(t)\equiv\hat{U}_0^{\dagger}(t,t_0)\hat{A}(t)\hat{U}_0(t,t_0), \tag{2.13}$$

$$\hat{H}_I(t) \equiv \hat{U}_0^\dagger(t,t_0)\hat{U}_M^\dagger(t,t_0)\hat{H}(t)\hat{U}_M(t,t_0)\hat{U}_0(t,t_0),$$

where $\hat{U}_0(t,t_0)$ and $\hat{U}_M(t,t_0)$ are the time evolution operators for the free system and measuring apparatus Hamiltonians respectively. If the observable $\hat{A}(t)$ is conserved in the absence of the interaction with the measuring apparatus, then it remains conserved if

$$[\hat{A}(t),\hat{H}_I]=0. \tag{2.14}$$

A simple method to satisfy this condition is to choose an interaction Hamiltonian that is linearly dependent on the observable one wishes to measure,

$$\hat{H}_I = K\hat{A}\hat{Q}, \tag{2.15}$$

where $\hat{Q}$ represents some observable of the measuring apparatus and K is a coupling constant which may be time dependent.

3. Quantum nondemolition measurement strategies for a harmonic oscillator

The harmonic oscillator is a useful model for a large number of physical systems, such as a mode of a mechanically resonant system, an electrically resonant circuit or a mode of a microwave or optical cavity. In this section we review the quantum-mechanical description of the harmonic oscillator and examine the nature of the various oscillator observables. According to the discussion in the previous section, in our description of a measurement on a harmonic oscillator we will neglect the thermodynamic coupling to the external environment, and treat the problem in the formalism of quantum mechanics for pure states. The oscillator is defined by its canonical coordinate, with the associated operator $\hat{x}$, by the conjugate momentum with operator $\hat{p}$—both Hermitian operators—and by the mass m and the angular frequency of free oscillation ω. The Hamiltonian of the free mechanical harmonic oscillator is

$$\hat{H}_0 = \frac{\hat{p}^2}{2m} + \frac{m\omega^2\hat{x}^2}{2}. \tag{2.16}$$

We introduce the operator representing the number of quanta,

$$\hat{N} = \frac{\hat{H}_0}{\hbar\omega} - \frac{1}{2} = \hat{a}^\dagger\hat{a}, \tag{2.17}$$

where the creation and annihilation operators have been introduced, respectively

$$\hat{a}^\dagger = \left(\frac{m\omega}{2\hbar}\right)^{1/2}\left(\hat{x} - i\,\frac{\hat{p}}{m\omega}\right) \quad \text{and}$$

$$\hat{a} = \left(\frac{m\omega}{2\hbar}\right)^{1/2}\left(\hat{x} + i\,\frac{\hat{p}}{m\omega}\right). \tag{2.18}$$

The dominant frequency dependence of the complex quantity $\hat{x}+i\hat{p}/(m\omega)$ can be factored out, and the oscillator complex amplitude $\hat{X}_1+i\hat{X}_2$ can be defined as

$$\hat{x} + i\,\frac{\hat{p}}{m\omega} = (\hat{X}_1 + i\hat{X}_2)e^{-i\omega t}. \tag{2.19}$$

The real and the imaginary parts of the complex amplitude operator can be written in terms of $\hat{x}$ and $\hat{p}/m\omega$ as

$$\hat{X}_1(\hat{x},\hat{p},t) \equiv \hat{x}\,\cos\omega t - \frac{\hat{p}}{m\omega}\,\sin\omega t,$$

$$\hat{X}_2(\hat{x},\hat{p},t) \equiv \hat{x}\,\sin\omega t + \frac{\hat{p}}{m\omega}\,\cos\omega t. \tag{2.20}$$

The two components of the complex amplitude are conserved in the absence of interactions with the external world:

$$\frac{d\hat{X}_j}{dt} = \frac{\partial\hat{X}_j}{\partial t} - \frac{i}{\hbar}[\hat{X}_j,\hat{H}_0] = 0 \tag{2.21}$$

so either component of the complex amplitude operator commutes with itself for all future times, which is the condition to be a continuous QND observable. The corresponding situation for position and momentum is more complicated. For the position and momentum we can calculate the different-time commutator

$$[\hat{x}(t),\hat{x}(t+\tau)] = \frac{i\hbar}{m\omega}\,\sin\omega\tau,$$

$$[\hat{p}(t),\hat{p}(t+\tau)] = i\hbar m\omega\,\sin\omega\tau, \tag{2.22}$$

which implies a vanishing commutator at times spaced by $\tau = n\pi/\omega$, with n an integer. This means that $\hat{x}$ and $\hat{p}$ are stroboscopic QND observables, that is, it is possible to perform a sequence of precise measurements of $\hat{x}$ or $\hat{p}$ at well-defined time intervals. The interaction Hamiltonian that would enable a stroboscopic measurement of the position consists of a sequence of pulses

$$\hat{H}_I \propto \sum_{n=0}^{\infty} \delta\left(t - \frac{n\pi}{\omega}\right)\hat{x}\hat{Q}; \tag{2.23}$$

or to measure the momentum we would have,

$$\hat{H}_I \propto \frac{1}{m\omega}\sum_{n=0}^{\infty} \delta\left(t - \frac{n\pi}{\omega}\right)\hat{p}\hat{Q}, \tag{2.24}$$

where $\hat{Q}$ is an observable of the measurement apparatus. A more realistic version of a stroboscopic measurement has a nonzero interaction between the harmonic oscillator and the apparatus for a time interval $\Delta\tau$ that is short compared to the harmonic oscillator period. If the precision of the initial position measurement is $\Delta x \ll [\hbar/(2m\omega)]^{1/2}$, the oscillator momentum will be perturbed by an amount $\Delta p \cong \hbar/(2\Delta x)$. This momentum dispersion will evolve into a position dispersion that will reach a maximum value at $t+\pi/2\omega$ and subsequently decrease, until at time $t+\pi/\omega$ the position dispersion will return to its original value that resulted from the initial measurement. Apparently one should therefore choose to perform repeated position measurements at the instants of time when the position dispersion has the minimum value; any observed deviation from the expected position would then signal that a force had acted on the mechanical oscillator since the preceding measurement. The accuracy obtainable in a series of stroboscopic measurements each of finite duration $\Delta\tau$ is Δx

$\cong[\hbar/(2m\omega)]^{1/2}(\omega\Delta\tau)^{1/2}$, where the improvement factor for a stroboscopic measurement over an amplitude and phase measurement is $(\omega\Delta\tau)^{1/2}$. The major practical limitation of a stroboscopic measurement is that unrealistically large electromechanical coupling strength is required to obtain a signal sufficiently large to be detectable in the face of the purely additive noise from practical measurement apparatuses. In light of this practical limitation, attention has focused on nonstroboscopic measurements in which the mechanical oscillator is monitored quasicontinuously, thereby allowing longer signal-averaging times. Measurement-time durations in such measurements typically extend over many periods of the mechanical oscillator, allowing the noise added by the measurement apparatus to be reduced by averaging.

The number of quanta $\hat{N}$ and the components of the complex amplitudes $\hat{X}_1$ and $\hat{X}_2$ are examples of continuous QND observables. Regarding the measurement of $\hat{N}$, using current technology efficient quantum counters are available for photons at submillimeter wave frequencies and above, but they are all demolition devices because the measurement process destroys the detected photons leaving the system in a different quantum state than the initial state before the measurement. Quantum nondemolition schemes to measure the number of photons in a microwave cavity without changing their number were proposed by Braginsky, Vorontsov, and Khalili (1977) and by Unruh (1978). A scheme to measure the number of phonons in a mechanical resonator was also proposed by Braginsky and Vorontsov (1974) in which a microwave cavity coupled to a resonant bar converts bar phonons into cavity photons, which provide a measure of the phonon number in the bar. This proposal was superseded by another proposed scheme in which an electromechanical transducer provided a quadratic coupling in $\hat{x}$, described by the Unruh-Braginsky interaction Hamiltonian

$$\hat{H}_I = K\hat{x}^2\hat{Q} = \frac{1}{2}K\left[\frac{2\hbar}{m\omega}\left(\hat{N}+\frac{1}{2}\right)+(\hat{X}_1^2-\hat{X}_2^2)\cos 2\omega t + (\hat{X}_1\hat{X}_2+\hat{X}_2\hat{X}_1)\sin 2\omega t\right], \tag{2.25}$$

provided an average is performed to filter out the components oscillating at 2ω. QND measurements of the number of quanta are plagued by two major drawbacks. From a practical point of view, it is difficult to design a transducer in which the dominant coupling is quadratic—it is difficult to reduce the linear coupling so that it is negligible compared to the quadratic terms. Moreover, a QND measurement of the number of quanta should allow the detection of an arbitrarily weak classical force, but the measurement cannot determine the precise time dependence of the force; in other words, it is not a QNDF measurement, according to the definitions in the previous section.

Subsequently, a style of QND measurement unaffected by these drawbacks was proposed (Thorne, Drever, *et al.*, 1978; Thorne, Caves, *et al.*, 1979). It consisted of measuring one component of the harmonic oscillator's complex amplitude. The complex-amplitude components are QND observables since they are constants of the motion in the absence of an external force; they are also QNDF observables and it is possible to show that, apart from an arbitrary phase factor, they are the only such QNDF observables that are a linear combination of the position and momentum operators (Braginsky *et al.*, 1980; Caves *et al.*, 1980). The simplest interaction Hamiltonian for a QND measurement of one component of the complex amplitude is therefore

$$\hat{H}_I = E_0\hat{X}_1\hat{Q} = E_0\left(\hat{x}\,\cos\omega t - \frac{\hat{p}}{m\omega}\sin\omega t\right)\hat{Q}, \tag{2.26}$$

from which it is apparent that transducers of position and momentum are needed, and that the coupling strengths between the mechanical oscillator and the two transducers must be modulated in a specific time-dependent fashion. Note that if Q is the charge of an electrical oscillator, the coupling constant E_0 must have units of the electric field. In practice this coupling could be modulated by an external generator that is excited in an arbitrarily energetic, coherent state, and therefore may be treated as a classical field (Unruh, 1979). In Caves *et al.* (1980), the feasibility of momentum transducers is discussed and it is shown that it would be difficult to develop a momentum transducer capable of reaching the quantum limit. Another interaction Hamiltonian was proposed by the same authors, by which a continuous single-transducer QND measurement could be performed

$$\begin{aligned}\hat{H} &= E_0\cos\omega t\hat{x}\hat{Q}\\ &= E_0\cos\omega t(\hat{X}_1\cos\omega t+\hat{X}_2\sin\omega t)\hat{Q}\\ &= \frac{E_0}{2}(\hat{X}_1+\hat{X}_1\cos 2\omega t+\hat{X}_2\sin 2\omega t)\hat{Q},\end{aligned} \tag{2.27}$$

where detection is followed by a low-pass filtering operation to select the information about the $\hat{X}_1$ phase and to reject the conjugate phase information. The low-pass filter should have a cutoff frequency $\omega_{co}\ll\omega$ so that the sinusoidally oscillating terms in the Hamiltonian will average to near zero over the time scales of interest. The measurement mediated by this interaction Hamiltonian is similar in concept to the phase-sensitive detection performed by a lock-in amplifier (Hollenhorst, 1979). In contrast to a lock-in amplifier however, the key feature of a QND measurement of one component of an oscillator's complex amplitude is that the phase-sensitive detection is performed before the amplification stage, which would unavoidably add noise to the measurement.

A convenient realization of the complex-amplitude QND measurement Hamiltonian would be to employ an electrically resonant circuit as the measurement apparatus and to modulate the coupling between this readout circuit and the system, i.e., the mechanical oscillator, at the sum and difference of the two subsystem natural resonant frequencies:

$$\hat{H}_I = E_0 \cos\omega_e t \, \cos\omega t \hat{x}\hat{Q} = \frac{E_0}{2}[\cos(\omega_e+\omega)t + \cos(\omega_e-\omega)t]\hat{x}\hat{Q}. \quad (2.28)$$

Moreover, the modulation does not need to be sinusoidal. For example, another single-transducer interaction Hamiltonian that has been proposed consists of stroboscopically monitoring the complex amplitude (Thorne *et al.*, 1978; Braginsky, Vorontsov, and Khalili, 1978). Each continuous QND observable can be monitored in a stroboscopic way, maintaining the QND feature—specifically, in the case under consideration, the interaction Hamiltonian would be

$$\hat{H}_I = E_0 \sum_{n=0}^{\infty} \delta\left(t - \frac{n\pi}{\omega}\right)\hat{X}_1\hat{Q} = E_0 \sum_{n=0}^{\infty} (-1)^n \delta\left(t - \frac{n\pi}{\omega}\right)\hat{x}\hat{Q}, \quad (2.29)$$

which differs from the interaction Hamiltonian for a stroboscopic QND measurement of x only by the presence of the alternating sign.

4. Quantum nondemolition strategies for coupled harmonic oscillators

The signal-to-noise ratio of a mechanically resonant gravitational wave antenna may conveniently be increased by coupling to the antenna a second, less massive mechanical resonator tuned to the resonant frequency of the antenna (Lavrent'ev, 1969; Paik, 1976). The vibrational energy imparted to the antenna by a signal force is transferred to the less massive secondary resonator, which serves as a mechanical amplifier to boost the mechanical signal to a level closer to the optimum level for common-readout electronics, achieving a sort of mechanical impedance matching. Thus it is natural to extend the theory developed so far to the case of a double harmonic oscillator (Bocko *et al.*, 1984; Onofrio, 1987; Onofrio and Rioli, 1993; Cinquegrana *et al.*, 1994).

Let us consider two coupled harmonic oscillators having classical displacement coordinates x and y, momenta p_x and p_y, masses m_x and m_y, and angular frequencies ω_x and ω_y. The two oscillators may represent the first longitudinal mode of a massive gravitational wave antenna and the resonant mode of a transducer attached to the end face of the antenna. For a cylindrical antenna the equivalent simple harmonic oscillator has an equivalent mass exactly equal to one half of the antenna's physical mass. The Lagrangian of the coupled system is written as

$$L = \tfrac{1}{2}m_x\dot{x}^2 + \tfrac{1}{2}m_y\dot{y}^2 - \tfrac{1}{2}m_x\omega_x^2x^2 - \tfrac{1}{2}m_y\omega_y^2(y-x)^2. \quad (2.30)$$

When the uncoupled frequencies ω_x and ω_y are exactly tuned to one another the coupled mode frequencies are

$$\omega_\pm^2 = \omega^2(1+\alpha_\pm), \quad \text{where} \quad \alpha_\pm = \frac{\mu}{2} \pm \sqrt{\mu(1+\mu/4)}, \quad (2.31)$$

in which $\mu = m_y/m_x$, and the normal coordinates are obtained from the physical coordinates using the transformations

$$\Xi_\pm = \sqrt{m_x/(2+\alpha_+)}\,x + \sqrt{m_y\alpha_\pm/\mu(2+\alpha_\pm)}\,y. \quad (2.32)$$

We thus define the quantum operators for the complex amplitudes of the two modes of the coupled system as follows

$$\hat{X}_{1\pm} = \hat{\Xi}_\pm \cos\omega_\pm t - \frac{\hat{P}_{\Xi_\pm}}{\omega_\pm}\sin\omega_\pm t,$$
$$\hat{X}_{2\pm} = \hat{\Xi}_\pm \sin\omega_\pm t + \frac{\hat{P}_{\Xi_\pm}}{\omega_\pm}\cos\omega_\pm t. \quad (2.33)$$

These observables obey the commutation rules,

$$[\hat{X}_{1+},\hat{X}_{2+}] = i\frac{\hbar}{\omega_+}, \quad [\hat{X}_{1-},\hat{X}_{2-}] = i\frac{\hbar}{\omega_-} \quad (2.34)$$

with all other combinations being zero. The Hamiltonian operator is written in terms of the components of the complex amplitudes of the normal coordinates as

$$\hat{H} = \frac{\omega_+^2}{2}[\hat{X}_{1+}^2 + \hat{X}_{2+}^2] + \frac{\omega_-^2}{2}[\hat{X}_{1-}^2 + \hat{X}_{2-}^2]. \quad (2.35)$$

Practical methods of detection for such coupled systems would use a measuring apparatus described by an interaction Hamiltonian proportional to the difference of the physical coordinates of the two oscillators,

$$\hat{H}_I = E_0(\hat{y}-\hat{x})\hat{Q}. \quad (2.36)$$

For example, the measuring apparatus could include a parallel-plate capacitor with one capacitor electrode mounted on the primary resonator and the other mounted on the secondary resonator. The interaction Hamiltonian would then have the form of Eq. (2.36) with Q representing the charge on the capacitor plates and E_0 the electric field in the capacitor. We can find the different-time commutator for the observed quantity by expressing the physical coordinates in terms of the two components of the normal mode complex amplitudes, obtaining

$$[\hat{y}(t)-\hat{x}(t),\hat{y}(t+\tau)-\hat{x}(t+\tau)] = \frac{i\hbar}{m_y\omega}\frac{1}{\sqrt{4+\mu}}\left(\frac{\omega_+^2}{\omega^2}\sin\omega_+\tau + \frac{\omega_-^2}{\omega^2}\sin\omega_-\tau\right), \quad (2.37)$$

where τ represents the time interval.

To check this result, we let the mass ratio μ go to zero, after which the commutator in Eq. (2.37) assumes the simple form

$$[\hat{y}(t)-\hat{x}(t),\hat{y}(t+\tau)-\hat{x}(t+\tau)] \xrightarrow{\mu\to 0} \frac{i\hbar}{m_y\omega}\sin\omega\tau, \quad (2.38)$$

which coincides with the commutator for the single oscillator, Eq. (2.22). In the limit of the mass ratio μ being very small, Eq. (2.37) can also be rewritten as

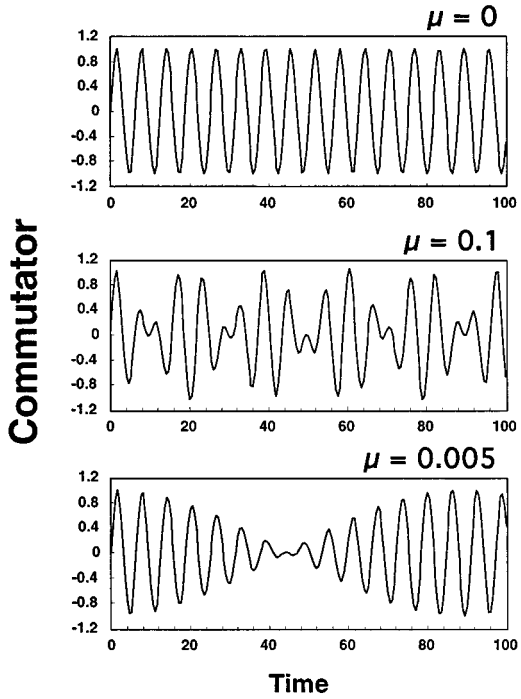

FIG. 1. The normalized different-time commutator for the observable that measures the difference of the displacements for two coupled harmonic oscillators is plotted as a function of time. The three cases correspond to different mass ratios. The uppermost plot, labeled μ=0, corresponds to the mass of the second harmonic oscillator going to zero, which yields a result identical to that for the single harmonic oscillator. In the other two cases the mass ratios are μ=0.1 and μ=0.005. It is assumed that the uncoupled natural frequencies ω of the two oscillators are the same. Results are expressed in units of $i\hbar/m_y\omega$ and the time is in units where the uncoupled harmonic oscillator period is 2π.

$$[\hat{y}(t)-\hat{x}(t),\hat{y}(t+\tau)-\hat{x}(t+\tau)] \cong \frac{i\hbar}{2m_y\omega}\left(\frac{\omega_+^2+\omega_-^2}{\omega^2}\sin\bar{\omega}\tau\cos\omega_B\tau\right) \tag{2.39}$$

where we defined the average frequency to be $\bar{\omega}=(\omega_+ + \omega_-)/2$, and the beat frequency as $\omega_B=(\omega_+ - \omega_-)/2$. The right-hand side of Eq. (2.39) is a sinusoidal function of the time τ, with period $\bar{T}=2\pi/\bar{\omega}\cong T$, modulated by a beating period $T_B\cong 2T/\sqrt{\mu}$. Shown in Fig. 1 is the value of the commutator given by Eq. (2.39) versus time for three different values of the mass ratio. As the mass ratio is decreased, the beating period between the normal modes becomes longer, and in the limit of the mass ratio going to zero, the commutator becomes identical to the commutator of the single harmonic oscillator. Similarly, in the case of two coupled harmonic oscillators detuned in frequency from one another, the energy transfer is reduced as the oscillator frequencies move farther apart, and in the limiting case of no energy transfer between the oscillators the commutator approaches that of the single harmonic oscillator—see Fig. 2. The periodicity of the commutator in Eq. (2.39) suggests a simple QND stroboscopic scheme in which measurements are performed for relatively long time intervals separated in time by one half the normal-mode beating period. The interaction Hamiltonian in this case would be of the form

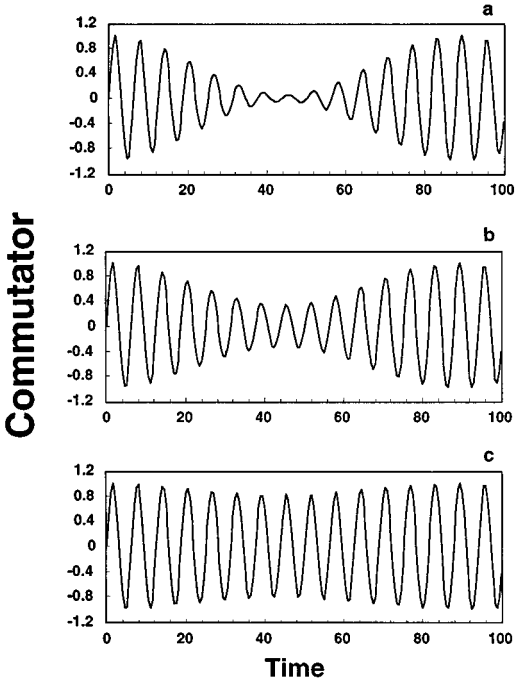

FIG. 2. Three plots of the same type as Fig. 1 for the case μ=0.005, for three different degrees of detuning of the harmonic-oscillator natural frequencies. In the plot labeled (a), the frequency detuning is such that 90% of the energy is transferred between the oscillators; case (b) corresponds to 50% energy transfer, and case (c) to 10% energy transfer. Units are the same as those in Fig. 1.

$$\hat{H}_I=\frac{E_0}{2}\sum_{n=0}^{\infty}\left[\theta\left(t-\frac{nT_B}{2}+\frac{\Delta T}{2}\right)+\theta\left(-t+\frac{nT_B}{2}+\frac{\Delta T}{2}\right)\right](\hat{y}-\hat{x})\hat{Q}, \tag{2.40}$$

where ΔT is of the order of the period of a single harmonic oscillator. It is interesting to observe that this interaction Hamiltonian may be derived from a different point of view as the limit of a continuous measurement scheme. Indeed, observing the periodicities in the commutator, a continuous interaction Hamiltonian of the kind

$$\hat{H}_I=E_0\cos\omega_e t\,\cos\bar{\omega}t\,\cos\omega_B t(\hat{y}-\hat{x})\hat{Q} \tag{2.41}$$

can be used provided one employs a band-pass filter to select only the frequency components centered on ω_e. This Hamiltonian can be written as

$$\hat{H}_I=E_0\cos\omega_e t[\cos\omega_+ t+\cos\omega_- t](\hat{y}-\hat{x})\hat{Q} \tag{2.42}$$

which shows that it is possible to perform a simultaneous approximate QND measurement on one of the complex amplitudes of each of the two normal modes. By analogy to the single oscillator case, it is possible to introduce additional frequency components in the interaction Hamiltonian,

$$\hat{H}_I \cong E_0 \cos\omega_e t \left[\sum_{n=0}^{\infty} \cos(2n+1)\omega_+ t + \sum_{n=0}^{\infty} \cos(2n+1)\omega_- t \right] (\hat{y}-\hat{x})\hat{Q} \tag{2.43}$$

that corresponds, in the limit of large n, to a stroboscopic measurement:

$$\hat{H}_I \cong \frac{E_0}{2} \left[\sum_{n=0}^{\infty} (-1)^n \delta\left(t - \frac{n\pi}{\omega_+} \right) + \sum_{n=0}^{\infty} (-1)^n \delta\left(t - \frac{n\pi}{\omega_-} \right) \right] (\hat{y}-\hat{x})\hat{Q}. \tag{2.44}$$

The two trains of impulsive measurements will coincide at times spaced by $T_B/2$, i.e., $T_B/2 = n\pi/\omega_+ = m\pi/\omega_-$, where $n = m+2$.

A small mass ratio implies a long coupled-oscillator normal-mode beating period, and consequently a small measurement duty cycle. One way to circumvent this inconvenience is to use a multimode configuration (Richard, 1982, 1984)—in particular the case of three coupled harmonic oscillators has been discussed in detail (Onofrio and Rioli, 1993). It turns out that the periodicity of a stroboscopic measurement on a multimode system has a higher frequency, i.e., the duty cycle is greater—however, the time dependence of the commutator becomes rather complex, with double beat frequencies present in the measurement coupling.

An analysis including classical sources of dissipation for the case of two coupled oscillators continuously monitored with a quantum nondemolition strategy has been discussed by Cinquegrana *et al.*, 1994. They also give estimates, as we will describe in Sec. V, of the sensitivity for actual gravitational wave antennas.

5. Quantum nondemolition measurements in nonlinear systems

Although it originated and developed in the particular context of the harmonic oscillator, the concept of quantum nondemolition measurement is in principle applicable to any dynamical system. Such a generalization has been proposed in the framework of the path-integral approach to quantum measurement theory (Mensky, Onofrio, and Presilla, 1993). In this approach the outcome of the measurements is considered known, the so-called *a posteriori* dynamics, and the goal of the method is to complete the knowledge of the state of the system during the measurement process. This is achieved by weighting the paths according to their average distance from the measurement outcome (Mensky, 1979, 1993; for similar attempts see Caves, 1986, 1987). It can be shown that a Gaussian weight satisfies all the properties of the Feynman propagator without the measurement process. Moreover, the link of this approach with other frameworks used to include the measurement process in quantum mechanics, such as the density-matrix master equation or the stochastic Schrödinger equation, have been made (Mensky, 1994, Presilla, Onofrio, and Tambini, 1995).

The Feynman kernel modified by the presence of the measurement result $a(t)$ of the observable A is written as

$$K_{[a]}(x'',\tau,x',0) = \int d[x] \exp\left\{ \frac{i}{\hbar} \int_0^{\tau} L(x(t),\dot{x}(t),t)dt \right\} \times \exp\left\{ -K(t) \int_0^{\tau} (x(t)-a(t))^2 dt \right\}, \tag{2.45}$$

where $[a]$ is the result of the continuous measurement ($[a] = a(t), 0 \leqslant t \leqslant \tau$) performed during the time τ, and $K(t)$ expresses the coupling of the observed system to the meter, in general a time-dependent coupling. The resulting path integral may be considered as describing a free system with an effective Lagrangian being a functional of the measurement result and having a non-Hermitian term due to the measurement process:

$$L_{\text{eff}}(x(t),\dot{x}(t),t) = L(x(t),\dot{x}(t),t) + iK(t)[x(t)-a(t)]^2. \tag{2.46}$$

The wave function evolves according to the effective Schrödinger equation:

$$i\hbar \frac{\partial \psi_{[a]}(x,t)}{\partial t} = H_{\text{eff}} \psi_{[a]}(x,t), \tag{2.47}$$

where H_{eff} is the effective Hamiltonian corresponding to the Lagrangian (2.46) (Mensky, Onofrio, and Presilla, 1991). This method allows one to evaluate the evolution of any system subjected to continuous measurements through numerical integration of the effective Schrödinger equation (2.47), thus completing the knowledge of the state during the continuous measurement with the already known outcome $a(t)$. This is called an *a posteriori* evaluation of the measurement process. Alternatively, one can evaluate the dynamical evolution *a priori* by choosing a measurement result at the initial time with probability $|\psi(x,0)|^2$, evolving the wave function at the instant of time Δt through the effective Schrödinger equation (2.47), and iterating the process by choosing the measurement result at the time Δt with probability $|\psi(x,\Delta t)|^2$. Thus the effective Schrödinger equation, together with the probability of having a particular result of a measurement chosen with the time-dependent probability distribution, allows one to evaluate the *a priori* dynamics. Of course, one can choose to extract the measurement result with a time-independent probability distribution using white noise. A stochastic effective Schrödinger equation is therefore obtained as

$$d|\psi_{[\xi]}(t)\rangle = \left[-\frac{i}{\hbar} \hat{H} - \frac{1}{2} K(t)[\hat{A} - a_{[\xi]}(t)]^2 \right] |\psi_{[\xi]}(t)\rangle dt + \sqrt{K(t)}[\hat{A} - a_{[\xi]}(t)]|\psi_{[\xi]}(t)\rangle dw(t), \tag{2.48}$$

where $dw(t)$ is a Wiener process expressed in terms of a white noise $\xi(t)$ as $dw(t) = \xi(t)dt$, and

$a_{[\xi]}(t)=\langle\psi_{[\xi]}(t)|\hat{A}(t)|\psi_{[\xi]}(t)\rangle$. This stochastic equation allows the description of individual trials of a quantum measurement (Gisin, 1984a, 1984b; Pearle, 1986; Diosi, 1988a, 1988b; Gisin and Percival, 1992a, 1992b; Belavkin, 1989; Belavkin and Staszewski, 1989; Belavkin, Hirota, and Hudson, 1995), the evolution of the measured system being a so-called *quantum trajectory* (Griffits, 1984; Zoller *et al.*, 1987; Carmichael *et al.*, 1989; Gagen and Milburn, 1993; Gagen, Wiseman, and Milburn, 1993).

The same formalism allows one to deal with stroboscopic QND measurements in a generic dynamical system (Mensky, Onofrio, and Presilla, 1993). This is obtained by simply modulating the measurement coupling $K(t)$ in such a way that it is always null, apart from small equally spaced time intervals. It has been shown that for particular values of the time spacing the uncertainty induced by the back-action of the measurement is minimized. These optimal periodicities are understood in terms of the spectral properties of the potential associated with the system. If the measurement result is known and assumed equal for each measurement the state will collapse to the measured eigenstate with a speed proportional to the measurement coupling $K(t)$. Therefore, the asymptotic dynamics will be dictated by the expansion of this eigenstate in terms of the energy eigenstates. Some of these eigenstates maximally contribute to the reformation of the asymptotic state and their eigenvalues will give the periods $T_{nm}=2\pi\hbar/(E_n-E_m)$. When the measurement-time spacing contains an integer number of periods for the eigenstates that contribute to the asymptotic state, we effectively will have a stationary situation at the instants of measurement. In the already understood case of the harmonic oscillator, the energy eigenstates are equally spaced and, for each initial state, the optimal measurement-time spacing is a multiple of the period of the harmonic oscillator as shown by the different-time commutators [Eq. (2.22)] in the Heisenberg picture. This does not occur for a generic system and the concept of QND strategy in this case is only applicable once the measurement result is known, an *a posteriori* situation.

Particular physical interest in generalizing QND measurements to nonlinear systems comes from the need to understand the role of quantum measurements in bistable potentials exhibiting tunneling and in the classical-to-quantum correspondence in chaotic systems.

In the first case, the interest is originated by the attempt to look for a comparison between quantum mechanics and realistic models through tests of the temporal Bell inequalities (Leggett and Garg, 1985). In this proposal, some correlation functions of different-time magnetic flux measurements in a rf SQUID (superconducting quantum interference device) were shown to satisfy a Bell inequality if realism were correct, but were shown to violate it in quantum mechanics. However, since repeated measurements on a single quantum object are performed, the measurement process must be included in the quantum predictions for the evolution of the system. When this is done (Calarco and Onofrio, 1995), the result is that impulsive quantum nondemolition measurements are performed if they are spaced by a tunneling period, and in all the other cases the back-action noise is large and can affect the distinguishability of the two signs of the magnetic flux of the rf SQUID (Onofrio and Calarco, 1995).

In the second case, the well-known discrepancy between the long-term behavior of classical systems and their corresponding quantum counterparts can be solved by including a measurement process that allows for the decoherence of the wave function. On the other hand, the measurement process has to be chosen in such a way as to not affect the observed quantity, so again a quantum nondemolition measurement has been suggested (Adachi, Toda, and Ikeda, 1989; Toda, Adachi, and Ikeda, 1989). Moreover, Weigert (1991) suggested the use of a QND basis to allow the distinction between chaos that is intrinsically due to the quantum nature of the system, which is quenched for this kind of observable, and chaos arising from the corresponding classical dynamics. In general, the role of the measurement process in quantum chaotic systems is still far from being understood (Casati and Chirikov, 1994, 1995).

As we will describe later, nonlinear oscillators have also been the subject of experiments performed to evade the amplifier noise in stabilized oscillators and frequency references (Greywall *et al.*, 1994). A quantum nondemolition method to track a resonator's phase gave a 10 dB reduction of the phase dispersion arising from the feedback amplifier in a driven oscillator with a cubic nonlinearity.

III. MODELS OF MEASUREMENT IN THE CLASSICAL REGIME

A quantum-mechanical description of a measurement on a mechanical harmonic oscillator was presented in Sec. II, and assorted strategies for monitoring a weak force acting on the mechanical oscillator were evaluated using the machinery of quantum mechanics. Here, in Sec. III, we bridge the gap from the idealized quantum-mechanical model of a measurement to the classical world of actual measurements using macroscopic laboratory apparatus. But before assembling the analytical apparatus to describe measurements in the classical regime, we begin this section by pointing out some of the assumptions and idealizations implicit in classical models of measurement.

The classical description of a mechanical oscillator and a measurement apparatus are idealizations since such macroscopic systems are composed of many atoms, and only chosen collective motions of the atoms are the subject of our classical description. For example, a macroscopic mechanical oscillator, which may be a mass of metal consisting of 10^{25} atoms, is described by the displacement of an equivalent ideal mechanical harmonic oscillator, and we ignore the remaining $(3\times10^{25}-1)$ normal modes of the solid body. Luckily, the collective mode of vibration of the real mechanical oscillator which we will monitor to sense the effect of a mechani-

cal force is very well described by an equivalent simple harmonic oscillator. The remaining modes of vibration of the real mechanical resonator are of no interest aside from their role as the thermal reservoir, which provides acoustic damping and the associated thermal noise to the mode of interest. The second macroscopic system that serves the role of the measurement apparatus is typically an electronic circuit made up of on the order of Avogadro's number of atoms and conduction electrons. Again, only specific collective motions of the conduction electrons will be of interest, and we will show below that these degrees of freedom can be well represented as an electrical simple harmonic oscillator.

The proof that the complex macroscopic objects under consideration may be represented by such simple idealizations is in the experimental results. In the following section we use our simple models to build the descriptive tools for analyzing the sensitivity of a harmonic oscillator to weak forces.

A. Detection of a weak force in the presence of noise: general formalism

The prototypical force-detection system consists of a mechanical oscillator, which responds directly to the force, followed by an electromechanical transducer that converts the motion of the mechanical oscillator into an electrical signal that may be detected and amplified by a classical amplifier up to a conveniently measurable level. The experimenter examines the output from the classical amplifier to search for the effect of a weak force that may be acting on the mechanical oscillator. The question addressed in this section is, how does one most effectively examine the available data to discern the presence of a weak signal force? There is a well-developed theory of optimal filtering that gives the prescription to carry out this task (Papoulis, 1977). In this section we briefly review the theory of optimal filtering and present some specific results relevant to weak-force detection with a mechanical oscillator.

The central goal of this section is to define a figure of merit by which one may characterize the sensitivity of a force detector. We will see that to define this figure of merit requires both some knowledge of the noise in the detector and of the nature of the signal that is to be detected. The class of signals that has been of greatest interest in this field is that of impulsive forces, which are characteristic of the interaction of a fleeting gravitational radiation event with a gravitational wave detector. Correspondingly, the figure of merit that has been widely adopted is called the burst equivalent-noise temperature, or simply the burst temperature, of the antenna. Below, we will precisely define the burst temperature for a mechanical harmonic oscillator, but first we must establish the framework for the analysis. This framework uses random variables to represent the dynamical observables in the mechanical oscillator/measurement apparatus system. We shall closely follow the notation and presentation of Papoulis (1977).

We assume that the unfiltered output data stream from a force-detection system is a Gaussian-distributed random variable $x(t)$, which consists of a part that is the signal $f(t)$, and another part which is purely noise, $n(t)$:

$$x(t)=f(t)+n(t). \tag{3.1}$$

We seek the filter function, $h(t)$, which when convolved with the unfiltered data maximizes the output signal-to-noise ratio. Convolution of a given filter function with the output signal may be accomplished in a straightforward way on a computer that has stored the data from the detector. The convolution is represented by an asterisk (*):

$$y(t)=x(t)*h(t)=y_f(t)+y_n(t). \tag{3.2}$$

The output of the filter is $y(t)$, which is composed of the filtered signal $y_f(t)$ and the filtered noise $y_n(t)$. We seek the specific filter $h(t)$ that will maximize the signal-to-noise ratio at a given time t_0:

$$\frac{S}{N}=\frac{|y_f(t_0)|}{\sqrt{E\{|y_n(t_0)|^2\}}}, \tag{3.3}$$

where $E\{y\}$ is the ensemble average of the random variable y and $|\cdots|$ denotes the magnitude of the complex variable. Note that the numerator in the expression for the signal-to-noise ratio is a deterministic signal, so ensemble averaging is not needed. If we represent the Fourier transforms of $f(t)$ and $h(t)$ by $F(\omega)$ and $H(\omega)$, then the filtered output signal, $y_f(t_0)$, may be represented as the following:

$$y_f(t_0)=\frac{1}{2\pi}\int_{-\infty}^{+\infty}F(\omega)H(\omega)e^{j\omega t_0}d\omega. \tag{3.4}$$

The spectral density S_{y_n} of the filtered noise $y_n(t)$, is given by the spectral density of the noise $n(t)$, represented by $S_n(\omega)$, and the Fourier transform of the filter function, $H(\omega)$:

$$S_{y_n}=\frac{1}{2\pi}\int_{-\infty}^{+\infty}S_n(\omega)|H(\omega)|^2d\omega. \tag{3.5}$$

To find the expression for the signal-to-noise ratio in terms of the frequency-domain quantities requires some manipulation. First, we write

$$F(\omega)H(\omega)=\frac{F(\omega)}{\sqrt{S_n(\omega)}}H(\omega)\sqrt{S_n(\omega)}, \tag{3.6}$$

and use the relationship

$$E\{|y_n(t)|^2\}=\int_{-\infty}^{+\infty}S_n(\omega)|H(\omega)|^2d\omega, \tag{3.7}$$

which holds if the noise $n(t)$ is stationary. Schwartz's inequality for integrals

$$\left|\int_a^b z(x)w(x)dx\right|^2\leq\int_a^b|z(x)|^2dx\int_a^b|w(x)|^2dx \tag{3.8}$$

may be used to find

$$\left| \int_{-\infty}^{+\infty} F(\omega) H(\omega) e^{j\omega t_0} d\omega \right|^2 \leq \int_{-\infty}^{+\infty} \frac{|F(\omega)|^2}{S_n(\omega)}\, d\omega \int_{-\infty}^{+\infty} S_n(\omega) |H(\omega)|^2 d\omega. \quad (3.9)$$

Therefore, the signal-to-noise ratio is given by

$$\left(\frac{S}{N}\right)^2 = \frac{y_f^2(t_0)}{E\{|y_n(t_0)|^2\}^2} \leq \frac{1}{2\pi} \int_{-\infty}^{+\infty} \frac{|F(\omega)|^2}{S_n(\omega)}\, d\omega, \quad (3.10)$$

which becomes an equality only when

$$\sqrt{S_n(\omega)} H(\omega) = K \frac{F^*(\omega)}{\sqrt{S_n(\omega)}} e^{-j\omega t_0}. \quad (3.11)$$

Therefore, the filter that maximizes the signal-to-noise ratio, the optimum filter, is given in the frequency domain by

$$H(\omega) = K \frac{F^*(\omega)}{S_n(\omega)} e^{-j\omega t_0}. \quad (3.12)$$

In summary, one needs only to know the spectrum of the noise in the detector, $S_n(\omega)$, and the form of the force that is to be detected to compute the maximum signal-to-noise ratio using Eq. (3.10). In order to achieve the signal-to-noise ratio computed from Eq. (3.10), the output of the detector must be filtered by the ''matched'' filter given by Eq. (3.12). In practice, the frequency-domain representation of the optimum filter is inverse Fourier transformed to find the time-domain representation of the filter that can be implemented on a digital computer.

The burst temperature of a force detector is defined by using Eq. (3.10) to find the amplitude of the impulse p_0 that yields a signal-to-noise ratio of unity. This value of p_0 is the amplitude of the noise-equivalent impulse. The burst noise temperature T_n is defined by the amount of energy that the noise-equivalent impulse would deposit in the harmonic oscillator:

$$T_n = \frac{p_0^2}{2mk_B}. \quad (3.13)$$

It is illuminating to express the burst noise temperature as an equivalent number of quanta that the noise-equivalent impulse would deposit in the harmonic oscillator. This quantity is called the burst noise number N and is written as

$$N = \frac{k_B T_n}{\hbar\omega} = \frac{p_0^2}{2m\hbar\omega}. \quad (3.14)$$

Within the framework of optimal filter theory, an analysis of a measurement strategy for a harmonic oscillator consists of the following steps. First, one must develop a dynamical model of the force-detection system, including both the mechanical oscillator and the electrical readout circuit, then the sources of noise in the harmonic oscillator and the electrical readout are identified and specified by their spectral densities. The response of the output observable, usually an output voltage from the amplifier following the readout, is calculated for the assumed signal and for the assumed noise. The output noise spectrum and the output-signal spectral density are then input to Eq. (3.10) to calculate the signal amplitude that yields a signal-to-noise ratio of unity. This minimum detectable signal defines the burst noise temperature [Eq. (3.13)] and the burst noise number [Eq. (3.14)] for the entire mechanical oscillator/transducer/amplifier force-detection system. In the following section, a specific model of a readout will be given to allow the explicit computation of the burst noise temperature.

B. Classical model of a back-action evasion measurement

Many innovative designs for electromechanical transducers having the potential to reach the quantum-noise-dominated regime of operation have been developed. First developed by Paik (1976), a superconducting modulated-inductance transducer with a superconducting quantum interference device (SQUID) amplifier is now widely being exploited in gravitational wave detectors, and it is conceivable that in a few years this scheme will approach quantum-limited operation. Another promising scheme, from the point of view of reaching the quantum regime, is the optical cavity transducer being developed by Richard (1986). A summary of the principles of all the various transducer schemes is beyond the intent of this review, however. In the following discussion we limit our attention to parametric electromechanical transducers, the reason being that, so far, parametric transducers are the only scheme that has been demonstrated to be capable of performing a quantum nondemolition measurement when the quantum-noise regime is reached. Variations of parametric transducers have been developed by groups in Moscow, Perth, Rome, Frascati, Louisiana State University, and the University of Rochester, and the experimental details of the various realizations of the parametric transducer will be presented in Sec. IV.

In this section we develop a model of a generic parametric transducer composed of a mechanical oscillator and an electrical oscillator coupled together via a time-dependent electromechanical coupling. In practice the coupling is achieved by rigidly attaching one plate of a parallel-plate capacitor to the moving mechanical oscillator and anchoring the other plate in such a way that the motion of the mechanical oscillator modulates the gap between the capacitor plates. This simple model contains the essence of any parametric transducer. Also, since sensitivity to the phase of the mechanical oscillator is a central feature of a quantum nondemolition measurement, the equations of motion must be cast into a form that lends itself to such an analysis, i.e., the equations will be written in terms of the complex amplitudes of the mechanical and electrical degrees of freedom. We will first find the noise-free equations of motion for the parametrically coupled electromechanical system and the equations will be solved to find the response of the system to an assumed signal. Later in this section we

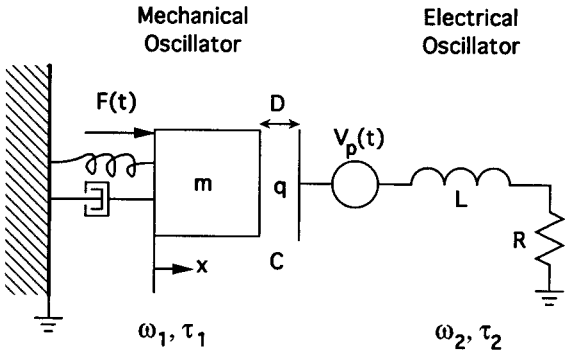

FIG. 3. A highly schematic representation of a parametric transducer coupled to a mechanical harmonic oscillator. The mechanical oscillator, which has a mass m, an angular resonant frequency ω_1, a relaxation time τ_1, and displacement x, is acted upon by an external signal force $F(t)$. The surface of the mechanical resonator serves as one plate of a capacitor C, contained in an electrical LCR resonator consisting of the capacitor, an inductor L, and a resistor R. A time-dependent voltage $V_p(t)$ drives the electrical resonator inducing a charge q on the capacitor plates thereby coupling the mechanical and electrical oscillators. The time-dependent gap of the capacitor is $D-x$, where D is the nominal capacitor gap.

present a more realistic model of the system that includes the major sources of noise. Following that, we shall use the optimal filter theory presented previously to predict the sensitivity of the parametric system to weak forces. We begin this detailed discussion by examining a highly simplified parametrically coupled mechanical and electrical oscillator system.

Refer to Fig. 3 for a schematized version of a parametric transducer. A mechanical oscillator of mass m, with a resonant frequency ω_1 and a relaxation time of τ_1 is acted upon by an external signal force $F(t)$. A surface of the mechanical resonator forms part of a capacitor C in an electrical resonator consisting of the capacitor, an inductor L and a resistor R. A time-dependent voltage $V_p(t)$ drives the electrical resonator inducing a charge q on the capacitor plates.

In Hamilton's form, the equations of motion for the mechanical oscillator are

$$\dot{x}=v,$$

$$\dot{v}-\frac{1}{\tau_1}\dot{x}=-\omega_1^2 x+\frac{F_T(t)}{m}, \tag{3.15}$$

where x is the displacement of the mechanical oscillator from its nominal position and v is the velocity of the mechanical oscillator. F_T is the sum of all the forces which act on the mechanical oscillator including the signal force $F(t)$ and the back-acting force $F_{BA}(t)$ of the electrical resonator acting on the mechanical resonator:

$$F_T(t)=F(t)+F_{\mathrm{BA}}(t). \tag{3.16}$$

The equations of motion for the electrical resonator, including the coupling to the mechanical resonator, are the following:

$$\dot{q}=I, \tag{3.17}$$

$$\dot{I}+\frac{1}{\tau_2}\dot{q}=-\omega_2^2 q+\frac{V_p(t)}{L}\left(1-\frac{x}{D}\right),$$

where q and I are, respectively, the charge on the capacitor plates and current in the inductor, τ_2 is the relaxation time, and ω_2 is the frequency of the electrical resonator; $V_p(t)$ is the excitation "pump" voltage and D is the capacitor spacing. In this simplified model the pump voltage source excites the electrical resonator through the "pump feedthrough" term $V_p(t)/L$ in Eq. (3.17). In a more realistic readout-circuit configuration one can employ a bridge circuit to cancel the pump feedthrough, leaving one with the $[V_p(t)/L](x/D)$ term that represents the "forward" coupling from the mechanical to the electrical resonator. Therefore, for convenience in the following analysis, we will drop the pump feedthrough term.

The back-action force of the transducer on the mechanical oscillator is given, to first order, by

$$F_{BA}(t)=-q\,\frac{V_p(t)}{D}. \tag{3.18}$$

This force, representing the "reverse" coupling, will drive the mechanical resonator in proportion to the excitation of the electrical resonator. Thus we have the complete equations for the mechanical and electrical resonators including the coupling between them. To facilitate the analysis of the phase-sensitive back-action evasion measurement, we now express the equations in terms of the complex amplitudes of the mechanical and electrical subsystems.

The complex amplitudes of the mechanical and electrical resonators are defined respectively as follows:

$$X_2+jX_1=\frac{1}{\omega_1'^*}(v+j\omega_1'^* x)e^{-j\omega_1 t},$$

$$Q_2+jQ_1=\frac{1}{\omega_2'^*}(I+j\omega_2'^* q)e^{-j\omega_2 t}, \tag{3.19}$$

where the complex angular frequencies $\omega_1'^*$ and $\omega_2'^*$ are defined to be

$$\omega_k'\equiv\omega_k\left[\left(1-\frac{1}{(2\omega_k\tau_k)^2}\right)+\frac{j}{2\omega_k\tau_k}\right]\quad k=1,2. \tag{3.20}$$

By forming linear combinations of Eqs. (3.15) and using the preceding definitions, one can cast the equations of motion for the mechanical oscillator into their complex-amplitude form:

$$\left(\frac{d}{dt}+\frac{1}{2\tau_1}\right)(X_2+jX_1)$$
$$=\frac{V_p(t)}{2D}\frac{1}{m\omega_1}[-Q_1(e^{j(\omega_2-\omega_1)t}+e^{-j(\omega_2+\omega_1)t})$$
$$+jQ_2(e^{j(\omega_2-\omega_1)t}-e^{-j(\omega_2+\omega_1)t})]+\frac{F(t)}{m\omega_1}e^{-j\omega_1 t}. \tag{3.21}$$

In like fashion, Eqs. (3.17) for the electrical oscillator may be put into the same form:

$$\left(\frac{d}{dt}+\frac{1}{2\tau_2}\right)(Q_2+jQ_1)$$
$$=\frac{V_p(t)}{2D}\frac{1}{L\omega_2}[-X_1(e^{j(\omega_1-\omega_2)t}+e^{-j(\omega_1+\omega_2)t})$$
$$+jX_2(e^{j(\omega_1-\omega_2)t}-e^{-j(\omega_1+\omega_2)t})]. \quad (3.22)$$

The specific form of the time-dependent pump voltage $V_p(t)$ must now be specified. As discussed earlier, the back-action evasion coupling requires establishing an electric field in the coupling capacitor with frequency components at both the sum and difference of the electrical and mechanical frequencies. To make possible a general analysis, we introduce the parameter f and write the pump in the following general form:

$$V_p(t)=\frac{V_0}{2}\{(1-f)\cos[(\omega_2+\omega_1)t]$$
$$+(1+f)\cos[(\omega_2-\omega_1)t]\}, \quad (3.23)$$

which, depending on the value of the parameter f, may represent any linear combination of the two pump frequency components, the two components being equal in amplitude for $f=0$. By inserting the general form of the pump into Eqs. (3.21) and (3.22), a set of four equations for the complex amplitudes of the mechanical and electrical oscillators may be found:

$$\left(\frac{d}{dt}+\frac{1}{2\tau_1}\right)X_1=\frac{V_0}{D}\frac{1}{4m\omega_1}\{Q_1\sin(2\omega_1t)+fQ_2$$
$$\times[1-\cos(2\omega_1t)]\}-\frac{F(t)}{m\omega_1}\sin(\omega_1t), \quad (3.24a)$$

$$\left(\frac{d}{dt}+\frac{1}{2\tau_1}\right)X_2=\frac{V_0}{D}\frac{1}{4m\omega_1}\{Q_1[1+\cos(2\omega_1t)]$$
$$+fQ_2\sin(2\omega_1t)\}+\frac{F(t)}{m\omega_1}\cos(\omega_1t), \quad (3.24b)$$

$$\left(\frac{d}{dt}+\frac{1}{2\tau_2}\right)Q_1=f\frac{V_0}{D}\frac{1}{4L\omega_2}\{X_1\sin(2\omega_1t)$$
$$+X_2[1-\cos(2\omega_1t)]\}, \quad (3.24c)$$

$$\left(\frac{d}{dt}+\frac{1}{2\tau_2}\right)Q_2=-\frac{V_0}{D}\frac{1}{4L\omega_2}\{X_1[1+\cos(2\omega_1t)]$$
$$+X_2\sin(2\omega_1t)\}. \quad (3.24d)$$

In Eqs. (3.24c) and (3.24d) for simplicity we have omitted the terms in which the voltage $V_p(t)$ is directly driving the electrical resonator. For now, we can assume that these terms are filtered out, and in practice the electrical resonator will be a bridge-type circuit that will cancel these ''direct feedthrough'' terms.

We may understand the essential features of a back-action evasion measurement by simplifying Eq. (3.24) for the case of $f=0$ and examining the nature of the dominant interaction between the two oscillators. Keeping in mind that the complex amplitudes $X_{1,2}$ and $Q_{1,2}$ have resonant frequencies of zero, we can neglect the terms at the frequency $2\omega_1$ since their effect will tend to average to zero for time intervals more than a few periods of the mechanical resonator—we shall show later that this time scale is typical of the signal averaging times that will be employed in practice. The simplified equations are the following:

$$\left(\frac{d}{dt}+\frac{1}{2\tau_1}\right)X_1=-\frac{F(t)}{m\omega_1}\sin(\omega_1t), \quad (3.25a)$$

$$\left(\frac{d}{dt}+\frac{1}{2\tau_1}\right)X_2=\frac{V_0}{D}\frac{1}{4m\omega_1}Q_1+\frac{F(t)}{m\omega_1}\cos(\omega_1t), \quad (3.25b)$$

$$\left(\frac{d}{dt}+\frac{1}{2\tau_2}\right)Q_1=0, \quad (3.25c)$$

$$\left(\frac{d}{dt}+\frac{1}{2\tau_2}\right)Q_2=-\frac{V_0}{D}\frac{1}{4L\omega_2}X_1. \quad (3.25d)$$

The key features of a back-action evasion measurement are immediately apparent from Eqs. (3.25). First of all, note that both complex amplitudes of the mechanical resonator are excited by the external force. For the specific choice of the pump voltage, we observe that the X_1 component of the mechanical system is unaffected by the back action of the electrical resonator; it is excited solely by the signal force and the Langevin force. We also note that the X_1 component of the mechanical resonator drives the Q_2 component of the electrical system, so a measurement of Q_2 will provide information about the X_1 phase of the mechanical resonator. We also see from Eq. (3.25b) that the X_2 phase of the mechanical resonator is driven by the back action of the electrical circuit, but that neither phase of the electrical circuit is driven by X_2. To summarize, the key features of the back-action evasion coupling are that one component of the mechanical oscillator's complex amplitude, X_1 in this case, can be measured without the electrical oscillator acting back and disturbing its evolution.

We now turn our attention to another related parametric transducer property, dynamic damping and frequency pulling. To examine this behavior we drop all of the external driving terms in Eq. (3.24) as well as the $2\omega_1$ and $2\omega_2$ frequency terms. However, we make no assumption as to the value of f. Under this set of assumptions, the equations may be easily solved for each of the complex amplitudes. The solutions all have the same form:

$$\left[\left(\frac{d}{dt}+\frac{1}{2\tau_1}\right)\left(\frac{d}{dt}+\frac{1}{2\tau_2}\right)+\frac{f\beta\omega_1^2}{8}\right]Z=0, \quad (3.26)$$

in which Z may represent $X_{1,2}$ or $Q_{1,2}$ and we have defined the dimensionless electromechanical coupling-strength coefficient β by the following:

$$\beta\equiv\left(\frac{V_0}{D}\right)^2\frac{\omega_2}{\omega_1}\frac{C}{m\omega_1^2}. \quad (3.27)$$

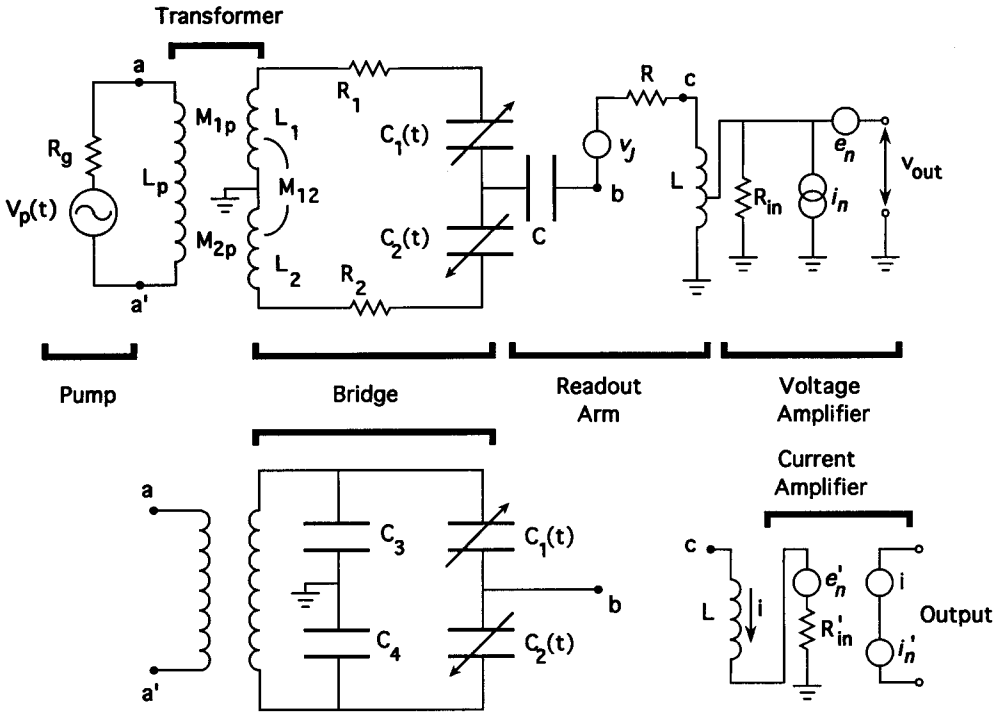

FIG. 4. A practical parametric transducer scheme and variations thereof. At the top is shown the schematic of a practical bridge-circuit parametric transducer. The bridge circuit consists of two capacitors $C_1(t)$ and $C_2(t)$ coupled to a mechanical harmonic oscillator in a push-pull configuration, and two inductors L_1 and L_2. The bridge circuit is excited symmetrically by a "pump" source and the bridge output is coupled through a capacitor C, in a resonant "readout" arm of the bridge to a voltage amplifier, such as a FET (field-effect transistor)—represented by its noise-equivalent circuit. The signal v_{out} is subsequently filtered and examined for the evidence of a signal acting on the mechanical oscillator. In the lower part of the figure are shown substitutions that have been implemented or studied. For example the bridge circuit may be constructed with four capacitors as shown, or the voltage amplifier may be replaced by a current amplifier, such as a SQUID, a noise-equivalent circuit of which is shown.

If we assume that Z has the form $Z=Z_0e^{st}$, where s is a parameter, we can find the characteristic equation associated with Eq. (3.27) and compute the roots. We find the following:

$$s=\frac{1}{2}\left[-\frac{1}{2\tau_1}-\frac{1}{2\tau_2}\pm\left(\frac{1}{2\tau_1}-\frac{1}{2\tau_2}\right)\times\left(1-\frac{f\beta\omega_1^2}{2}\Big/\left(\frac{1}{2\tau_1}-\frac{1}{2\tau_2}\right)^2\right)^{1/2}\right]. \tag{3.28}$$

In the back-action evasion case, $f=0$, the two roots of the characteristic equation are $s=-1/(2\tau_1)$ and $s=-1/(2\tau_2)$, so the electrical and mechanical variables will exhibit decaying solutions with the characteristic decay times of the uncoupled mechanical and electrical resonators. In the case $f=1$, the contents under the radical in Eq. (3.28) will always be less than or equal to unity, so s can never be positive real; therefore no exponentially growing solutions may exist. However, when β is large enough, s becomes complex and the resonant frequencies begin to shift. The threshold value of β at which frequency shifts begin to occur is $\beta\geqslant(1/8\omega_1^2)(1/\tau_1-1/\tau_2)^2$. Below this threshold, the coupling between the mechanical and electrical oscillators only serves to change their characteristic decay times, and above the threshold the resonant frequencies are shifted as well.

For the case $f=-1$ it can be shown that s becomes positive real for $\beta\geqslant(2/\omega_1^2)(1/\tau_1\tau_2)$, and exponentially growing solutions will exist. This corresponds to the threshold for parametric oscillation of the mechanical resonator. Below this value of β, the transducer acts as a mechanical parametric amplifier and the electrical resonator serves to read out the state of the mechanical system, but this scheme offers no sensitivity advantage over the parametric upconvertor mode, $f=+1$, and the BAE mode, $f=0$.

Now that the main features of a back-action evasion measurement of a mechanical resonator have been discussed, we turn our attention to estimating the force sensitivity of a system consisting of a mechanical resonator coupled to a readout electrical resonator. To facilitate this discussion we will use a more realistic model for the transducer, including the main sources of noise in the system. We also introduce the balanced-bridge transducer configuration which, as we will show, has significant practical advantages over the idealized system discussed above.

We refer to Fig. 4, which shows a practical transducer scheme and variations on the basic transducer configuration. In the upper part of the figure we show a schematic representation of the transducer realized as a resonant bridge circuit consisting of two inductors L_1

and L_2, and two capacitors C_1 and C_2. The capacitors are coupled to the mechanical resonator in a push-pull configuration. In Sec. IV of this review a number of practical realizations of the transducer scheme will be described. The bridge also has some unavoidable loss represented by R_1 and R_2, and there is mutual inductive coupling M_{12} between L_1 and L_2. The bridge is inductively coupled through a transformer to a pump represented by a voltage generator $V_p(t)$ with internal resistance R_g. Below we will also show how to include the phase and amplitude fluctuations of the pump voltage $V_p(t)$. The mutual inductances between the transformer primary L_p and the bridge inductors are M_{1p} and M_{2p}. The readout arm of the bridge consists of a capacitor C and inductor L—also with an unavoidable small resistance R in series with L—and associated with the resistor R is a Johnson-voltage noise source v_J. The current through the readout-arm inductor L is sensed by a voltage amplifier connected across a chosen segment of L to properly impedance-match the amplifier input. The voltage amplifier has an assumed input impedance $R_{\rm in}$ (in practice a resistor of a few kilo-ohms is used to stabilize the amplifier circuit) and the amplifier has an assumed input noise, represented by a current source i_n, and a purely additive noise represented as a voltage noise e_n. This is a conventional representation of a field-effect transistor amplifier. One should also allow that the two sources of noise in the amplifier may exhibit some degree of mutual correlation. It is straightforward to include these effects through the introduction of a complex correlation impedance; however, to maintain simplicity we will not explicitly do so in the following analysis.

Variations on this transducer configuration are shown in the lower part of Fig. 4. For example, the bridge circuit may be constructed of all capacitors with a parallel transformer used to couple the pump signal into the bridge. The other major variation may be in the amplifier. We have shown an alternative current amplifier, which would be placed in series with the readout-arm inductor L. In this case the input noise is represented by a voltage source e_n' and the additive noise is shown as a current source i_n'. This current-amplifier model is a convenient representation of a SQUID amplifier.

The fluctuations of the pump do not appear as an explicit noise source in Fig. 4, but the fluctuations of the pump combined with any bridge imbalance effectively create a new noise source that appears in series with the Johnson noise source coming from the loss in the readout arm of the bridge. The magnitude of this effective pump-noise source is proportional to the product of the fractional imbalance factor of the bridge circuit and the spectral density of the pump source. Thus it is important that the bridge circuit be well balanced to minimize the effect of the pump noise and, in fact, it turns out that balancing and phase noise are major factors limiting the sensitivity of parametric transducers. Alternative pump feed through reduction schemes that serve to effectively balance the transducer by external cancellation of the pump have also been employed in systems that we describe in Sec. IV.

We generalize our expression for the pump voltage $V_p(t)$ to include the fluctuations of both the amplitude and the phase of the pump components:

$$V_p(t)=\frac{V_0}{2}\left\{\begin{array}{l}(1-f)(1+a_1)\cos[(\omega_2+\omega_1)t+\phi_1]\\+(1+f)(1+a_2)\cos[(\omega_2-\omega_1)t+\phi_2]\end{array}\right\}. \tag{3.29}$$

We use the dimensionless random variables a_1 and a_2 to represent the small random component of the pump amplitudes and we use ϕ_1 and ϕ_2 to represent the phase fluctuations. It is assumed that these random variables represent mutually uncorrelated Gaussian random processes. Returning to Eq. (3.22), we substitute the expression (3.29) for the noisy pump to find the following equations of motion for the electrical variables:

$$\begin{aligned}\left(\frac{d}{dt}+\frac{1}{2\tau_2}\right)Q_1=&\frac{V_0}{4D}\frac{1}{L\omega_2}\left\{fX_2-\frac{X_1}{2}[f(\phi_2-\phi_1)\right.\\&+(\phi_2+\phi_1)]+\frac{X_2}{2}[f(a_2+a_1)\\&\left.+(a_2-a_1)]\right\},\\\left(\frac{d}{dt}+\frac{1}{2\tau_2}\right)Q_2=&\frac{V_0}{4D}\frac{1}{L\omega_2}\left\{-X_1-\frac{X_1}{2}[f(a_2-a_1)\right.\\&+(a_2+a_1)]+\frac{X_2}{2}[f(\phi_2+\phi_1)\\&\left.+(\phi_2-\phi_1)]\right\}.\end{aligned} \tag{3.30}$$

The imbalance of the bridge readout circuit may be represented by a static, or slowly time-dependent displacement x_0 of the mechanical oscillator. To find an expression for the spectral density of the pump-noise contribution, the bridge circuit imbalance is expressed in terms of the complex amplitudes, chosen as $X_1=x_0\cos\omega_1 t$, $X_2=x_0\sin\omega_1 t$, substituted into Eqs. (3.30), and the squared modulus of the Fourier transforms of those equations is computed. Confining attention to the equation for Q_2, one finds the following expression for the pump-noise term that appears on the right-hand side of that equation of motion:

$$\begin{aligned}S_{\rm pump}(\omega)=&\left(\frac{V_0}{4D}\right)^2\left(\frac{1}{L\omega_2}\right)^2\frac{x_0^2}{8}\\&\times\left[\begin{array}{l}(1+f)^2S_{a_2}(\omega+\omega_1)+(1-f)^2S_{a_1}(\omega+\omega_1)\\+(1+f)^2S_{\phi_2}(\omega+\omega_1)+(1-f)^2S_{\phi_1}(\omega+\omega_1)\end{array}\right],\end{aligned} \tag{3.31}$$

in which $S_\phi(\omega)$ and $S_a(\omega)$ represent respectively the double-sided spectral densities of the phase and amplitude fluctuations associated with the pump at a frequency offset of ω from the pump carrier frequency. Upon examination of Eq. (3.31), we note that in order to

drive the Q_2 variable on resonance, i.e., at ω=0, the pump phase and amplitude fluctuations at a frequency that is offset from the carrier by ω_1 come into play. This has a simple interpretation in the frequency domain. An examination of the spectrum of the pump source would show sharp peaks at $\omega_2 \pm \omega_1$, depending on the chosen value of f, and the phase and amplitude fluctuations would appear as low-amplitude wings centered about these sharp peaks. The pump phase and amplitude fluctuations offset from the carriers by $\pm\omega_1$ will drive the bridge circuit on resonance, i.e. at the frequency ω_2.

Our attention is now turned to computing the response of the coupled electromechanical system including all the noise sources. The electrical variables are the experimentally accessible quantities, so the set of equations will be solved for one of these quantities. Referring back to Eqs. (3.25), it is noted that, for f=0 and the choice of pump phases made in Eq. (3.29), only the Q_2 phase of the electrical mode will contain information about the state of the mechanical oscillator. Q_2 is also a directly measurable quantity and in practice may be measured by monitoring the time-dependent voltage on the center capacitor plate of the three-plate capacitor in the bridge circuit and extracting the Q_2 information by demodulating using a reference frequency of ω_2. Thus Q_2 will be considered to be the output observable and the system equations will be solved to compute the spectral density of Q_2.

The solution of Eqs. (3.25) is carried out in the frequency domain so that the noise sources can be explicitly specified in terms of their spectral densities. Solving the equations for Q_2 by substitution, we arrive at

$$Q_2(\omega)=\frac{V_0}{8D}\frac{j}{m\omega_1 L\omega_2}\frac{1}{J(\omega)}[F(\omega+\omega_1)-F(\omega-\omega_1) +f_L(\omega+\omega_1)-f_L(\omega-\omega_1)]+\frac{1}{2L\omega_2}\frac{G_1(\omega)}{J(\omega)} \times[\nu(\omega+\omega_2)-\nu(\omega-\omega_2)], \tag{3.32}$$

in which $J(\omega)\equiv G_1(\omega)G_2(\omega)+(\omega_1^2\beta/8)$ and $G_{1,2}(\omega) \equiv j\omega+1/(2\tau_{1,2})$. As before, F is the signal force acting on the mechanical resonator, and f_L is introduced to represent the Langevin force that acts on the mechanical resonator and is responsible for its Brownian motion. Finally, ν is used to represent the sum of all the voltages driving the electrical resonator. At this point it is appropriate to elucidate the choice of representation for the noisy amplifier. Referring back to Fig. 4, for the current-amplifier model the input noise of the amplifier is represented by a voltage-noise generator e_n, which adds to the Johnson noise and effective pump-noise voltage sources. In this case ν may be written as the sum of three terms—$\upsilon=\nu_J+\nu_{\text{pump noise}}+e_n$. Given the voltage-amplifier representation for the actual amplifier in use, it would be straightforward to transform the voltage-amplifier representation to the Thévenin equivalent current-amplifier representation. If, as shown in Fig. 4, the noisy voltage amplifier has an input noise current of i_n' and an additive voltage noise of e_n', it can be transformed into an equivalent current amplifier with an effective input noise of $e_n=\omega L i_n'$ and an effective additive noise of $i_n=e_n'/(\omega L)$, where ω is the frequency; note that the model transformation is frequency dependent but in general the operating frequency is confined to a narrow band and may be regarded as constant. These expressions are based on the assumption that the voltage amplifier is connected across all the turns of the inductor L, while one could connect the amplifier input across only part of the inductor turns, which would modify the apparent magnitudes of the two noise generators to allow one to reach the optimum noise impedance. Of course the noise temperature of the amplifier, which is proportional to the product of the current and voltage noise terms, is maintained. This is a practical technique for impedance matching an amplifier to a source to obtain optimum system signal-to-noise performance.

Returning to the expression for Q_2, Eq. (3.32), we note that the purely additive contribution of the amplifier current-noise source at the output of the amplifier may be added. The expression for Q_2 is multiplied by the complex conjugate Q_2^* to obtain the following expression for the spectral density of Q_2:

$$S_{Q_2}(\omega)=\frac{V_0^2}{64D^2}\frac{1}{m^2\omega_1^2L^2\omega_2^2}\frac{2S_{f_L}(\omega_1)}{|J(\omega)|^2} +\frac{1}{4L^2\omega_2^2}\left|\frac{G_1(\omega)}{J(\omega)}\right|^2 2S_\nu(\omega_2)+\frac{2S_{i_n}(\omega_2)}{\omega_2^2}, \tag{3.33}$$

where the double-sided spectral densities of the Langevin force, the voltage noise, and the current noise are represented respectively by S_{f_L}, $S_{e_n'}$, and $S_{i_n'}$. To simplify the analytic result, it was assumed that there were no correlations among the various noise sources. However, transistors operated at radio frequencies often display a significant degree of mutual correlation between the amplifier's input and additive noise sources. This introduces an analytical complication and is more easily accounted for in numerical calculations, so for the remainder of the present analysis the amplifier noise correlations will be ignored. The double-sided spectral density of the Langevin force is given by $S_{f_L}\equiv 4k_BTm/\tau_1$, and the voltage noise is composed of the contribution of the amplifier plus the Johnson noise associated with the losses in the electrical circuit, with spectral density $S_{\nu_J}=4k_BTL/\tau_2$.

It is convenient to introduce two dimensionless quantities, α and γ:

$$\alpha\equiv\frac{T}{T_E}\frac{\omega_2}{\omega_1}\frac{1}{\omega_1\tau_1},$$

$$\text{in which } T_E\equiv\sqrt{S_{i_n'}(\omega_2)S_{\nu_n}(\omega_2)}/k_B, \tag{3.34}$$

and

$$\gamma \equiv \omega_2 C \frac{\omega_2}{\omega_1} \sqrt{S_{v_n}(\omega_2)/S_{i_n}(\omega_2)}$$

for the current-amplifier model,

$$\gamma \equiv \frac{1}{4\omega_2 C} \frac{\omega_2}{\omega_1} \sqrt{S_{i_n}(\omega_2)/S_{e'_n}(\omega_2)}$$

for the voltage-amplifier model. (3.35)

The noise spectral density may be expressed in terms of the normalized frequency $y \equiv \omega/\omega_1$ and the above-defined dimensionless parameters as follows:

$$S_{Q_2}(y) = \frac{S_{i'_n}(\omega_2)}{{\omega_2}^2} \left\{ 1 + \frac{\alpha\beta\gamma}{8} \frac{1}{|J(y)|^2} + \gamma^2 \left| \frac{G_1(y)}{J(y)} \right|^2 \right\}. \tag{3.36}$$

To find the optimum filter and the maximum signal-to-noise ratio, the response of Q_2 to the signal, which is assumed to be an impulse arriving at the time $t=0$, $F_s(t) = p_0 \delta(t)$ must be computed. This calculation follows the lines of the preceding noise calculation so the details will not be repeated. Combining the signal and noise responses with the noise in the expression for the maximum signal-to-noise ratio, Eq. (3.10), yields the expression

$$\left(\frac{S}{N}\right)^2_{\max} = \frac{p_0^2}{2m} \frac{\omega_2}{\omega_1} \frac{1}{k_B T_E} \left\{ \frac{\beta\gamma}{8\pi} \int_{-\infty}^{+\infty} \left(|J(y)|^2 + \frac{\alpha\beta\gamma}{8} + \gamma^2 |G_1(y)|^2 \right)^{-1} dy \right\}, \tag{3.37}$$

which can be integrated to determine the maximum signal-to-noise ratio for an impulsive signal of amplitude p_0. The *noise-equivalent impulsive signal* is the one that gives a signal-to-noise ratio of unity, and the mechanical oscillator impulse noise number N [Eq. (3.14)] is given by

$$N = \frac{k_B T_E}{\hbar \omega_2} \frac{1}{r} = N_E \frac{1}{r}. \tag{3.38}$$

In Eq. (3.38) it is convenient to represent the total electronic noise by an electronic noise number N_E, and the factor r is used to represent the expression in curly brackets in Eq. (3.37). It remains to evaluate the factor r as a function of α, β, γ, and f. Carrying out the integration yields the following result:

$$\frac{1}{r} = \left[\left(f^2 + \frac{8\alpha\gamma}{\beta} \right) \left\{ 1 + \frac{\beta}{4\gamma^2} \left[\left(f^2 + \frac{8\alpha\gamma}{\beta} \right)^{1/2} - f \right] \right\} \right]^{1/2}. \tag{3.39}$$

In Fig. 5 appear contour plots of constant values of $1/r$ in the $\beta\gamma$ plane for fixed values of α in the two cases of most practical interest: $f=1$, the conventional upconvertor, and $f=0$, the back-action evasion mode. For the $f=1$ case, the value of $1/r$ cannot be less than unity; this is referred to as the amplifier limit for a conventional measurement. In the back-action evasion operating mode $1/r$ may be considerably less than unity, and the smaller the value of α, the larger r may be. Thus the back-action evasion technique yields the greatest reduction in the system noise for small values of α, i.e., when the Brownian noise is small compared to the electronic noise in the mechanical oscillator/electrical oscillator system.

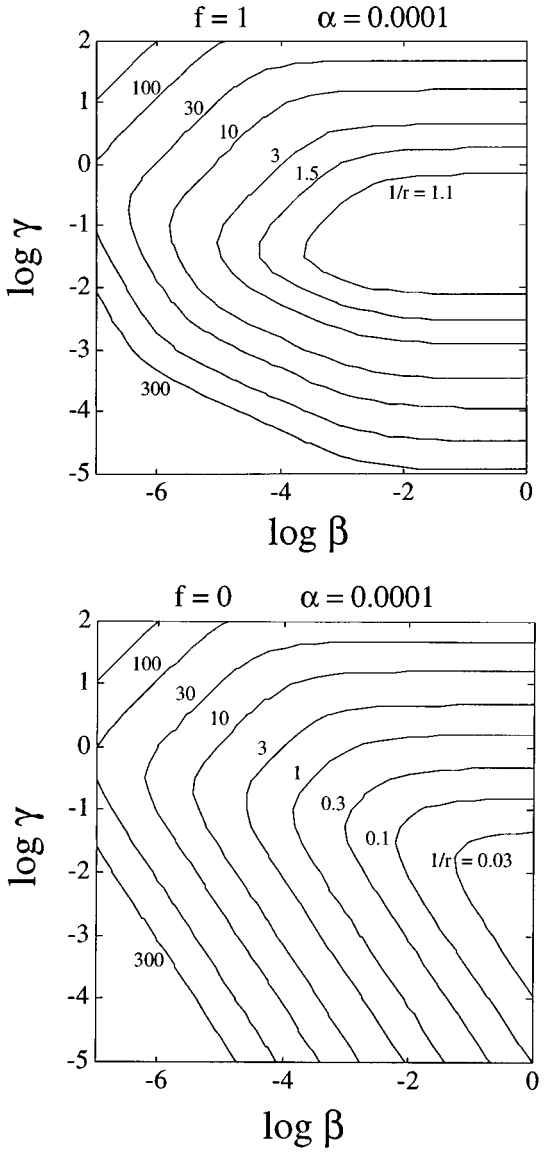

FIG. 5. Contour plots of the BAE noise-reduction factor $1/r$, for different values of the parameters α, β, and γ (defined in the text): (a) the parametric upconvertor, labeled by $f=1$; (b) and the BAE measurement scheme, $f=0$. The parameter β is a measure of the strength of the electromechanical coupling of the readout circuit to the mechanical oscillator and γ is a measure of the impedance ratio of the readout circuit and the amplifier. The quantity α characterizes the ratio of the thermal Brownian motion to the total electrical noise—$\alpha=0$ in the case of the physical temperature going to zero. One observes in Fig. 5(a) that the parametric upconvertor is incapable of exceeding the sensitivity limit enforced by the noisy amplifier, i.e., $1/r \geq 1$; however, as shown in Fig. 5(b) in the BAE case ($f=0$), the amplifier limit may be exceeded by significant factors (Bocko and Johnson, 1982).

In the preceding analysis a simplified set of dynamical equations—Eqs. (3.25)—was solved to find the signal

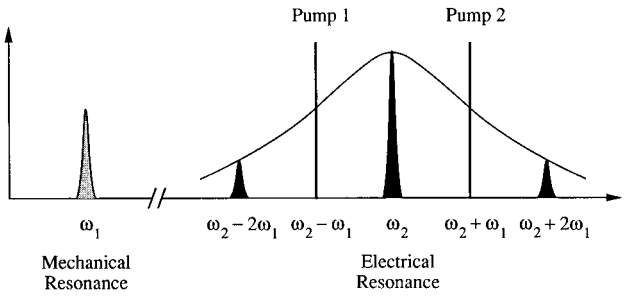

FIG. 6. A frequency-spectrum representation of a back-action evasion measurement. A narrow-band mechanical signal, near ω_1, from the mechanical oscillator is simultaneously upconverted by pump 1 and pump 2 to the peak of the electrical-oscillator resonance at ω_2. Simultaneously, noise in the electrical oscillator, in the vicinity of ω_2, arising from the amplifier input is downconverted by the pumps to produce a back-acting force on the mechanical oscillator. The electrical noise near ω_2 is downconverted to a phase-sensitive force by the simultaneous action of the two pumps. However, electrical noise near $\omega_2 \pm 2\omega_1$ is downconverted by the individual pumps and thus produces a phase-insensitive back-action force.

and noise content of the parametric transducer output. The complete equations governing the behavior of the system—Eqs. (3.24)—contain "sideband" terms that oscillate at a frequency $2\omega_1$ and which drive the mechanical and electrical resonators at frequencies off resonance. The consequences of the $2\omega_1$ sidebands is examined in the following discussion.

The details of the tedious calculations to determine the influence of the additional sideband components at $2\omega_1$ will not be reproduced here, but the result may be summarized rather simply. The $2\omega_1$ terms introduce a small fluctuating back action of the electrical readout system on the mechanical resonator and the effect of this may be represented as additional Brownian noise in the mechanical resonator by modifying the parameter α as follows:

$$\alpha \rightarrow \alpha + \frac{3\beta\gamma}{64}. \tag{3.40}$$

The physical interpretation of this is straightforward and we refer to Fig. 6 to facilitate the interpretation (Bocko *et al.*, 1986). In Fig. 6 we show the frequency spectrum of the electromechanical system operating in the back-action evasion mode. The function of the transducer is to convert energy between the mechanical and electrical resonators, so an excitation of the mechanical oscillator at the frequency ω_1 is upconverted to an electrical signal at the frequencies ω_2 and $\omega_2 - 2\omega_1$ by pump 1; pump 2 upconverts the mechanical signal to the electrical frequencies ω_2 and $\omega_2 + 2\omega_1$. The upconverted signal at $\omega_2 \pm 2\omega_1$ can be easily filtered out if desired, so it presents no practical problem. The problem arises from the downconversion of energy in the electrical resonator to produce a force acting on the mechanical resonator. The electrical resonance is typically broad enough so that there will be a non-negligible response of the electrical resonator to electrical noise at the frequencies $\omega_2 \pm 2\omega_1$. These noise sidebands are downconverted to a mechanical force at the frequency ω_1, which coincides with the mechanical resonance. This downconverted electrical noise can conveniently be represented as additional Brownian motion. The following intuitive description of the excess back-action noise represented in Eq. (3.40) is helpful. The excess noise is proportional to the electromechanical coupling strength β, so that if the electromechanical coupling is reduced to zero, the excess noise vanishes as well. The excess noise is also jointly proportional to the factor γ which is large when the back-acting input noise of the amplifier is large compared to the additive noise. The numerical factor 3/64 emerges from the analysis after making the assumption that $\omega_1 \tau_2 \gg 1$.

C. Back-action evasion and parametric processes

In the preceding section a detailed signal-to-noise analysis of a parametric transducer operated in the back-action evasion measurement mode was presented. In this section the more general qualitative features of the back-action evasion measurement are examined, and the relationship to previously well-understood parametric processes is explored.

The back-action evasion measurement scheme is the linear superposition of two parametric interactions already familiar in the theory of parametric amplifiers (Louisell *et al.*, 1961; Decroly *et al.*, 1973). In a general parametrically coupled system, two subsystems are interacting through a time-varying parameter containing degrees of freedom of both the subsystems. The modulation of this coupling parameter gives rise to so-called parametric coupling of modes of the two subsystems. The transfer of energy from one subsystem to the other is controlled by the choice of the frequency, amplitude, and phase of the modulation. A common mechanical example of a parametrically coupled system is a playground swing. The operator sitting on the swing modulates the effective length of the swing by lowering and raising their center of gravity. The most satisfying operating mode of a swing is to parametrically pump the system at twice its resonant frequency with the pump phase chosen so that the swing's effective length is increased at the lowest point of the swing's motion and raised at the instants of the swing's maximum angular displacement. Pumping the swing in this manner transfers energy from the user to the swing leading to the familiar enjoyable sustained oscillations.

The principles of parametric coupling are applied to electromechanical force-detection systems composed of a mechanical resonator and an electrical resonator by parametrically coupling the two subsystems via a capacitor to which is applied a time-dependent electric field. The characteristic frequencies in the parametric system are the mechanical and the electrical oscillation frequencies and the pump frequency of the electric field in the capacitor. Thus a three-frequency parametric transducer can be operated in two different regimes, the modulation occurring either at the sum of the electrical and mechanical frequencies (phase-conjugating upconver-

tor) or at the difference of the electrical and mechanical frequencies (phase-preserving upconvertor). The main differences between these two parametric interactions can be illustrated in a quantum description, in which the process can be described as the destruction or creation of phonons and photons at the various subsystem frequencies. In the phase-preserving upconvertor, a photon of the pump and a phonon of the harmonic oscillator mutually annihilate to create a photon at the electrical mode frequency. In the phase-conjugating upconvertor case, a phonon at the mechanical frequency and a photon at the pump frequency combine to create a photon at the electrical frequency and an additional phonon in the mechanical oscillator. This case is also a mechanical parametric amplifier with the electrical mode serving as a readout, containing information about the state of the mechanical mode.

In the above description, the terms phase-preserving and phase-conjugating were used to describe the two single-pump parametric processes. The significance of these designations can be understood by the following simple mathematical demonstration. Assuming that there is a signal represented by $\cos[\omega_s t+\phi(t)]$, where $\phi(t)$ is a time-dependent phase factor, and a pump, $\cos(\omega_p t)$, one can multiply these two terms together to find

$$\cos(\omega_p t)\cos[\omega_s t+\phi(t)]=\tfrac{1}{2}\{\cos[(\omega_p+\omega_s)t+\phi(t)] +\cos[(\omega_p-\omega_s)t-\phi(t)]\}. \tag{3.41}$$

Equation (3.41) shows that the upconverted signal at the sum of the pump and signal frequencies follows the time-dependent phase of the signal, but the upconverted signal at the difference of the two frequencies is a phase-reversed version of the signal. Therefore the designations phase-preserving and phase-conjugating are attached to the two processes.

The back-action evasion measurement is the coherent superposition of the phase-preserving and phase-conjugating three-frequency parametric interactions; therefore BAE is a four-frequency parametric process. One may gain insight into the essential feature of a BAE measurement by considering the reverse transfer characteristics of the BAE parametric converter, i.e., the conversion of photons at the electrical readout frequency to phonons at the mechanical frequency. Let us assume the electrical fluctuations in the readout circuit exhibit a Lorentzian spectrum centered at the frequency ω_2 with a bandwidth determined by the quality factor of the electrical resonator. The electrical noise that lies in a band extending from $\omega_2-\omega_1$ to $\omega_2+\omega_1$ is simultaneously downconverted by the two pumps to produce a force acting on the mechanical resonator. The parametric process associated with the pump at $\omega_2-\omega_1$ preserves the phase of the electrical fluctuations upon downconversion to a mechanical force and the fluctuating force from the other pump at $\omega_2+\omega_1$ is phase reversed. The coherent superposition of the two processes leads to a cancellation of the fluctuating back-action force on one phase of the mechanical oscillator and the enhancement of the back-acting force noise on the other phase of the mechanical oscillator. Electrical noise lying outside the electrical frequency band extending from $\omega_2-\omega_1$ to $\omega_2+\omega_1$ does not cancel mutually upon downconversion and so leads to a fluctuating force on both of the mechanical oscillator phases. The magnitude of the overall back-action noise reduction depends upon the relative magnitude of the electrical noise near $\omega_2\pm 2\omega_1$ compared to the electrical noise at ω_2. Therefore, a large quality factor for the electrical mode is a key feature in a back-action evasion measurement system and most of the back-action force noise will be canceled in one phase of the mechanical system if $\omega_1\tau_2$ is much greater than unity. In the following section on multipump and stroboscopic measurements, we describe a scheme to recover a high degree of back-action noise cancellation even when this condition is not met.

In conclusion, in the above discussion it was shown that the BAE technique is a close relative of conventional, well-known parametric processes and it's tempting to conjecture that the back-action evasion measurement technique could have been discovered eventually without any reference to quantum nondemolition measurements. Moreover, the description of the BAE measurement technique in the familiar language of parametric interactions may enable us to find broader applications, in other types of parametric detectors, beyond its use in the detection of small mechanical displacements.

D. Multipump and quasistroboscopic schemes

In the previous section we indicated that when the width of the Lorentzian peak of the electrical resonator response is comparable to or larger than the mechanical frequency, the two-pump back-action evasion measurement offers limited back-action noise reduction. One pair of pumps at $\omega_2\pm\omega_1$ can cancel the back-action noise arising from a band of frequencies of width $2\omega_1$ centered on the electrical resonance at ω_2, but downconverted electrical noise outside of this band does not mutually cancel. However, by adding additional pumps at specific frequencies we could arrange for the cancellation of back-action noise originating from a broader band of frequencies in the electrical system noise spectrum. For example, if another pair of pump components were introduced at the frequencies $\omega_2\pm 3\omega_1$, it would result in the back-action cancellation of all the downconverted electrical noise in a band of width $6\omega_1$ centered on the electrical resonance. If there remained significant electrical noise outside of this band, i.e., if the electrical Q were that low, one could add additional pairs of pumps at $\omega_2\pm(2n+1)\omega_1$ until the majority of the back-action noise was canceled. In the limit of a very large number of pump frequencies this technique becomes the stroboscopic measurement technique discussed by Braginsky, Vorontsov, and Thorne (1980).

Stroboscopic QND measurements of the position of a harmonic oscillator have been discussed in detail (Bra-

ginsky and Nazarenko, 1969; Braginsky, Vorontsov, and Khalili, 1978; Thorne *et al.*, 1978). In this scheme, as described in Sec. II, "quick" measurements of the position of the mechanical oscillator are performed at equally spaced time intervals twice per mechanical oscillation cycle. In this context quick means that the instrument that measures the mechanical oscillator position interacts with it for a time interval that is short compared to the period of oscillation. During the time interval between two consecutive measurements, the Schrödinger wave function of the mechanical oscillator spreads out and then contracts to its initial dispersion. The key feature of a stroboscopic measurement is that repeated quick measurements are performed at the time instants when the position dispersion is minimum. An observed deviation from the expected position at those time instants would signal that a force had acted on the mechanical oscillator since the previous measurement.

A more quantitative noise performance estimate for the multipump measurement scheme may be carried out by calculating the ratio of the variances for the two quadrature phases of the electrical output observable, under the assumption that the mechanical oscillator is sensitive to the downconverted electrical noise only near resonance, i.e., in a band of frequencies centered around ω_1 within a bandwidth $\Delta\omega_1=\omega_1/2Q_1$, and that $\Delta\omega_1 \ll \Delta\omega_2$ (Onofrio and Bordoni, 1991). In the quiet mechanical phase the electrical noise contribution to the back-action force will be due only to the electrical noise in a band of frequencies ($\Delta\omega_1$) centered around $\omega_2 \pm 2n\omega_1$, where n is the number of pump pairs. All the pumps at the frequencies between $\omega_2 \pm (2n-1)\omega_1$ yield the phase-sensitive cancellation of the remaining back-acting noise. The quiet mechanical phase will only feel the fluctuating back action from electronic noise lying outside the frequency band spanned by the pumps; this residual back-action noise may be quite small when the frequency range spanned by the pumps is broad compared to the width of the electrical resonance. The calculation of the effective back-action noise squeezing factor is presented in the following simplified model of a generalized multipump BAE measurement apparatus.

To analyze a generalized BAE measurement, we return to the model developed in Sec. III.B and assume a more general form of the parametric pump source. Recall that in the earlier analysis we assumed a pump that contained one or both of the frequency components at the sum or difference of the electrical and mechanical resonator frequencies, $E(t)=E_0\cos[(\omega_2 \pm \omega_1)t]$. For the generalized BAE measurement, we assume a general form of the pump:

$$E(t)=\sum_{n=1}^{N} \frac{E_0}{2N}\{\cos[\omega_2 t+(2n-1)\omega_1 t] + \cos[\omega_2 t-(2n-1)\omega_1 t]\}, \tag{3.42}$$

where $2N$ is the total number of pump frequency components. If $N=1$ then we recover the simple BAE case discussed above,

$$E(t)=\frac{E_0}{2}[\cos(\omega_2+\omega_1)t+\cos(\omega_2-\omega_1)t]. \tag{3.43}$$

Under the simplifying assumption that ω_2 is an integer multiple of ω_1, in the limit of an infinite number of pump components, $N\to\infty$, the electric field becomes a series of impulses at regularly spaced intervals:

$$E(t)=\sum_{n=0}^{\infty} E_0(-1)^n \delta\left(t-\frac{n\pi}{\omega_1}\right). \tag{3.44}$$

For the pump field in Eq. (3.44) the interaction Hamiltonian of the coupled mechanical oscillator electrical oscillator system becomes

$$\hat{H}_I=E_0\sum_{n=0}^{\infty} \delta\left(t-\frac{n\pi}{\omega_1}\right)\hat{X}_1\hat{Q}, \tag{3.45}$$

which shows that at certain instants of time, i.e., when $t=n\pi/\omega_1$, the interaction between the two oscillators is proportional to the mechanical oscillator complex amplitude component X_1 and zero at other times. This means that when $t=n\pi/\omega_1$ X_1 will be measured.

The multipump field of Eq. (3.42) has a Fourier spectrum with an infinite number of frequency components, which in the time domain is a series of pulses of infinitesimal duration. In practice, the pulses will have a finite duration τ, in which case the amplitudes of the pump's Fourier components are given by the formula

$$E_{2n+1}=E_0\tau\frac{\omega_1}{\pi}\frac{\sin[(2n+1)\omega_1\tau/2]}{(2n+1)\omega_1\tau/2}, \tag{3.46}$$

where n denotes the nth harmonic of the mechanical resonant frequency. If $\tau\to 0$, with $E_0\tau$ held constant, the pump consists of an infinite number of equal-height components at the frequencies $\omega_1, 3\omega_1, 5\omega_1, \ldots, (2n+1)\omega_1$.

It is more realistic to consider a quasistroboscopic measurement, i.e., one having finite values for both the electric field and the measurement duration τ, with the practical constraint that the frequency components of the pump within the electrical circuit bandwidth have the same amplitude. Thus to complete our analysis we write the equations of motion in terms of the complex amplitudes, using the definitions above and the expressions for $E(t)$ for $2N$ pumps:

$$\left[\frac{d}{dt}+\frac{1}{2\tau_1}\right]X_1=\frac{E_0}{4Nm\omega_1}Q_1\sin(2N\omega_1 t)-\frac{F(t)}{m\omega_1}\sin(\omega_1 t), \tag{3.47}$$

$$\left[\frac{d}{dt}+\frac{1}{2\tau_1}\right]X_2=\frac{-E_0}{4Nm\omega_1}Q_1\left[\cos(2N\omega_1 t)+1+2\sum_{n=1}^{N-1}\cos(n\omega_1 t)\right]+\frac{F(t)}{m\omega_1}\cos(\omega_1 t), \tag{3.48}$$

$$\left[\frac{d}{dt}+\frac{1}{2\tau_2}\right]Q_1=-\frac{\nu_n}{L\omega_2}\sin(\omega_2 t), \tag{3.49}$$

$$\left[\frac{d}{dt}+\frac{1}{2\tau_2}\right]Q_2=\frac{-E_0}{4NL\omega_2}\left\{X_1\left[\cos(2N\omega_1 t)+1+2\sum_{n=1}^{N-1}\cos(n\omega_1 t)\right]+X_2\sin(2N\omega_1 t)\right\}+\frac{\nu_n}{L\omega_2}\cos(\omega_2 t). \tag{3.50}$$

The terms that oscillate at ω_2 were dropped because they average to zero over the time scales of interest. The above set of equations will serve as the basis of our further analysis. Equations (3.47)–(3.50) may be solved to determine the response of the mechanical resonator to the fluctuating back-action force from the electrical resonator. The externally applied force is assumed to be zero and it is assumed that the electrical resonator is excited by phase-insensitive random noise. The spectral densities of X_1 and X_2 are calculated from the Fourier transformed equations, and for the case of $2N$ pumps, the ratio of the spectral densities of X_1 and X_2 is (Marchese, Bocko, and Onofrio, 1992):

$$\frac{S_{X_2}}{S_{X_1}}=3+4\sum_{n=1}^{N-1}\frac{1+16N^2(\omega_1\tau_2)^2}{1+16n^2(\omega_1\tau_2)^2}+32N^2(\omega_1\tau_2)^2. \tag{3.51}$$

Equation (3.51) applies in the case when the Langevin force responsible for the Brownian motion of the mechanical resonator is negligible compared to the back-action force. In this case, the reduction of the burst noise number N, for a mechanical oscillator monitored by the multipump technique, is directly related to the back-action evasion noise reduction factor r:

$$N=N_E\frac{1}{r},\quad \text{where}\quad r\cong\left(\frac{S_{X_2}}{S_{X_1}}\right)^{1/2}. \tag{3.52}$$

This relationship between r, the BAE reduction factor, and the squeezing factor is only approximate because our earlier calculation of r, Eq. (3.39), also accounted for the Brownian motion of the mechanical oscillator and the match between the amplifier noise impedance and the readout-circuit impedance.

The multipump BAE scheme also has an analog in quantum optics, where both four-wave mixing (Schumaker, 1985, 1986; Schumaker *et al.*, 1987) and pulsed light (Slusher *et al.*, 1987; Yurke *et al.*, 1987) have been used to successfully demonstrate squeezing.

E. Other models of back-action evasion measurements

An alternative noise and sensitivity analysis for a system of two parametrically coupled harmonic oscillators has been described by Fuligni (1982). The equations of motion for the two coupled oscillators are solved in the time domain using Mathieu function theory, and from that one can calculate the minimum detectable energy in a measurement time Δt. When the sampling time is optimized to give the maximum value of r, one obtains for the parametric upconvertor pumping $f=1$:

$$r=\left(1+\frac{\alpha}{\beta}\frac{\omega_2}{\omega_1}\frac{1}{Q_1}\right)^{-1/2}, \tag{3.53}$$

and when the BAE pump is used, r becomes

$$r=\left[\frac{1}{8}\left(\frac{\omega_2}{\omega_1}\right)^2\frac{1}{Q_2^2}+8\frac{\alpha}{\beta}\frac{\omega_2}{\omega_1}\frac{1}{Q_2}\right]^{-1/2}. \tag{3.54}$$

In Fuligni's calculations, the matching between the electrical oscillator impedance and the amplifier noise impedance was not considered, and the solutions are meaningful only in the small-coupling limit, in which $\beta\ll 1$, though they display the correct trend and provide simple expressions for estimating the sensitivity of a parametric electromechanical system. Even with these provisos we see that, in the limit of negligible Brownian noise ($\alpha\to 0$), r approaches the limiting value of unity for the single-mode pumping and may exceed this for the BAE mode pumping. In the limit $\alpha\to 0$, Eq. (3.54) reduces to $r=\omega_1\tau_2/2\sqrt{2}$, which agrees qualitatively with the earlier results.

Cinquegrana *et al.* (1993) presented an independent analysis of a BAE measurement scheme that they later generalized to a two-mode mechanical system (Cinquegrana *et al.*, 1994). The model applies specifically to a capacitive bridge readout, and separate equations are written for the noise and signal terms. The assumptions made in the calculations are that an ideal filter is used to completely reject the terms near twice the electrical frequency, a reasonable assumption in practice, and that there is no correlation among the noise sources. They defined an equivalent temperature that is a measure of the energy distribution of the harmonic oscillator, and showed that it is equal to the oscillator's thermodynamic temperature provided that perfect bridge-circuit balance is achieved, giving complete cancellation of the amplitude and phase fluctuations of the pump at the readout-circuit output. They also parametrize the sensitivity to impulsive forces in terms of the burst noise temperature, defined in Eq. (3.14), and the mechanical oscillator noise number, expressed in Eq. (3.38), in terms of a noise-reduction merit factor r that, for the optimal arrival time of the signal, is found to be

$$r=\frac{1}{64\pi}\beta\frac{\omega_1^2 I}{C}, \tag{3.55}$$

where I is a function of the noise impedance of the amplifier, the mechanical and electrical quality factors, the pump amplitude and phase noise, and the remaining electrical parameters of the readout circuit. The authors compared the predictions of their model to the performance of their parametric transducer, which will be de-

scribed in Sec. IV, obtaining agreement over the experimentally accessible range of parameters. Furthermore, they compared their BAE transducer to a commonly used constant-voltage biased capacitive transducer and showed that the BAE pumping scheme is not subject to the electromechanical loading of the mechanical oscillator, which complicates the use of the dc capacitive scheme. They also demonstrated that the noise in the BAE transducer-output quadrature containing the signal was solely due to the Brownian motion of the mechanical oscillator.

The models discussed in this section, although very different in detail, all confirm that the two-pump parametric process corresponding to a continuous quantum nondemolition measurement of one phase of a harmonic oscillator's complex amplitude also allows one to evade the classical amplifier noise limit. We identified the key parameter that determines the back-action evasion capability of any parametric transducer: the product of the mechanical angular frequency and the relaxation time of the electrically resonant transducer idler mode, $\omega_1\tau_2$. This parameter determines the ability of the transducer to filter out electrical noise that would otherwise be converted to a mechanical back-action noise force on the "quite" mechanical oscillator phase. Only under the condition $\omega_1\tau_2 \gg 1$, and provided that the pump fluctuations and the mechanical oscillator Brownian noise do not dominate, will the back-action evasion scheme yield a sensitivity gain with respect to conventional parametric transduction schemes. Although it is intuitively obvious that practical back-action evasion schemes will require small mechanical and electrical dissipation, low pump amplitude and phase noise, and large electromechanical coupling factors, the models described in this section give quantitative predictions for the parameters required to achieve back-action evasion and will guide the experiments to the quantum regime.

IV. EXPERIMENTAL RESULTS

The quantum-noise regime of a mechanical oscillator has not been reached yet in laboratory experiments. However, the dynamics of the interaction between the measuring apparatus and the mechanical oscillator are the same for quantum noise dominated quantum nondemolition measurements and corresponding measurements dominated by classical sources of noise. The most practical quantum nondemolition strategy is the back-action evasion measurement, and in a variety of experiments summarized in this section all of the essential features of the back-action evasion measurement have been experimentally demonstrated in the classical limit. The key practical difficulties blocking the way to the quantum regime have been identified, and promising avenues for the exploration of the quantum behavior of macroscopic mechanical oscillators have been charted (Cinquegrana *et al.*, 1995).

The demonstration of a back-action evasion measurement consists of two factors. First, the reverse-transfer characteristics of the transducer must be demonstrated; specifically, it must be shown that the fluctuating back-action force of the transducer on the mechanical resonator is squeezed, i.e., that the back-action force is a function of the phase of the mechanical oscillator and at its minimum it is reduced from the level of back action in a conventional non-BAE measurement. Second, it must be demonstrated that the forward-transfer characteristic is phase sensitive, specifically that the transducer output contains only information about the "quiet" phase of the mechanical oscillator. The essence of a BAE measurement is that the transducer "reads out" information about the phase of the mechanical oscillator that is isolated from the fluctuating back-action force of the transducer.

In Sec. III we showed that the BAE measurement was one member of a larger class of parametric electromechanical converters. There has been substantial experimental work on conventional and BAE parametric transducers, and in this section we review the experiments. We will describe the essential features of the various designs for mechanical resonators and electrical readout circuits and we will summarize the salient features of parametric conversion and BAE measurements that have been demonstrated. We organize our presentation by the various research groups that have produced experimental results.

A. Moscow State University

The theoretical contributions of the Moscow State University group to the field of quantum measurements on macroscopic mechanical systems were complemented by considerable experimental efforts. In this review we will not attempt to summarize the entire body of work from this group—for a review see Braginsky (1988) or Braginsky and Khalili (1991). Rather, we will focus our attention on the Moscow State University work concerning the capacitive parametric transducer.

Shown in Fig. 7 is a diagram of the capacitive parametric transducer developed by Braginsky and his collaborators (Braginsky, Mitrofanov, and Panov, 1985). The mechanical resonator was a niobium disk 3 cm in diameter clamped at the perimeter and possessing a lowest drumhead mode at a frequency of $\omega_1/2\pi$=40 kHz. The surface of the disk formed one wall of a niobium reentrant microwave cavity with the capacitive cavity element having a gap of 3.4×10^{-4} m. The drumhead vibration of the disk modulated the capacitance of the microwave cavity resonator being pumped by a microwave source stabilized by a high-quality factor tunable sapphire resonator. The microwave cavity had an electrical quality factor of $Q_2=4\times10^4$ which, given the cavity resonant frequency of $\omega_2/2\pi$=3 GHz leads to an electrical relaxation time $\tau_2=Q_2/\omega_2$=2.1 μsec. The product $\omega_1\tau_2$ is only 0.5 for this device, and to enable a back-action evasion measurement this parameter should be much greater than unity. To enable a BAE measurement, the electrical relaxation time of the microwave cavity would have to be increased substantially. However, operating their transducer in the single-pump, non-BAE mode

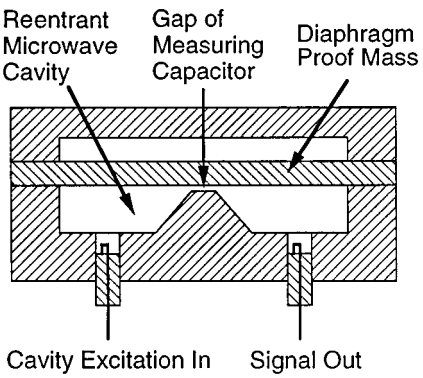

FIG. 7. The reentrant cavity parametric transducer built by the Moscow University group. The motion of a diaphragm-shaped proof mass modulates the capacitive stub of a reentrant microwave cavity. The cavity is excited by a weakly coupled loop, and the signal in the cavity is monitored by a second weakly coupled probe. Motion of the proof mass creates sidebands on the cavity excitation that are monitored to infer the proof-mass displacement.

they reported the impressive effective displacement noise of the mechanical diaphragm at 8 kHz of $\Delta x = 6\times10^{-19}$ m/$\sqrt{\text{Hz}}$.

A novel design for a mechanical harmonic oscillator that could be coupled to a parametric transducer was the "horned" bar developed by Braginsky's group—see Fig. 8,—which provided a means of coupling the vibration of a cylindrical gravitational wave antenna to a transducer. In this design a pair of tapered horns translated the motion of the ends of a cylinder to the center of the cylinder. There was a small gap between the horn ends forming a capacitor that was part of an electrically resonant circuit tuned to 5–10 MHz in early designs (Braginsky, 1974), or in a later design, using a single crystal sapphire horned bar, the horn ends modulated the capacitive element of a reentrant microwave cavity (Panov and Khalili, 1980).

Later, this group shifted attention to measurement schemes based on the exploitation of whispering-gallery modes in high-quality sapphire optical cavities (Braginsky, Il'chenko, and Bagdassarov, 1987) both for optomechanical transducers and to make a QND measurement of the number of photons in an optical cavity (Braginsky and Vyatchanin, 1988; Braginsky, Gorodetsky, and Il'chenko, 1989; Braginsky and Khalili, 1990). This interesting proposal has been studied further at Stanford University (Schiller and Byer, 1991) and at the Ecole Normale Supérieure in Paris (Collot *et al.*, 1993); this last group confirmed and studied the scheme in detail showing the splitting of the high-quality whispering gallery modes into the doublets already observed by Ilchenko and Gorodetsky (1992), which are attributable to internal light backscattering (Weiss *et al.*, 1995), therefore limiting the performance of the optical cavity transducer as a high-sensitivity electromechanical transducer.

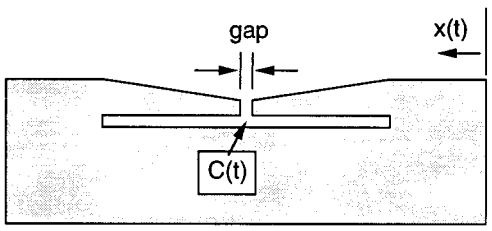

FIG. 8. A method to couple the end-face motion of a cylindrical gravitational wave antenna to a centrally located capacitor was developed by the Moscow State University group. The capacitor formed by the horns attached to the ends of the bar could serve as a component in a rf circuit or a reentrant microwave cavity.

B. University of Rochester

The earliest attempts by the Rochester group at implementing the back-action evasion measurement strategy were conducted with a very-low-mass mechanical resonator fabricated from sapphire (Bocko and Johnson, 1984). The mechanical oscillator was the first bending mode of a nearly-free plate of sapphire of dimensions 2.5 cm×1.5 cm×0.1 cm, which had a frequency of 16.1 kHz and an effective mass of 4×10^{-4} kg (see Fig. 9). A face of the resonator was coupled capacitively to a superconducting radio-frequency bridge circuit with a resonant readout of frequency 4.15 MHz. The highest electrical quality factor achieved with the superconducting readout circuit was approximately 4300, so the product $\omega_1\tau_2$ was 16, large enough to allow significant back-action evasion in a two-pump experiment. However, the strength of the electromechanical coupling between the mechanical resonator and the electrical readout circuit was insufficient to make the back-action force measurable, but a complete study of the transducer forward-transfer characteristics, i.e., the mechanical to electrical conversion, was conducted and the phase-sensitive nature of the BAE measurement strategy was demonstrated for the first time.

The pump voltage used to excite the readout circuit can be represented in the standard form [Eq. (3.23)]. To demonstrate the various parametric processes achieved by modifying the pump, the mechanical resonator was excited by a sinusoidal force and monitored by a weakly coupled strain-gauge transducer, the output of which was fed into a two-phase lock-in detector. The outputs of the two channels of the lock-in detector were proportional to the X_1 and X_2 amplitudes of the mechanical oscillator, and the signal amplitudes were plotted to produce the topmost plot in Fig. 10, which shows the excitation of the mechanical oscillator in the X_1X_2 plane for a series of five measurements, each one for a different phase of excitation of the mechanical oscillator. The amplitude and phase of the electrical signal at the output of the transducer were also monitored as a function of the mechanical oscillator excitation phase. The other three plots shown in the lower part of Fig. 10 display the output of the transducer in the Q_1Q_2 plane. It was observed that when $f=+1$, the upconverted electrical signal

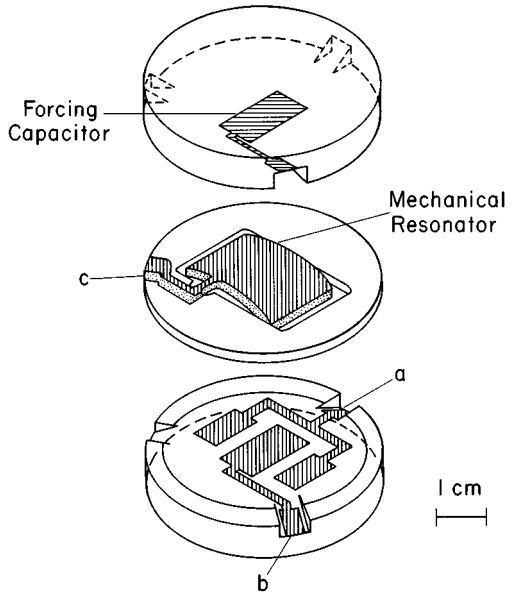

FIG. 9. A scheme to couple a parametric bridge-circuit transducer to the fundamental bending mode of a rectangular sapphire plate was developed by researchers at the University of Rochester. When assembled the electrodes labeled a, b, and c, formed two capacitors operating in a push-pull configuration, i.e., bending of the plate increased one capacitance while the other capacitance was decreased. The forcing capacitor on the other side of the sapphire plate was used to provide calibration forces.

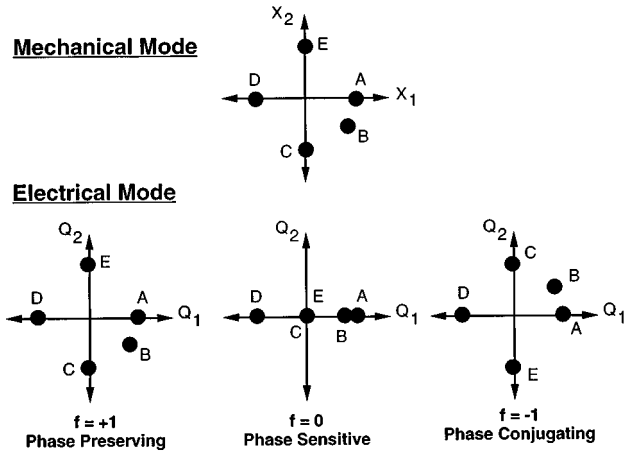

FIG. 10. Experimentally obtained phase-plane plots showing the phase sensitivity of the parametric upconversion in the BAE configuration. The plotted data at the top of the figure shows the excitation of the mechanical oscillator in the X_1X_2 phase plane. The mechanical oscillator was monitored by sending the signal from a weakly coupled auxiliary transducer to a two-phase lock-in detector, and the phase of the mechanical excitation force was changed to obtain the five data points labeled $A-E$. During each of the five measurements the output of the parametric transducer, the electrical mode, was similarly monitored with a two-phase lock-in detector. The experiments were repeated for three types of parametric conversion corresponding to f=0,±1. There is a unique mapping of the mechanical-mode phase-space points onto the electrical mode for each parametric process. In the case f=+1, the rotational order of the points is preserved; it is a phase-preserving parametric conversion process, whereas for f=−1, the phase is conjugated, and for f=0, the superposition of the phase-preserving and phase-conjugating processes, the conversion is phase sensitive. The mechanical excitations labeled E and C yielded no output signal in the transducer, i.e., the transducer was not sensitive to the X_2 phase of the mechanical oscillator (Bocko and Johnson, 1984).

is a phase preserved version of the mechanical excitation—note, in the plot of Fig. 10 labeled f=+1, that the output-signal phase tracks the mechanical drive phase, i.e., it is a phase-preserving parametric process. In the plot of the transducer output data labelled f=−1, the sense of rotation of the points is reversed, demonstrating the phase-conjugating parametric process. In the remaining data plot, taken with equal pump components, f=0, the BAE case, information about only one mechanical oscillator phase is present at the transducer output.

Continued work on a parametric transducer coupled to a more massive mechanical oscillator—0.15 kg effective mass—suitable for a gravitational wave antenna transducer was reported (Bocko, Johnson, and Iafolla, 1989; Bocko and Johnson, 1989). The main improvements were to decrease the residual imbalance of the transducer bridge circuit to 20 parts per million and to increase the electromechanical coupling coefficient to approximately $\beta=2\times10^{-4}$. This value of the coupling coefficient was sufficient to see clearly the parametric loading effect of the electrical transducer circuit on the mechanical resonator. For the phase-preserving parametric upconvertor the effect of the transducer is to damp the mechanical oscillator. Pumping the transducer at the sum of the electrical and mechanical frequencies has the opposite effect and gives rise to a parametric instability. The demonstration of these effects is shown in Fig. 11. An absolute sensitivity calibration of the transducer was also performed. The equivalent displacement noise spectral density (in $\mathrm{m}/\sqrt{\mathrm{Hz}}$) was limited by the combination of pump phase noise and residual bridge imbalance (see Fig. 12) but the equivalent-displacement noise of the transducer approached 10^{-15} $\mathrm{m}/\sqrt{\mathrm{Hz}}$.

A complete demonstration of the forward- and reverse-coupling characteristics of a BAE measurement was subsequently performed by the Rochester group (Marchese, Bocko, and Onofrio, 1992) using a room-temperature version of a parametric transducer. Noise was introduced in the experiment to simulate a noisy amplifier, making possible a clear demonstration of the back-action evasion capability of the transducer. The mechanical oscillator used in the experiments was a torsional resonator with a frequency of 1870 Hz at room temperature, its effective mass was 0.2 Kg, and the measured mechanical quality factor at room temperature in vacuum was 10^3. The electrical readout circuit consisted of a lumped-element LC bridge circuit with the two electrically resonant modes of the circuit having frequencies near 50 kHz. The measured electrical quality factor for the readout circuit was 13.

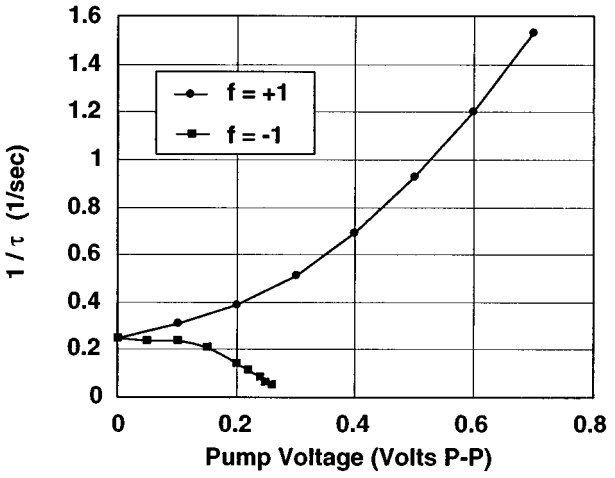

FIG. 11. The inverse of the measured mechanical relaxation time ($1/\tau$) of a mechanical oscillator coupled to a parametric transducer is plotted as a function of the pump voltage. For the phase-preserving parametric upconvertor, f=+1, an increase of the electromechanical coupling strength, measured by the pump voltage, decreases the mechanical relaxation time, i.e., the parametric interaction produces dynamical damping of the mechanical oscillator. The phase-conjugating parametric upconverter produces dynamical antidamping of the mechanical oscillator, with the mechanical oscillator breaking into oscillation above some threshold coupling strength (Bocko, Johnson, and Iafolla, 1989).

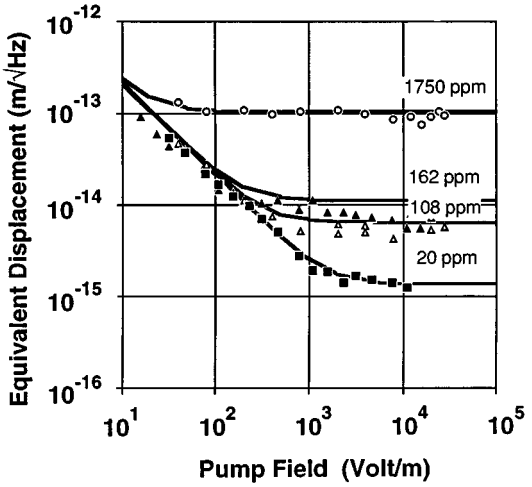

FIG. 12. The equivalent mechanical-oscillator displacement noise versus the pump electric-field amplitude for different values of parametric transducer bridge-circuit imbalance. As the bridge circuit approaches balance, the equivalent displacement noise due to the combination of pump phase fluctuations and imbalance is decreased (Bocko, Johnson, and Iafolla, 1989).

The complete BAE measurement demonstration consisted of two stages; the first was to show that one quadrature phase of the mechanical oscillator was isolated from the fluctuating back action of the transducer and the second stage was to show that the transducer responds only to the quiet mechanical phase. To perform the first part of the demonstration, the mechanical oscillator noise was measured as a function of its phase. The construction shown in Fig. 13(a) is an aid for predicting the noise for any mechanical oscillator phase ϕ, which is defined relative to the mechanical-oscillator complex-amplitude components X_1 and X_2. The projections of the major and minor axes of the "noise ellipse" on the phase direction ϕ are added in quadrature because the noise in the X_1 and X_2 components is uncorrelated. The measured phase dependence of the noise in the mechanical oscillator is displayed in Fig. 13(b). An arbitrary vertical scale has been added to the back-action noise versus mechanical oscillator phase plot to aid comparisons of relative magnitudes.

In the other part of the demonstration, the response of the electrical readout circuit to the mechanical oscillator was measured. Expressing a sinusoidal force acting on the mechanical oscillator as $F(t)=F_0\cos(\omega_1 t+\theta)$ where θ is the phase of the force measured relative to the readout pump field it was seen that, for certain θ values, the output of the readout circuit was zero, i.e., the readout contained no information concerning the force acting on the mechanical resonator. In Fig. 13(b) the measured relative conversion gain is shown simultaneously with the measured mechanical noise. The conversion gain is scaled to fit on the same plot as the back-action noise.

The key feature of a BAE measurement is displayed in Fig. 13(b). That is, since one has the freedom to set $\theta=\phi$, the phase of the mechanical resonator to which the readout circuit responds is the back-action-immune phase, i.e., the mechanical oscillator phase benefiting from the reduced back-action force noise. Furthermore, the readout contains no information about the noisy phase of the mechanical resonator. In the specific example above, taking θ=90°, the X_2 phase of the mechanical resonator is excited by the force. This is also the phase of the mechanical resonator, which suffers the maximum back-action noise. However, the output of the transducer is proportional to $\cos\theta$, zero for θ=90°, so there is no information about the noisy X_2 phase (nor the force) at the output of the transducer. On the other hand, if θ=0°, then the force excites the quiet X_1 phase of the mechanical resonator that is measured by the readout. We also note the small 15° phase shift between the conversion-gain maximum and noise minimum, which we believe is due to a slight detuning of the frequency of the mechanical oscillator drive from the oscillator's resonant frequency in the conversion-gain measurements. This would yield a small phase shift of the mechanical oscillator response from the phase of the applied driving force.

Multipump BAE techniques were also demonstrated with this transducer. The transducer bridge circuit was driven with two pumps, four pumps, or quasistroboscopically with multiple pumps. The phase sensitivity of the noise for two- and four-pump schemes was measured, and it was shown that the back-action noise squeezing increased with the addition of more pumps.

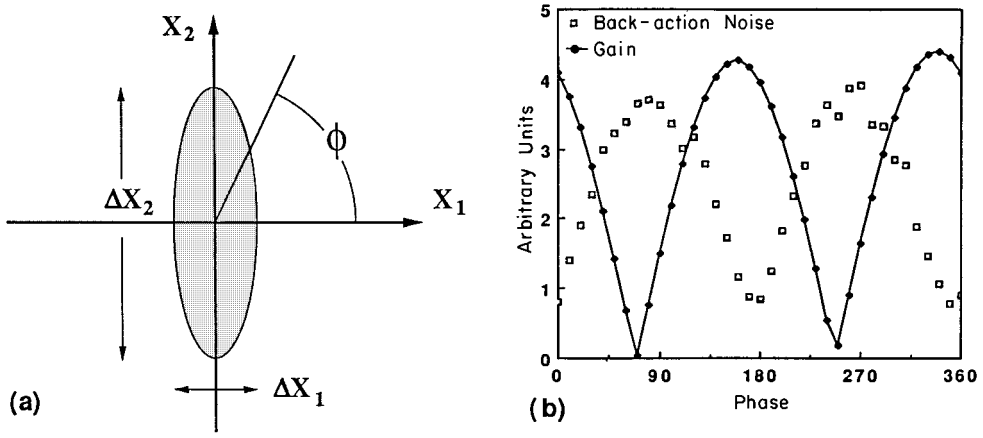

FIG. 13. Back action noise in a mechanical oscillator and phase-sensitive electromechanical conversion: (a) schematic representation of back-action noise measurements in a parametric transducer system; (b) measurements in which the noise of the mechanical oscillator and the electromechanical conversion gain of the parametric transducer are plotted as functions of the phase of the mechanical oscillator. If the noise in the mechanical oscillator is squeezed, as shown in (a), the measured rms mechanical-oscillator noise displays a sinusoidal dependence on the mechanical-oscillator phase. The electromechanical conversion gain is also a function of the mechanical-oscillator phase, and there are certain phases of excitation of the mechanical oscillator for which no signal appears at the transducer output. The essence of a BAE measurement is that the conversion gain is maximum for the phases of the mechanical oscillator that display the minimum back-action noise (Marchese, Bocko, and Onofrio, 1992).

The ratio of the maximum to minimum rms mechanical noise is the experimentally determined squeezing factor. For the two-pump case, the measured squeezing factor was 3.8; for the four pump case the measured squeezing factor was 5.1, in reasonable agreement with theory (Marchese, Bocko, and Onofrio, 1992). The demonstration of a multipump quasistroboscopic BAE measurement was also demonstrated by this group using the same transducer.

The most recent experimental work in the Rochester group has been the refinement of the parametric transducer for use on a resonant gravitational wave antenna. This transducer consisted of a torsional mechanical oscillator coupled capacitively to a microstrip bridge circuit, shown in Fig. 14. The bridge circuit was fabricated from niobium sheet stock 1 mm thick and was designed to have the two electrically resonant bridge modes near 230 MHz (Fisher *et al.*, 1995). A number of favorable factors influenced the decision to operate the transducer readout at 230 MHz. The first was the availability of low-noise amplifiers at that frequency, the second, the compact circuit design possible at the chosen frequency lent itself to achieving high electrical quality factors, and finally, there are very-low-noise frequency sources available to use as the pump.

In tests of the 230 MHz transducer in the non-BAE operation mode, it was found that unloaded electrical quality factors of 200 000 were attainable, and the readout bridge-circuit balance could be controlled to 6 parts in 10^7. A low-noise GaAs FET (field-effect transistor) amplifier with a noise number approximately 5400 times the quantum limit was used to measure the output of the bridge circuit. Large electromechanical coupling strength was achieved by tuning the bridge-circuit pump mode to the idler mode frequency and a dimensionless coupling constant β of about 1% was achieved. The transducer was tested in the non-BAE operation mode to demonstrate its potential as a transducer for a gravitational wave detector, and although the measured noise was limited by the environmental vibration noise, the transducer would allow the detection of displacements on the order of 5×10^{-19} m on a 2000 kg gravitational wave antenna. In terms of displacement sensitivity, the quantum limit is still more than a factor of 10^5 below the present transducer sensitivity.

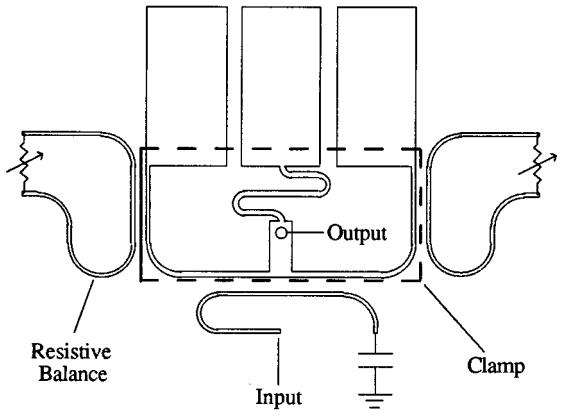

FIG. 14. A stripline bridge circuit operated at 230 MHz. The three rectangular plates form capacitors with the surface of a torsional (teeter-totter) resonator so that oscillation of the mechanical resonator modulates the two outer capacitors in a push-pull fashion, while the central capacitor maintains a fixed value. The inductive elements of the bridge are formed by stripline covered by a dielectric clamp and surrounded by a ground plane. The pump and resistive-balance controlling signals are introduced via edge-coupled striplines (Fisher *et al.*, 1995).

C. CNR-Frascati

The group at the CNR in Frascati, Italy, began their investigations of parametric transducers using low-electrical-frequency prototypes (Fuligni and Iafolla, 1983; Bordoni *et al.*, 1986). The mechanical resonator used by them employed torsion springs to achieve a low resonant frequency, 59 Hz, and served as the central plate in a three-plate capacitor. The low mechanical frequency was motivated by applications as a gravimeter or a force sensor to search for the mechanical interaction of neutrinos with matter (Bordoni *et al.*, 1990). They also found it essential to use a balanced-bridge configuration for the readout circuit to reduce the output noise contributed by the combination of pump fluctuations and bridge-circuit imbalance. Provided that the two capacitor plates coupled to the transducer mass have the same area and that the gaps are the same, the pump noise could be canceled at the output of the readout circuit. This was demonstrated by their measurements of the transducer output noise as a function of the imbalance of the transducer bridge circuit.

The reverse-coupling behavior of the BAE scheme was also demonstrated by injecting a high-level voltage-noise source into the bridge circuit along with the two-frequency pump represented by Eq. (3.23) with $f=0$. This technique simulated the back-action noise of an amplifier. The bridge circuit was driven by the two-frequency pump plus noise with a variable bandwidth to simulate the noise-filtering capability of the resonant bridge readout circuit. The lower pump was at a frequency of 20 KHz and the upper pump component was at a frequency of 20.118 KHz. The mechanical oscillator was monitored by a weakly interacting auxiliary transducer with its output sent to a lock-in detector with a reference at the mechanical frequency. The output of the lock-in detector yielded a direct measurement of both the in-phase and quadrature components of the mechanical oscillator. When a single-frequency pump was used, injection of noise at the central electrical frequency caused a back-action force on the oscillator with no preferred direction in the X_1X_2 phase space. When the two-frequency BAE pump was employed, the back-action noise was squeezed by a factor of approximately 4, i.e., the noise in the quiet phase was one fourth of its value for the single pump case. The imperfect cancellation of the noise in the ''quiet'' mechanical oscillator phase was due to the noise present at $\omega_e \pm 2\omega_m$, which acts back on both of the mechanical phases. Despite this drawback, the squeezing of the noise was demonstrated by plotting a histogram of the signal at the output of the lock-in by changing the phase of the local oscillator. The noise distribution was shown to be a symmetric two-dimensional Gaussian in the case of a conventional parametric scheme, confirming the absence of contamination from non-Gaussian noise sources, while in the BAE mode of operation the two-dimensional Gaussian was found to be asymmetric (Bordoni *et al.*, 1986; Bocko *et al.*, 1986). This can also be viewed as the mechanical, classical counterpart of the later introduced quantum tomography of optical states (Vogel and Risken, 1989) experimentally demonstrated by Smithey *et al.* (1993).

To overcome the limited back-action reduction capability of a low-Q electrical readout circuit, a multipump configuration was first employed by Bordoni and Onofrio (1990). The pump excitation of the transducer circuit was the sum of a set of phase-locked synthesizers; some of the sources served as sinusoidally varying pumps and others served as simulated noise sources by introducing a random narrow-band frequency sweep centered around a fixed frequency. Using this configuration, the effect of multiple pumps on the back-action noise was demonstrated, providing the first experimental demonstration that the multifrequency pumping technique relaxes the requirement on the electrical quality factor of the readout circuit.

D. University of Rome ''La Sapienza''

The Rome gravitational wave group started to develop QND/BAE schemes in 1986. Their efforts concentrated on developing a transducer to be used with one of the gravitational wave antennae operating in Italy (Rapagnani, 1982). The mechanical resonator in their system was a center-clamped disk of 17.0 cm diameter and 0.65 cm thickness, having an equivalent mass of 0.38 kg and a resonant frequency of 930 Hz (Barro *et al.*, 1988). The decay time of the mechanical mode was measured at 4.2 K to be 320 s, corresponding to a mechanical quality factor of 927 000. The disk is the central plate in a three-plate capacitor in which the two capacitances of the assembled transducer each had a capacitance value $C=1780$ pF and loss angle $\tan(\delta)\leqslant 10^{-4}$ at 1 KHz (see Fig. 15). The remainder of the electrical readout circuit consisted of two other fixed-value capacitors and an inductor to form the central arm of a bridge circuit, the same configuration as in the Frascati experiments. The central inductor was a superconducting Nb coil shielded in a Pb container, and the measured inductance at $T=4.2$ K was $L=1.7$ mH. The measured electrical frequency of the resonant bridge was 126 kHz and the electrical quality factor was 6300.

A bridge-circuit balancing mechanism used a piezoelectric actuator that gave a displacement of 33 microns for a dc voltage of 800 V. The actuator was arranged to push on one of the outer capacitor plates in the transducer and the minimum value of the static imbalance obtained at room temperature was $(8.20\pm0.08)\times10^{-7}$, which corresponded to a variation of capacitance $\Delta C=5.6\times10^{-3}$ pF, and a minimum imbalance of $(5.8\pm0.4)\times10^{-6}$ was achieved at 4.2 K.

Based upon noise measurements of the transducer output, an effective burst-noise temperature of $T_{\rm eff}=8$ K was determined, which was slightly lower than the noise temperature of the amplifier used to monitor the bridge output, $T_n=14$ K, implying that the product $(\omega_1/\omega_2)(1/r)$ was equal to 1.75, giving a value of $r=2.9\times10^{-3}$. This limit was attributed to the relatively high value of the static imbalance and the limited electrical quality factor of the transducer bridge circuit. With all other param-

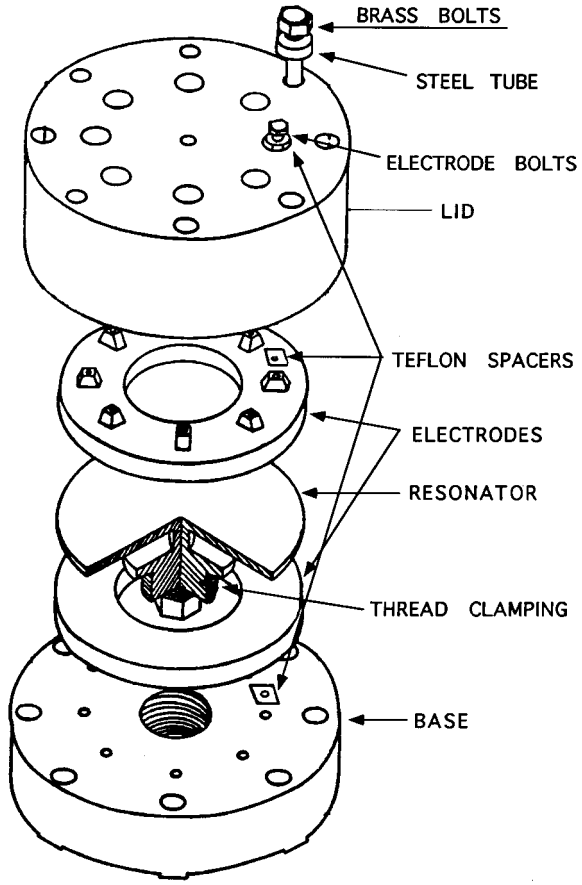

FIG. 15. Exploded view of the differential capacitive transducer used by the Rome group (Barro *et al.*, 1988; Cinquegrana *et al.*, 1993). A scaled version of this transducer, with a resonant frequency at 1.8 KHz, has been implemented on the cryogenic antenna at CNR, Frascati—see Sec. V.B for details.

eters held constant, if the imbalance were improved to 10^{-7}, a value of $r=1$ would have been achieved, giving $T_{\rm eff}=71$ mK. The conclusion of the early Rome experiments was therefore that the sensitivity was most strongly limited by the amplitude and phase noise of the pump source and the minimum achievable bridge imbalance.

In more recent experimental developments in Rome a refined version of the transduction system has been developed with improvements in the suspension systems, the shielding of the superconducting coil and the balancing system (Cinquegrana *et al.*, 1993). A mechanical quality factor of 2.8 million and an electrical quality factor of 6000 were achieved, but a vastly improved bridge residual imbalance of 8×10^{-7} was the main new feature. Their measured noise temperature was limited to about $T_{\rm eff}=0.5$ K, but the pump noise continued to be the limiting factor in the sensitivity of their transducer. Finally, the Rome group succeeded in observing the Brownian motion of their transducer at 4.5 K (Majorana *et al.*, 1993). The noise of electrical origin was the same in either transducer output phase, being limited by the phase noise of the pump source and the bridge imbalance. The Brownian noise appeared as a narrow spectral peak in

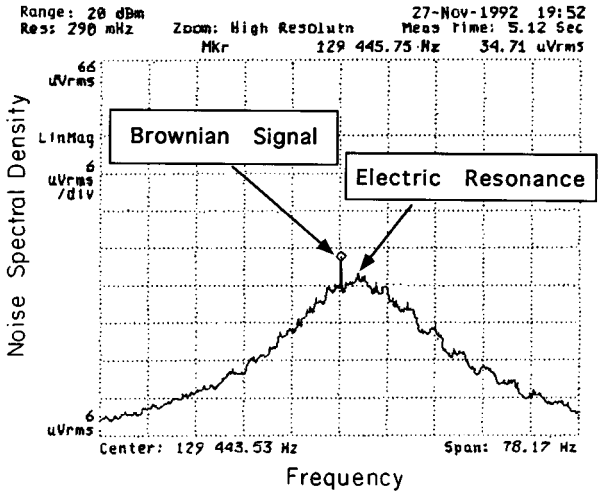

FIG. 16. Frequency spectrum of the output of the transducer shown in Fig. 15, showing the 4.5 K Brownian-noise peak and the shape of the electrical resonance near 130 KHz (Cinquegrana *et al.*, 1993).

the signal-containing output phase and its magnitude was in agreement with the predicted value within the uncertainty of their calibration, as shown in Fig. 16. The Fourier spectra of the two phases of the output signal shows that the measurement was phase sensitive, with bandwidth and amplitude in agreement with the theoretical predictions of the model developed by Cinquegrana *et al.* (1993) for the signal due to the Brownian motion (see Fig. 17). It is notable that this was the first BAE transducer to reach the Brownian-motion limit and to demonstrate the phase-sensitive forward-transfer characteristics of a BAE measurement using the Brownian motion as the signal.

E. Louisiana State University

The first demonstration of the reverse-coupling characteristics of a BAE measurement was made by the group at Louisiana State University (Spetz *et al.*, 1984). They used a transducer coupled to a low-mass mechanical oscillator via the two-frequency BAE pumping scheme to demonstrate phase-sensitive squeezing of the back-action noise. The mechanical oscillator was a niobium diaphragm with an effective mass of 2×10^{-5} kg and a frequency of 4.1 kHz. The transducer was a double reentrant microwave cavity, similar in geometry to the single reentrant cavity used by Braginsky (shown in Figure 7) with separate cavity resonances of 602 and 618 MHz and Q's of 300 000 and 500 000 respectively (Oelfke and Hamilton, 1978, 1983). Amplified thermal noise and the two-frequency pump were injected into one of the cavities and the diaphragm motion was observed with the other cavity weakly pumped by a single frequency. Although this readout cavity performed an amplitude and phase measurement of the mechanical os-

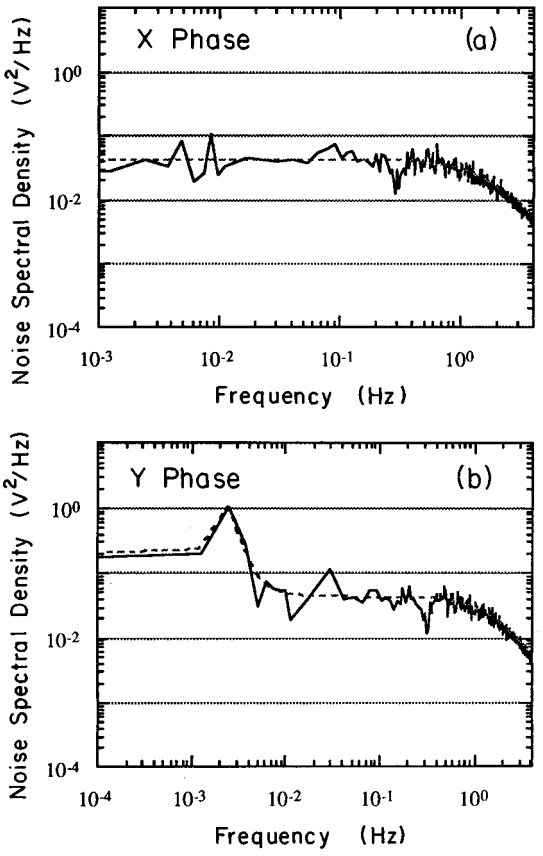

FIG. 17. Spectra of the two quadrature phases, labeled X and Y, of the parametric transducer output for a Brownian limited back-action-evasion measurement. The amplitude and bandwidth of the peak present in the Y-phase plot are compatible with the Brownian noise of the transducer at a thermodynamic temperature of (4.5+0.3) K (Majorana *et al.*, 1993).

cillator, the field strength in the readout cavity was very weak and did not perturb the motion of the mechanical resonator.

The maximum squeezing factor measured for the 4.1 kHz diaphragm mode was 4.0±0.5. Higher-frequency modes of the transducer displayed higher squeezing factors: modes at 8.5 and 13.9 kHz showed squeezing factors of 6.3±0.7 and 15±3, respectively. The results were in general agreement with the theoretical prediction that the squeezing factor should increase as the ratio of the mechanical to electrical frequencies, but the observed squeezing was approximately a factor of 2 below the ideal value they predicted. This discrepancy was attributed to the large amount of noise injected into the microwave cavity to simulate the back action of a noisy amplifier. It was necessary to inject a high noise level to make the back-action force on the mechanical oscillator larger than the influence of environmental vibrations, and the injected noise created an additional phase-insensitive back-action force, thus reducing the squeezing factor.

More recently, the same group developed a parametric transducer composed of a niobium resonant diaphragm at 929 Hz and coupled through a superconducting bridge circuit to a two-stage metal-semiconductor FET cryogenic amplifier (Aguiar *et al.*, 1991). The bridge circuit consisted of a three-plate capacitor with lumped-element superconducting inductors and transformers. A very high degree of bridge mode tuning and balance control was achieved and the novel feature of being able to tune the bridge idler and pump resonances to a highly stable 5 MHz quartz oscillator serving as the pump source allowed the researchers to achieve a high electromechanical coupling factor, β=0.054, and a low noise level of 4×10^{-16} m/$\sqrt{\text{Hz}}$. No attempt was made to operate the transducer in the BAE pumping configuration.

F. University of Western Australia, Perth

The gravitational radiation detector group at the University of Western Australia developed a 9.6 GHz double reentrant cavity transducer that could be operated in a continuous back-action evasion mode (Blair, 1982). This transducer was similar in geometry to the 600 MHz reentrant cavity used by the LSU group, but much smaller—0.8 cm diameter—to achieve the high frequency. The advantage of the high frequency of the UWA transducer was that it allowed them to achieve very high values of the electromechanical coupling coefficient β, approaching unity for their two-mode 1.5 ton niobium antenna.

Other notable features of the UWA transducer were the following. Although the single-cavity transducer is an intrinsically unbalanced system, in contrast to the lower frequency bridge-circuit transducers, a high-precision carrier-suppression circuit external to the antenna was employed, which gave a carrier suppression of 70 dB. This was equivalent to balancing the bridge to approximately 3 parts in 10^4. The combination of this degree of carrier suppression with the ultralow-noise pump sources developed at UWA, with phase and amplitude noise spectral densities of −160 dBc/Hz and −180 dBc/Hz (dBc=decibels referenced to the carrier) respectively, yielded a measured transducer noise-equivalent displacement spectrum of 3×10^{-17} m/$\sqrt{\text{Hz}}$ and will allow operation of the UWA gravitational wave antenna at a burst strain sensitivity below 10^{-19} (Tobar and Blair, 1993, 1995). Another innovative technical feature of the UWA parametric transducer system is the microstrip patch antenna that is used to electrically couple the transducer to the external electronics (Ivanov, Turner, and Blair, 1993; Ivanov, Turner, Tobar, and Blair, 1993). The noncontacting electrical connection makes it possible to operate the antenna without any directly attached cables or wires that can transmit vibrations and damp the antenna's mechanical quality factor. The high mechanical quality factor of the UWA niobium antenna, 250 million at 4.2 K, is another notable feature. In principle the UWA parametric transducer will be capable of operation in a BAE mode.

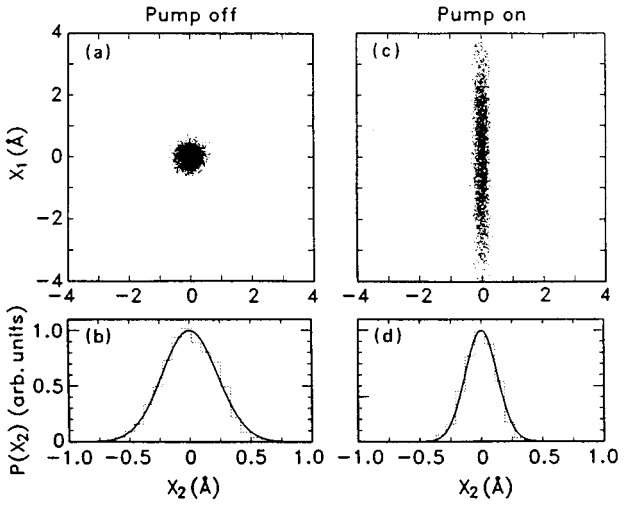

FIG. 18. The measured noise of a microfabricated cantilever-beam mechanical parametric amplifier built by the IBM, Almaden group: (a), (b) when the parametric amplifier pump was turned off the cantilever displayed phase-insensitive noise with an rms value near 0.5 Å; (c), (d) when the pump was turned on the noise was deamplified in the X_2 phase to one-half of its "pump-off" value. The noise of the X_1 phase increased by a factor equal to the parametric gain, which could be as high as 100 in their experiment (Rugar and Grutter, 1991).

G. IBM-Almaden

A related experiment that demonstrated squeezing of the thermal Brownian noise in a mechanical oscillator was conducted at the IBM Almaden Research Center (Rugar and Grutter, 1991). Their mechanical oscillator was a micromachined silicon cantilever, 500 μm long, 10 μm wide, and a few microns thick, with an effective mass of 2.2×10^{-11} kg. The spring constant of the cantilever was modulated at twice the cantilever's natural frequency of 33.57 kHz by forming a capacitor from a nearby electrode and the surface of the cantilever. A sinusoidal electric field, at 67.14 kHz, was then established in the capacitor, effectively modulating the restoring spring constant of the mechanical oscillator. In this way they succeeded in building a degenerate mechanical parametric amplifier capable of stable mechanical gain up to 100. The gain of a degenerate parametric amplifier is phase sensitive, defined by the phase of the pump, and in quadrature to the high-gain phase there is a low-gain phase with a theoretical gain of 1/2. They took advantage of this feature of degenerate parametric amplifiers to squeeze the mechanical Brownian noise of the cantilever, see Fig. 18. In one of the mechanical oscillator phases the rms thermal vibration of the cantilever was reduced by a factor of 2, while the noise in the other phase was increased by the maximum gain factor.

The small mass of their micromachined oscillator, combined with their sensitive optical-interferometer readout, placed their experiment relatively close to the quantum limit, falling short by a factor of about 1000. However, the Brownian motion of their room-temperature resonator was another factor of 1000 above the transducer noise level.

The IBM degenerate parametric amplifier may be used to improve the sensitivity for the detection of a weak force acting on a mechanical oscillator similar to a BAE measurement. However, the mechanical degenerate parametric amplifier differs from the BAE transducer in that the degenerate parametric amplifier is not intended to function as the transducer, but rather as an auxiliary means to squeeze the fluctuations that are intrinsic to the mechanical oscillator. In contrast, in the BAE scheme, the back-acting force noise of the transducer on the mechanical oscillator is squeezed while at the same time the transducer also provides a readout of the state of the mechanical oscillator.

The IBM researchers suggested two ways in which the mechanical degenerate parametric amplifier could improve the performance of a system for detecting weak forces. One possibility is to use the parametric amplification as a form of impedance matching (Yurke, 1991). In a situation in which the mechanical signals may be lost in the noise of a sensor used to monitor the mechanical oscillator, the parametric amplifier could be used to boost the mechanical signal to a level at which it would be detectable. An alternative scheme would be to use the noise deamplification capability of the parametric amplifier to prepare a mechanical oscillator in a reduced-fluctuation initial state before interaction with a weak force.

H. AT&T Bell Laboratories-Murray Hill

Another related experiment using micromechanical resonators, performed at AT&T Bell Laboratories, Murray Hill, showed how the amplifier limit can be evaded by using nonlinear oscillators (Greywall *et al.*, 1994). A micromechanical resonator having significant nonlinearities was driven into oscillation, and the amplitude and phase of one of its modes were measured. The authors used a micromachined rectangular silicon beam of size 3600 μm$\times$127 μm$\times$26 μm anchored at its ends, with a thin film of gold evaporated onto one surface of the beam to form a conductor with a resistance of 17 Ω. The end-anchored beam displayed a significant cubic nonlinearity due to the change of the beam length as a function of the beam's transverse displacement. The beam was cooled down to 100 mK and the lowest resonant mode at 15.994 KHz was measured to have a quality factor of 375 000. The beam was placed in a uniform magnetic field in the plane containing the beam, perpendicular to its long dimension, and the beam was mechanically excited by passing an alternating current through the gold film. The amplitude of the beam motion was measured by monitoring the voltage induced across the conducting film. The presence of the cubic nonlinearity in the restoring force led to a distortion of the resonance curve dependent on the drive level and it was possible to find operating points where the slope of the displacement versus frequency curve was infinite. At these points, the phase versus frequency curve tangent was also vertical and therefore the frequency was independent of the phase of the drive. Thus the influence of

TABLE I. Summary of the performance for various parametric transducers. The second column gives the operating frequency of the parametric transducer, the next column gives the mass of the mechanical oscillator that was monitored by the transducer, followed by the mechanical oscillator's resonant frequency and the back-action evasion figure of merit, $\omega_1\tau_2$, which is a measure of the ability of the transducer, if operated in the BAE mode, to isolate the mechanical oscillator from back-action noise. The next column reports the measured displacement equivalent noise of the transducer and the last column, the transducer displacement equivalent-noise spectral density divided by the quantum-noise spectral density $(\hbar/m\omega_{\rm mech}^2)^{1/2}$ indicates how far from the quantum limit each transducer performed.

Reference	f (readout)	Mass (kg)	Mechanical resonant frequency	$\omega_1\tau_2$	Displacement equivalent noise	(Displacement equivalent noise)/(Quantum noise)
Braginsky *et al.*, 1985[a]	3 Ghz	0.05	40 kHz	0.53	6×10^{-19} m/$\sqrt{\rm Hz}$	3.3×10^3
Bocko and Johnson, 1984	4.2 MHz	4×10^{-4}	16.1 kHz	16	8×10^{-16} m/$\sqrt{\rm Hz}$	1.6×10^5
Bocko *et al.*, 1989b	4.1 MHz	0.15	2.3 kHz	2.2	1×10^{-15} m/$\sqrt{\rm Hz}$	5.5×10^5
Fisher *et al.*, 1995	230 Mhz	0.08	980 Hz	0.85	1.7×10^{-15} m/$\sqrt{\rm Hz}$	2.9×10^5
Barro *et al.*, 1988[b]	126 kHz	0.38	930 Hz	47	4×10^{-15} m/$\sqrt{\rm Hz}$	1.4×10^6
Majorana *et al.*, 1993[c]	130 kHz	0.31	928 Hz	43	1.7×10^{-15} m$\sqrt{\rm Hz}$	5.4×10^5
Spetz *et al.*, 1984[d]	618 MHz	2×10^{-5}	4.1 kHz	4.0	not measured	
Aguiar *et al.*, 1991	5 MHz	0.26	929 Hz	0.41	4×10^{-16} m/$\sqrt{\rm Hz}$	1.2×10^5
Tobar and Blair, 1995	10 GHz	0.45	700 Hz	0.007	3×10^{-17} m/$\sqrt{\rm Hz}$	8.6×10^3
Rugar and Grutter, 1991[e]	optical	2.2×10^{-11}	33.6 kHz		1×10^{-14} m/$\sqrt{\rm Hz}$	9.9×10^2

[a]Displacement-equivalent noise measured at 8 kHz.
[b]Displacement-equivalent noise inferred from the quoted noise temperature.
[c]Brownian-motion peak used as calibration to infer displacement equivalent noise.
[d]Demonstration of back-action force noise reduction, noise level and sensitivity not measured.
[e]Nonparametric optical readout, Brownian noise of cantilever-beam oscillator is about 10^6 times the quantum-noise spectral density.

the phase fluctuations of the driving voltage, which are determined by the feedback amplifier that maintains the resonator in oscillation, could be reduced.

By working at these critical bias points Greywall *et al.* were able to suppress the phase diffusion of the driven oscillator by 10 Db, making it possible to reach the regime in which the long-term frequency stability of the oscillator is determined by the noise associated with the intrinsic loss of the resonator alone. This is of great interest for metrological devices such as continuous-wave frequency sources and precision clocks (Braginsky, Caves, Thorne, 1977; Braginsky, 1988). This experiment is the first example of a continuous back-action evasion measurement of the phase of a resonator (Caves, 1989).

The last two experiments reported in this section demonstrate the possible benefits of phase-sensitive techniques for mechanical measurements in the realm of microminiaturized mechanical structures where the influence of the measurement apparatus is most strongly felt.

To close this section we refer the reader to Table I, which summarizes the key physical parameters and the experimentally obtained sensitivities for the different parametric transducers discussed in this section. The last column of the table is indicative of how far we have to go in order to reach the quantum limit. To form this column we have taken the reported displacement equivalent-noise spectral densities and divided each by the spectral density of the quantum noise $(\hbar/m\omega_{\rm mech}{}^2)^{1/2}$ for a mechanical resonator of the mass and frequency used in the respective experiments.

V. APPLICATIONS TO HIGH-PRECISION EXPERIMENTS

In addition to the fundamental interest in reaching and surpassing the standard quantum limit, there have been a number of efforts in the last decade to apply the general concepts of back-action evasion measurements to high-precision experiments, in particular to mesoscopic mechanics, gravitational wave detection, single-electron and single-ion spectroscopy, and superconducting tunnel junction mixers. These efforts are reviewed below to complement the previous section, which was oriented more to a description of the laboratory activities aimed at testing the predictions of the measurement models described in Sec. III. Due to the rapid developments in many areas, we expect (and hope) that the present section will soon become outdated, although it may maintain its value as an introduction to this expanding subject area.

A. Quantum mechanics at a mesoscopic scale

The possibility of performing experiments to monitor macroscopic objects at the quantum level of sensitivity has been discussed since the beginning of quantum theory, especially in the context of the debate over the loss of realism when quantum theory is applied to the macroscopic world (Schrödinger, 1935; Przibram, 1967; Wheeler and Zurek, 1983) and the dynamics of the decoherence induced by the environment (Zurek, 1990). Only in recent times, due to the development of microfabrication technologies and advances in low-noise elec-

tronics and cryogenics, have these experiments become feasible. Some of the most difficult to overcome constraints imposed on the design of gravitational wave detectors are relaxed for experiments dedicated to the study of repeated quantum measurements on a macroscopic mechanical oscillator (Bocko and Johnson, 1986; Onofrio 1990). Specifically, in such dedicated experiments, a much smaller mass than that required in a gravitational wave antenna transducer may be used, thus increasing the amplitude of the quantum zero-point displacements. Additionally, it is easier to reach and maintain very low temperatures for a small mass than for a multiton gravitational wave antenna. A small resonant mass also implies naturally large mechanical frequencies, which makes it easier to isolate the experiment from environmental vibrations.

The drawback is that capacitive transducer schemes are difficult to implement on small-mass oscillators because of the small available surface area and corresponding small capacitance. A small capacitance makes it difficult to obtain substantial electromechanical coupling strength, and impedance-matching available amplifiers to low-capacitance/high-impedance sources adds complications. To overcome these problems an alternative transduction scheme was proposed, the tunneling transducer (Niksch and Binnig, 1988), and its application to gravitational wave-detection was discussed (Bordoni *et al.*, 1990). The tunneling transducer is the ultimate, quantum version of a variable-resistance transducer. Electron tunneling current between a tip and a surface held a few angstroms distant is very sensitive to modulations of the distance; the distance scale over which the current modulation is appreciable depends upon the quantum features of the system. A tunneling transducer may be modeled as a resistor in which the resistance is exponentially dependent upon the separation of the probe tip from the surface of the object being monitored. If the separation of the tip from the object is $d-x(t)$, in which d is the nominal gap and $x(t)$ is the small time-dependent part of the gap, the probe resistance can be expressed as $R=R_0e^{-\kappa x}$, where R_0 is typically 10^4–10^8 Ω for a nominal separation d of several angstroms, and κ is typically 10^{10} m^{-1}. It has been shown (Bocko, Stephenson, and Koch, 1988) that this class of transducers displays reduced back action of the amplifier when the stray capacitance of the tunneling probe is small enough. This allows the effect of the amplifier to be ignored, and from a practical point of view it implies that amplifiers considerably above the quantum limit could be used in quantum-noise experiments. A detailed comparison of the sensitivity of a tunneling transducer to a capacitive transducer, with particular attention to the dependence upon the test mass, has been carried out (Stephenson, Bocko, and Koch, 1989; Bocko, 1990). As shown in Fig. 19, when the mass of the resonator is small, the noise number for a tunneling transducer is far below that for a capacitive transducer.

The question then arises: ''how is the standard quantum limit enforced in the tunneling transducer?'' The answer is that the tunneling electrons contribute two independent noise sources, analogous to the voltage- and current-noise sources in an amplifier, which together enforce the standard quantum limit. First, the statistical nature of the tunneling process is responsible for fluctuations of the tunneling current, the so-called shot noise. Shot noise is indistinguishable from the current fluctuations that would result from fluctuations in the gap of the tunneling probe; therefore the shot noise implies an uncertainty in the inferred position of the test mass. Furthermore, the momentum imparted to the test mass by each electron as it is transferred between the test mass and the tunneling probe is a fluctuating quantity, thereby giving rise to uncertainty in the momentum of the test mass. Even if the electrons were being transferred from the test mass to the tunneling probe at perfectly regular intervals of time, i.e., no shot noise, the momentum of each electron is uncertain, leading to an uncertainty of the net momentum transferred to the test mass. The tunneling probe resembles a Michelson interferometer, where both the shot-noise fluctuations of the photon flux and the fluctuations in the momentum imparted by each photon to the mirror enforce the uncertainty relations for the momentum and position of the mirror. The standard quantum limit for this class of transducers was explored by Mitrofanov and Yanikov (1989). More detailed calculations have been done in a second-quantization approach (Yurke and Kochansky, 1990) and in a first-quantization approach (Presilla, On-

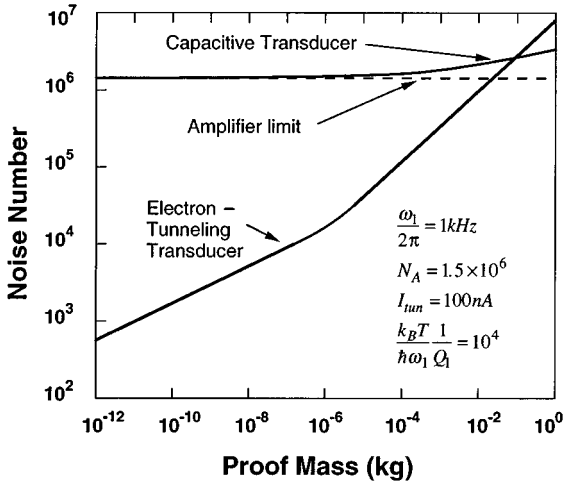

FIG. 19. The equivalent noise number vs the mass of a mechanical oscillator monitored by a conventional, non-BAE, capacitive transducer and by the electron-tunneling transducer. The capacitive transducer cannot surpass the limit imposed by the amplifier, assumed to be a conventional room-temperature field-effect transistor, whereas using the same amplifier, the near absence of back action by the tunneling transducer allows it to exceed the amplifier limit by very large factors for small proof masses. The assumed parameters are a mechanical resonant frequency of 1 kHz, an amplifier noise number N_A of 1.5×10^6, and the tunneling current $I_{\rm tun}$ is 100 nA. The values of the temperature T and the mechanical quality factor Q_1 were chosen to yield a value of 10^4 for the parameter $(k_BT/\hbar\omega_1)(1/Q_1)$ (Stephenson, Bocko, and Koch, 1989).

ofrio, and Bocko, 1992). In the latter paper practical configurations that allow one to reach the quantum limit were also presented.

The first fundamental obstacle to observing quantum noise with the tunneling transducer is the thermal noise of the mechanical resonator, so we compare the Brownian-noise spectral density of the test mass to the effective noise spectral density due to the quantum measurement process. Dominance by the quantum noise will be assured, provided that the following condition is satisfied:

$$\frac{10^{-6}A}{I_0}\frac{m}{10^{-10}\ \mathrm{kg}}\frac{\theta}{10\ \mathrm{mK}}\frac{f_0}{10^5\ \mathrm{Hz}}\frac{10^7}{Q}<1. \tag{5.1}$$

We assume that $\kappa=10^{10}\ \mathrm{m}^{-1}$; the mass, frequency and Q used in Eq. (5.1) are appropriate to micromachined silicon resonators at low temperatures. A mechanical quality factor of 600 000 was obtained at room temperature in a micromachined silicon torsional resonator of mass 7×10^{-6} kg (Buser and De Rooij, 1990) and a more massive resonator of mass 10^{-3} kg had a similar Q at room temperature and a Q approaching 10^8 at 10 mK (Kaminsky, 1985; Kleiman *et al.*, 1985). Further progress can be expected because systematic studies of the acoustic losses of silicon resonators at cryogenic temperatures indicate that the intrinsic quality factors of silicon are over one billion (Lam, 1979; Braginsky, Mitrofanov, and Panov, 1981; Wajid, 1984). It therefore seems possible to achieve a quality factor of 10^7 with a 10^{-10} kg mechanical resonator at a temperature $T=10$ mK. Microresonators with characteristics close to those required to test quantum mechanics on a mesoscopic scale are routinely used in atomic force microscopy (Akamine, Barrett, and Quate, 1990) and low-temperature scanning tunneling microscopes have been demonstrated (Smith and Binnig, 1986; Lang, Dovek, and Quate, 1989).

Modeling of the electron-barrier interaction in a tunneling transducer has shown that even when only a portion of the tunneling electron energy is imparted to the test mass, the standard quantum limit for the test mass may be approached, even for a small electron mean-free path (Onofrio and Presilla, 1992). More recently it was proposed that a resonant tunneling barrier be employed in a tunnel-probe transducer (Onofrio and Presilla, 1993). A resonant tunneling barrier could be fabricated by depositing a thin-film quantum well on the surface of the test mass. For a given probe-sample bias voltage, the resonant tunneling barrier has a greater tunneling current compared to the nonresonant barrier, thereby increasing the electromechanical coupling of the tunneling transducer to the test mass. To reach the transducer noise limit it is necessary for the transducer momentum-transfer noise to dominate the test-mass Brownian noise; the increased tunneling current in the resonant-barrier configuration allows one to achieve this condition at a higher temperature than the nonresonant case. By using resonant-tunnel barriers, experiments to reach the quantum limit could be performed at 4.2 K provided the other parameter values in Eq. (5.1) are maintained.

In Fig. 20(a) the schematic of a double resonant barrier is shown. The optimal displacement sensitivity versus the energy of the tunneling electrons is shown in Fig. 20(b) for the resonant barrier, the nonresonant barrier for zero temperature and for a finite temperature. It is evident that, in the case of the resonant tunneling configuration, the sensitivity on the tunneling resonance exceeds the nonresonant tunneling transducer by almost two orders of magnitude. Experiments conducted with fixed resonant barriers have shown that the shot noise is reduced in comparison to the expected theoretical value: this has been explained as being due to incoherent tunneling with the so-called sequential model (Li, Tsui, *et al.*, 1990; Li, Zaslasky, *et al.*, 1990; van der Roer *et al.*; 1991, Liu *et al.*, 1995). It is an open question how to evade the standard quantum limit in this class of transducers. The most practical way could be to use stroboscopic techniques by exploiting the ease of charging and discharging the small dynamical capacitance of the tunneling gap, measured in the range of 10^{-17} F (van Bentum *et al.*, 1988).

The Rome group has developed an independent strategy for reaching and surpassing the standard quantum limit using improved versions of their parametric bridge-circuit transducer (Cinquegrana *et al.*, 1995). Since they consider a relatively large mass for the mechanical resonator, a capacitive transducer is a practical alternative to a tunneling-based scheme, thus without the gain of the tunneling transducer it will be crucial to employ a nearly quantum-limited amplifier following the transducer. The primary requirement to perform a QND measurement is that the amplifier noise, N_A, be sufficiently close to the quantum limit that the value of the BAE noise-reduction factor r achievable by the transducer can allow the system to surpass the quantum limit, i.e., $N_A/r<1$. At frequencies below 1 MHz the lowest-noise amplifier available is a SQUID. Intrinsic SQUID noise very close to the quantum limit has been demonstrated (Awschalom, 1988) and the noise of practical SQUID amplifiers that are optimized for gravitational wave antennae are at present about a factor of 100 above the quantum limit. SQUIDs have the further advantage that they have extremely low power dissipation and so would provide nearly no heat load to the experiment's refrigeration system. At frequencies above several MHz there is no reason in principle why a SQUID could not be operated, though such wide-bandwidth SQUIDs do not exist at present. However, very-low-noise transistor amplifiers have been demonstrated at frequencies of several MHz up to 10 or 20 GHz. Below 1 GHz, the best transistor amplifiers operate with noise numbers of several hundred times the quantum limit, but from 1–10 GHz it is possible to obtain amplifiers with noise numbers of 10 to 20, which make the prospect of a QND measurement plausible.

The analysis of the Rome group shows that the transducer developed so far and described in Sec. IV, if cooled down to 1.5 K and equipped with a low-noise SQUID amplifier, can reach a burst noise temperature of 4.4 microkelvin, corresponding to a minimum number

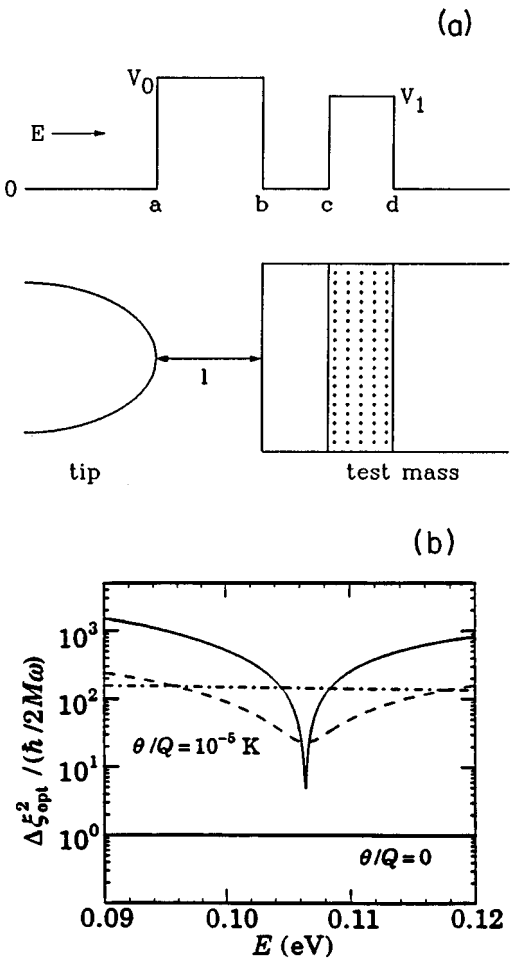

FIG. 20. The resonant electron-tunneling transducer: (a) resonant tunneling barrier and its corresponding potential-energy diagram. A second tunneling barrier, indicated by the textured region, is fabricated on the surface of the test mass. The barrier heights for the vacuum-metal and barrier-metal interfaces are assumed to be V_0 and V_1, respectively. (b) The maximum achievable displacement sensitivity (in units of the standard quantum limit) vs the energy of the tunneling electrons for resonant (solid line) and nonresonant (dashed-dotted line) barriers for a temperature θ of zero and for a finite temperature, where Q is the mechanical quality factor of the microresonator. At finite temperatures the tunneling current is greatly enhanced at the resonant energy of the tunneling barrier, and the optimally achievable noise is reduced. Of course, at zero temperature both the resonant and the nonresonant tunneling transducers are quantum limited. The dashed line is relative to the case of sequential tunneling with a damping factor of the wave function—proportional to the inelastic phonon scattering along the barrier—of 0.95 (instead of 1 for the coherent tunneling of the solid line), which slightly diminishes the gain in the resonant configuration. Calculations have been made for microresonators with masses of the order of 10^{-10} kg and other parameters close to those in Eq. (5.1) (Onofrio and Presilla, 1993).

of one hundred detectable phonons with a signal-to-noise ratio of unity. If the same transducer is cooled down to a temperature of 8 mK, they estimate an effective noise temperature of about 20 nK, corresponding to about one-half a phonon. The model used to evaluate such figures is based upon classical equations of motion (Cinquegrana *et al.*, 1993), and therefore the results obtained in the quantum limit should be taken only as a guide.

B. The first back-action-evading gravitational wave antenna

A joint effort of the groups at the University of Rome and at the CNR in Frascati resulted in the first implementation of a back-action evasion scheme on a cryogenic gravitational wave bar antenna coupled to a resonant transducer (Bonifazi *et al.*, 1996). The antenna used was the 270 Kg aluminum alloy 5056 cryogenic bar located at the CNR in Frascati-Altair—operating since 1978 (Giovanardi, 1981) and recently upgraded for long-term runs (Bassan *et al.*, 1990; Bonifazi and Visco, 1993). A resonant transducer similar to the one described in Sec. IV.D was designed to have its frequency at the first longitudinal mode of the bar. The measured frequencies of the two normal modes of the coupled system were equal to ν_-=1783.845 Hz and ν_+=1826.079 Hz at 4.2 K, and the mass ratio was $\mu=5.7\times10^{-4}$. Both the normal modes showed mechanical quality factors of 3×10^6. A push-pull capacitive coupling scheme to the transducer was part of a capacitive bridge circuit in which two other variable capacitors were present, one for coarse-range (0–120 pF) and one for fine-range (0–20 pF) balancing of the bridge circuit at 4.2 K. Two superconducting niobium transformers were used to decouple the capacitance bridge from the pumps and the output amplifier. The transduced signal was amplified and processed through a conventional FET amplifier and a lock-in amplifier.

In a previous analysis, Cinquegrana *et al.* (1994) considered a back-action-evading measurement for a two-mechanical-mode system with normal-mode angular frequencies at ω_+ and ω_-. Their conclusion was that, by supplying a parametric pump excitation of the form

$$V(t)=V_0(\cos\omega_2 t\,\cos\omega_+ t+\cos\omega_2 t\,\cos\omega_- t), \qquad (5.2)$$

one may perform a back-action evasion measurement simultaneously on each of the two antenna normal modes. Measurements were carried out both with the usual single-mode BAE pumping and in the double-mode configuration, described by Eq. (5.2), using four pumps at the sum and the difference of the electrical and the two normal mode frequencies. The minimum bridge imbalance was obtained at an electrical frequency of 210 kHz, but it was quite large—2×10^{-4}; consequently the sensitivity of the antenna for reasonable values of the pump voltage used in the tests (V_0 was in the 10 V range) was dominated by the pump amplitude and phase noise. Even with this limitation they were able to test the forward transducer coupling and the noise behavior in both the BAE configurations. In the pumping mode of Eq. (5.2), a continuous run of about two hours resulted in the power spectra for the lock-in integrated data shown in Fig. 21. On the x spectrum two mechani-

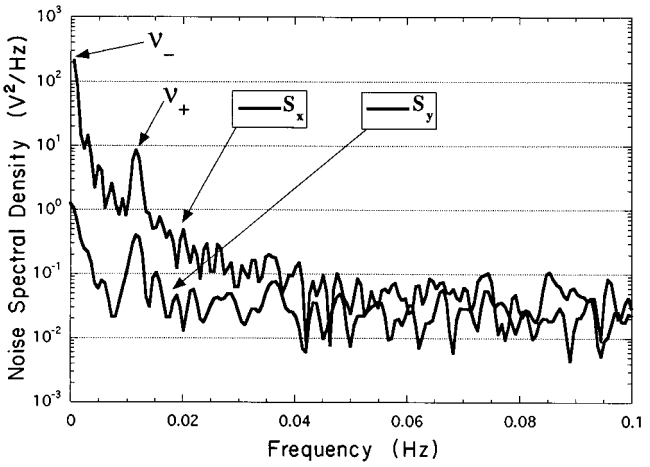

FIG. 21. Power spectra of the two quadrature phases of the Altair BAE gravitational wave antenna (Bonifazi *et al.*, 1996). The two mechanical modes are labeled ν_- and ν_+.

cal peaks shifted by 11 mHz appear due to a small difference in the frequency setting of the pumps, while the spectrum of the *y* component is depressed with respect to the former, around zero frequency, by two orders of magnitude. The best balance of the transducer bridge circuit operated separate from the antenna was measured to be 2×10^{-6}; the difference from the best achieved balance of the transducer working with the antenna was attributed to residual resistive imbalance. If this imbalance were achieved for the transducer working on the antenna and by employing commercially available low-noise synthesizers as pump sources and low-noise FET amplifiers to read out the bridge signal, the burst noise temperature of Altair could be improved to 100 μK. The tests on Altair are encouraging for the implementation of back-action evasion transduction schemes on resonant gravitational wave antennae and give experimental support to the sensitivity analysis discussed in Cinquegrana *et al.* (1994). With readily available commercial technologies it should be possible to operate the Rome 2 K antenna Explorer (Astone *et al.*, 1993) at a burst noise temperature below 100 μK, and that the 100 mK antenna Nautilus (Astone *et al.*, 1991) should be able to surpass 10 μK in noise temperature. The predicted performance levels will require bridge-circuit imbalance of the order of one part in 10^7 and pump phase noise of –165 dBc/$\sqrt{\text{Hz}}$—these are, however, within reach.

C. Single-electron and single-ion spectroscopy

Quantum nondemolition concepts also have been applied to spectroscopy of trapped electrons and ions, both in theoretical proposals and in experiments, with the aim of performing quantum measurements on microscopic single particles and improving the sensitivity in the cases where the results are limited by the measurement apparatus. In the first approximation, the axial motion of an electron or an ion in a Penning trap is harmonic, the nonlinearities arising from the magnetic fields used to confine the transverse motion of the particle or by the relativistic corrections to the particle mass (for a review, see Brown and Gabrielse, 1986).

Back-action evasion techniques were suggested as a means to control the bistability of the cyclotron motion of an electron in a Penning trap, specifically by using a phase-sensitive detection scheme proposed by Bagini, Lerner, and Tombesi (1992), and by Lerner and Tombesi (1993). Taking the nonlinearities into account, the steady-state solution of a trapped particle's cyclotron motion branches into two regions, which can be experimentally accessed by changing the relative phase of the coupling to the macroscopic measurement device and the cyclotron resonance. The hysteresis curve of the bistable cyclotron motion thereby may be modified by varying the quantum properties of the measuring apparatus. In a further analysis, Marzoli and Tombesi (1993) proposed quantum nondemolition measurements of the cyclotron energy through the relativistic coupling to the axial motion of the electron in the Penning trap.

Concrete ways to perform phase-sensitive measurements on trapped ions have been studied (DiFilippo *et al.*, 1992). Amplitude squeezing can be obtained, as in the Almaden experiment described in the previous section, by driving the motion of the ion at twice its axial frequency. Due to the presence of controllable anharmonicities however, it is also possible to exploit the amplitude-dependent dephasing without driving oscillations. The expected reduction of the thermal uncertainty in the relativistic frequency shift in single-ion spectroscopy is about a factor of 5. An experiment has been performed by using a single Ne^+ ion in a Penning trap (Natarajan, DiFilippo, and Pritchard, 1995). The thermal motion of the ion in the axial mode was squeezed by modulating the ion-trapping potential at twice the axial frequency. Before squeezing, the rms thermal motion of the ion was about 100 μm at 4.2 K and after squeezing the quiet phase was reduced to about 15 μm rms motion. The squeezed axial excitation was read out in the following way. First, the squeezed noise was transferred to the ion cyclotron motion by applying an electromagnetic pulse that coupled the two modes, then the cyclotron mode was provided a further excitation which could be varied in phase angle with respect to the phase of the squeezed noise. The cyclotron motion energy was then read out by measuring the frequency of the axial mode. Repeating this experiment a large number of times for each phase value allowed the experimenters to determine the variance in axial frequency as a function of the phase of the parametric squeezing excitation pulse. They observed a noise reduction of about 6 dB in the quiet phase of the oscillator, as shown in Fig. 22. Although the experiment was performed in the classical limit, it was pointed out that it may be possible to squeeze quantum noise by applying their technique to laser-cooled ions thereby possibly reducing the noise of spectroscopic measurement.

A spectroscopic application in which the pure quantum noise should instead be reduced below the standard quantum limit in ensembles of two-level or spin-1/2 sys-

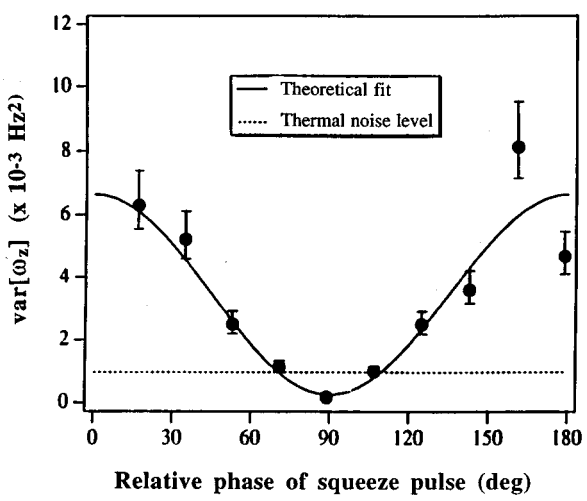

FIG. 22. Variance plot of the axial frequency noise versus the relative phase of a pulse used to squeeze one quadrature component of the axial motion of a trapped Ne ion. The maximum noise reduction is 6 dB, obtained for a phase difference of 90° (Natarajan, DiFilippo, and Pritchard, 1995).

tems has been discussed by Wineland *et al.* (1992). The preparation of correlated squeezed states of N two-level atoms could allow an increase of the signal-to-noise ratio in state population measurements by a factor approximately equal to $N^{1/2}$.

D. Superconducting tunnel junctions

QND measurements have been applied to nearly quantum-limited superconducting tunnel junctions in the attempt to circumvent the quantum noise in purely electrical systems. Josephson junctions have very low dissipation and also present a strong quadratic dependence of their effective inductance upon the current. Thus they can be exploited, as suggested by Braginsky and Viatchanin (1983), to measure energy through the Unruh-Braginsky interaction Hamiltonian [Eq. (2.25)]. This proposal was not pursued further: instead, the back-action evasion scheme proposed by Caves *et al.* (1980) was used in rf SQUIDs (Bordoni *et al.*, 1985) and in superconducting tunnel junction mixers (Bocko *et al.*, 1991).

In the first experiment the SQUID was coupled to two resonant circuits, an input and an output one, tuned to 2 MHz and 23.4 MHz respectively (with quality factors of 2000 and 200). Parametric upconversion was obtained by providing a pump to the Josephson junction via a third coil through which a superposition of the sum and the difference of the other two frequencies was sent. The phase sensitivity of the scheme was experimentally shown, but noise measurements to show the expected reduction of the back action were not possible due to the overwhelming pump noise relative to the intrinsically low SQUID noise.

In other experiments, a superconducting tunnel junction mixer was simultaneously pumped at the sum and difference of a signal input frequency and the lower output frequency, called the RF and the IF in keeping with mixer convention, to attempt to achieve phase-sensitive response and reduced noise in one of the mixer phases (Bocko, Wengler, and Zhang, 1989; Wengler and Bocko, 1989).

Experiments on a 65.5 GHz microwave cavity coupled to a superconducting tunnel junction mixer pumped by two coherent local oscillators at frequencies of 64 and 67 GHz demonstrated the expected phase-sensitive response of the mixer to the cavity mode (Bocko *et al.*, 1991). A reduction of the mixer noise was not demonstrated however, due to excess shot noise from the leakage current of the tunnel junctions available for these experiments. However, simulations suggested that for ideal tunnel junctions, with very low subgap current, a modest improvement over the mixer's quantum-limited noise temperature should be possible (Zhang *et al.*, 1989).

Finally, analogous to the mechanical parametric amplifier, amplification and deamplification of thermal noise has been observed with a Josephson parametric amplifier (Yurke *et al.*, 1988, 1989). By varying the relative phase between the amplifier's local oscillator and the input signal, the phase dependence of the amplifier gain was measured, observing parametric deamplification of the signal. The excess noise of the amplifier was measured to be 0.28 K referred to the input, smaller than the vacuum fluctuation level equal to 0.47 K. Thus deamplification of the quiet phase to a sub-quantum-limit noise temperature was achieved.

VI. CONCLUSIONS

In this review, we have summarized the results obtained from experiments in the last two decades to understand whether the *gedanken* experiments on the uncertainty principle discussed by Heisenberg at the beginning of quantum theory will be practical with currently available or near-future technology. Models to guide the design of concrete experimental configurations for monitoring macroscopic harmonic oscillators have been discussed in the classical limit. It is noteworthy that quantum nondemolition strategies also have an imprint in the classical limit, an illustration of the correspondence principle, by allowing one to evade the amplifier noise limit in measurements well above quantum-limited sensitivity. This result also has been shown to appear without any reference to quantum theory but rather as an extension of well-known parametric processes. Furthermore, we have reviewed the first generation of electromechanical QND experiments.

Measurements of displacements of macroscopic mechanical oscillators are still far from reaching the quantum regime, in contrast to the recent progress in nonlinear optics where production and manipulation of nonclassical photon states is becoming a routine activity in many laboratories. It is a formidable experimental challenge to reach the quantum limit in the low-frequency mechanical experiments, due to the effect of

the environment, and other sources of noise such as the fluctuations present in the pump oscillators used to modulate the interaction of the mechanical oscillator with the electrical readout system. However, continuing experimental efforts in these areas will reward researchers with the opportunity to reach a number of other ambitious experimental goals. One such goal is the production of nonclassical states of single macroscopic degrees of freedom. The creation of nonclassical states in macroscopic systems will demand a reconciliation of the predictions of quantum mechanics for individual trials of an experiment with the results predicted by semiclassical theories. Another experiment of this sort will address the interplay between quantum and classical fluctuations in open quantum systems by studying the decay of nonclassical states through decoherence induced by the environment (Zurek, 1990; Zurek, Habib, and Paz, 1993). Both of these issues have been studied in the context of rf SQUIDs (Leggett and Garg, 1985; Tesche, 1990) and cavity QED (Brune *et al.*, 1990, 1992; Haroche, 1992). In the context of measurements on mechanical oscillators, the same issues appear simultaneously in a relatively simply modeled system. This apparent simplicity of the model itself gives rise to some fundamental questions. A macroscopic object is composed of an enormous number of microscopic degrees of freedom, each one well described by quantum-mechanical laws, but is the quantum behavior of macroscopic degrees of freedom completely deducible from the dynamics of the microscopic constituents? If not, what is the kinematic origin for the degree of *macroscopic quantum complexity* one must introduce? Some of these issues will also be studied in a near future through Bose-Einstein condensates of atomic clouds recently obtained in various laboratories (Anderson *et al.*, 1995; Bradley *et al.*, 1995; Davis *et al.*, 1995), and quantum measurements on macroscopic degrees of freedom could complement these investigations.

In addition to the fundamental issues, work on back-action evasion measurements is yielding improvements in the sensitivity of measurement apparatuses for several high-precision physics experiments. Gravitational wave antennae are the most mature among the applications of these principles—indeed, the effort to improve their sensitivity provided the motivation for QND measurements. Gravitational wave astronomy requires measurements of perturbations of the space-time metric of the order of 10^{-21}, requiring a similar sensitivity for measurements of the relative displacement of the macroscopic objects comprising a gravitational wave antenna. The De Broglie wavelength associated with a macroscopic gravitational wave antenna is the same magnitude, so unless antennae masses are scaled up by a factor of 10^2 or more, which is highly unlikely, every sensitive gravitational wave bar detector will face the standard quantum limit as it approaches the interesting range of sensitivity. Back-action evasion measurement techniques offer a viable road to overcome this limit. The impact of back-action evasion measurements in high-precision spectroscopic measurements and other quantum-limited devices such as SQUID's is still in its infancy: however, besides stimulating theoretical proposals we have described a few experiments that are moving in these directions.

Finally, we briefly mention the importance of the quantum nondemolition concepts in quantum estimation theory (Helstrom, 1976). From this point of view quantum nondemolition measurements provide a way to achieve optimal information transfer, i.e., one in which the detection probability is maximized for a fixed false-alarm probability (Hollenhorst, 1979; Braginsky and Khalili, 1983; for entropic considerations see also Vourdas, 1990). The connection of this aspect of QND measurements with quantum communication theory (Bekenstein and Schiffer, 1990; Caves and Drummond, 1994) and quantum-mechanical computers (Feynman, 1986) remains an open question.

ACKNOWLEDGMENTS

We are grateful to our collaborators and colleagues working to make quantum-limited macroscopic measurements an experimental reality, and whose efforts have made the writing of this review worthwhile. In particular we would like to acknowledge F. Bordoni, V. B. Braginsky, T. Calarco, D. Douglass, M. Fisher, the late F. Fuligni, V. Iafolla, W. W. Johnson, M. Karim, E. Majorana, L. Marchese, M. B. Mensky, C. Presilla, P. Rapagnani, F. Ricci, S. Schiller, P. Tombesi, G. Zhang, and Z. Zhang. We would like to acknowledge the support of the National Science Foundation under Grant No. PHY 9102164. One of us (R.O.) also acknowledges the Consiglio Nazionale delle Ricerche and the Istituto Nazionale di Fisica Nucleare, Sezioni di Roma 1 and Padova, for financial support.

REFERENCES

Adachi, S., M. Toda, and K. Ikeda, 1989, J. Phys. A **22**, 3291.
Aguiar, O. D., W. W. Johnson, and W. O. Hamilton, 1991, Rev. Sci. Instrum. **62**, 2523.
Aharonov, Y., and D. Bohm, 1961, Phys. Rev. **122**, 1649.
Aharonov, Y., and D. Bohm, 1964, Phys. Rev. B **134**, 1417.
Aharonov, Y., and A. Petersen, 1971, in *Quantum Theory and Beyond*, edited by T. Bastin (Cambridge University, Cambridge), p. 135.
Akamine, S., R. C. Barrett, and C. F. Quate, 1990, Appl. Phys. Lett. **57**, 316.
Amaldi, E., and G. Pizzella, 1979, in *Relativity, Quanta and Cosmology in the Development of the Scientific Thought of Albert Einstein*, edited by F. De Finis (Johnson Reprint, New York), p. 282.
Anderson, M. H., J. R. Ensher, M. R. Matthews, C. E. Wieman, and E. A. Cornell, 1995, Science **269**, 198.
Astone, P., M. Bassan, P. Bonifazi, P. Carelli, M. G. Castellano, G. Cavallari, E. Coccia, C. Cosmelli, V. Fafone, S. Frasca, E. Majorana, I. Modena, G. V. Pallottino, G. Pizzella, P. Rapagnani, F. Ricci, and M. Visco, 1993, Phys. Rev. D **47**, 362.
Astone, P., M. Bassan, P. Bonifazi, M. G. Castellano, E. Coccia, C. Cosmelli, V. Fafone, S. Frasca, E. Majorana, I.

Modena, G. Pallottino, G. Pizzella, P. Rapagnani, F. Ricci, and M. Visco, 1991, Europhys. Lett. **16**, 231.
Awschalom, D. D., J. R. Rozen, M. B. Ketchen, W. J. Gallagher, A. W. Kleinsasser, R. L. Sandstrom, and B. Bumble, 1988, Appl. Phys. Lett. **53**, 2108.
Bachor, H. A., M. D. Levenson, D. F. Walls, S. H. Perlmutter, and R. M. Shelby, 1988, Phys. Rev. A **38**, 180.
Bagini, V., P. Lerner, and P. Tombesi, 1992, in *Quantum Measurement in Optics*, edited by P. Tombesi and D. F. Walls (Plenum, New York), p. 105.
Barchielli, A., 1983, Nuovo Cimento B **74**, 113.
Barchielli, A., 1985, Phys. Rev. D **32**, 347.
Barchielli, A., 1986, Phys. Rev. A **34**, 1642.
Barchielli, A., L. Lanz, and G. M. Prosperi, 1982, Nuovo Cimento B **72**, 121.
Barro, E., R. Onofrio, P. Rapagnani, and F. Ricci, 1988, in *International Symposium on Experimental Gravitational Physics: Guangzhou, China, 3–8 August 1987*, edited by P. F. Michelson (World Scientific, Singapore), p. 363.
Bassan, M., P. Bonifazi, F. Bordoni, M. G. Castellano, V. Iafolla, and M. Visco, 1990, Astron. Astrophys. **233**, 285.
Bekenstein, J. D., and M. Schiffer, 1990, Int. J. Mod. Phys. C, Phys. Comput. **1**, 355.
Belavkin, V. P., 1989, Phys. Lett. A **140**, 355.
Belavkin, V. P., O. Hirota, and R. L. Hudson, Eds., 1995, *Quantum Communications and Measurements* (Plenum, New York).
Belavkin, V. O., and P. Staszewski, 1989, Phys. Lett. A **140**, 359.
Blair, D., 1982, Phys. Lett. A **104**, 335.
Bocko, M. F., 1990, Rev. Sci. Instrum. **61**, 3763.
Bocko, M. F., F. Bordoni, F. Fuligni, and W. W. Johnson, 1986, in *Physical Noise and 1/f Noise*, edited by A. D'Amico and P. Mazzetti (Elsevier, Amsterdam), p. 47.
Bocko, M. F., and W. W. Johnson, 1982, Phys. Rev. Lett. **48**, 1371.
Bocko, M. F., and W. W. Johnson, 1984, Phys. Rev. A **30**, 2135.
Bocko, M. F., and W. W. Johnson, 1986, in *New Techniques and Ideas in Quantum Measurement Theory*, edited by D. M. Greenberger, Annals of the New York Academy of Sciences Vol. 480 (New York Academy of Sciences, New York).
Bocko, M. F., and W. W. Johnson, 1989, in *Gravitational Wave Data Analysis*, edited by B. F. Schutz (Kluwer Academic, Dordrecht/Boston), p. 125.
Bocko, M. F., W. W. Johnson, and V. Iafolla, 1989, IEEE Trans. Magn. **25**, 1358.
Bocko, M. F., L. Narici, D. H. Douglass, and W. W. Johnson, 1984, Phys. Lett. A **104**, 335.
Bocko, M. F., K. A. Stephenson, and R. Koch, 1988, Phys. Rev. Lett. **61**, 726.
Bocko, M. F., M. J. Wengler, and Z. N. Zhang, 1989, IEEE Trans. Magn. **25**, 1038.
Bocko, M. F., Z. Zhang, and S. Martinet, 1991, IEEE Trans. Magn. **27**, 3391.
Bohm, D., 1951, *Quantum Theory* (Prentice-Hall, Englewood Cliffs, NJ), p. 583.
Bohr, N., and Rosenfeld, L., 1933, Mat.-Fys. Medd. K. Dan. Vidensk. Selsk. **12**, No. 8 [English translation by A. Petersen, in *Selected Papers of Leon Rosenfeld*, edited by R. S. Cohen and J. J. Stachel (Reidel, Dordrecht, 1979), p. 357].
Bohr, N., and L. Rosenfeld, 1950, Phys. Rev. **78**, 794.
Bonifazi, P., C. Cinquegrana, E. Majorana, N. Pergola, P. Puppo, P. Rapagnani, F. Ricci, G. Vannaroni, and M. Visco, 1996, Phys. Lett. A **215**, 141.
Bonifazi, P., and M. Visco, 1993, Nuovo Cimento C **15**, 943.
Bordoni, F., P. Carelli, V. Foglietti, and F. Fuligni, 1985, IEEE Trans. Magn. **21**, 421.
Bordoni, F., S. De Panfilis, F. Fuligni, V. Iafolla, and S. Nozzoli, 1986, in *Proceedings of the Fourth Marcell Grossmann Meeting on General Relativity*, edited by R. Ruffini (North-Holland, Amsterdam), p. 523.
Bordoni, F., F. Fuligni, and V. Iafolla, 1990, Nuovo Cimento C **13**, 49.
Bordoni, F., M. Karim, M. F. Bocko, and T. Mengxi, 1990, Phys. Rev. D **42**, 2952.
Bordoni, F., and R. Onofrio, 1990, Phys. Rev. A **41**, 21.
Bradley, C. C., C. A. Sackett, J. J. Tollett, and R. G. Hulet, 1995, Phys. Rev. Lett. **75**, 1687.
Braginsky, V. B., 1967, Zh. Eksp. Teor. Fiz. **53**, 1434 [Sov. Phys. JETP **26**, 831 (1968)].
Braginsky, V. B., 1971, *Physical Experiments with Test Bodies* (Nauka, Moscow) [English translation published as NASA-TT F672, National Technical Information Service, Springfield, VA (1971)].
Braginsky, V. B., 1974, in *Gravitational Radiation and Gravitational Collapse, Proceedings of IAU Symposium No. 64*, edited by Cecile DeWitt-Morette (Reidel, Dordrecht), p. 28.
Braginsky, V. B., 1988, Usp. Fiz. Nauk. **156**, 93 [Sov. Phys. Usp. **31**, 836 (1989)].
Braginsky, V. B., 1989, in *Proceedings of the Third International Symposium on Foundations of Quantum Mechanics*, edited by S. Kobayashi, H. Ezawa, Y. Murayama, and S. Nomura (The Physical Society of Japan, Tokyo), p. 135.
Braginsky, V. B., C. M. Caves, and K. S. Thorne, 1977, Phys. Rev. D **15**, 2047.
Braginsky, V. B., M. L. Gorodetsky, and V. S. Il'chenko, 1989, Phys. Lett. A **137**, 393.
Braginsky, V. B., V. S. Il'chenko, and Kh. S. Bagdassarov, 1987, Phys. Lett. A **120**, 300.
Braginsky, V. B., and F. Ya. Khalili, 1983, Zh. Eksp. Teor. Fiz. **84**, 1930 [Sov. Phys. JETP **57**, 1124 (1983)].
Braginsky, V. B., and F. Ya. Khalili, 1990, Phys. Lett. A **147**, 251.
Braginsky, V. B., and F. Ya. Khalili, 1991, *Quantum Measurements* (Cambridge University Press, Cambridge).
Braginsky, V. B., and F. Ya. Khalili, 1996, Rev. Mod. Phys. **68**, 1.
Braginsky, V. B., V. P. Mitrofanov, and V. I. Panov, 1981, *Sistemi s maloi dissipatsei* (Nauka, Moscow) [English translation: *Systems with Small Dissipation* (University of Chicago, Chicago, 1985)].
Braginsky, V. B., and V. S. Nazarenko, 1969, Zh. Eksp. Teor. Fiz. **57**, 1421 [Sov. Phys. JETP **30**, 770 (1970)].
Braginsky, V. B., V. I. Panov, V. G. Petnikov, and V. D. Popel'nyuk, 1977, Prib. Tekh. Eksp. **20**(1), 234 [Instrum. Exp. Tech. (USSR) **20**, 269 (1977)].
Braginsky, V. B., and Yu. I. Vorontsov, 1974, Usp. Fiz. Nauk **114**, 41 [Sov. Phys. Usp. **17**, 644 (1975)].
Braginsky, V. B., Yu. Vorontsov, and F. Ya. Khalili, 1977, Zh. Eksp. Teor. Fiz. **73**, 1340 [Sov. Phys. JETP **46**, 705 (1977)].
Braginsky, V. B., Yu. Vorontsov, and F. Ya. Khalili, 1978, Zh. Eksp. Teor. Fiz. Pis'ma Red. **27**, 296 [Sov. Phys. Lett. JETP **27**, 276 (1978)].

Braginsky, V. B., Yu. I. Vorontsov, and V. D. Krivchenkov, 1975, Zh. Eksp. Teor. Fiz. **68**, 55 [Sov. Phys. JETP **41**, 28 (1975)].
Braginsky, V. B., Yu. Vorontsov, and K. S. Thorne, 1980, Science **209**, 547.
Braginsky, V. B., and S. P. Vyatchanin, 1983, IEEE Trans. Magn. Vol.-MAG **19**, No. 3, 570.
Braginsky, V. B., and S. P. Vyatchanin, 1988, Phys. Lett. A **132**, 206.
Breuer, H. P., and F. Petruccione, 1995, Phys. Rev. Lett. **74**, 3788.
Brown, L., and G. Gabrielse, 1986, Rev. Mod. Phys. **58**, 233.
Brune, M., S. Haroche, V. Lefevre, J. M. Raimond, and N. Zagury, 1990, Phys. Rev. Lett. **65**, 976.
Brune, M., S. Haroche, J. M. Raimond, L. Davidovich, and N. Zagury, 1992, Phys. Rev. A **45**, 5193.
Buser, R. A., and N. F. De Rooij, 1990, Sensors and Actuators **A21–A23**, 323.
Calarco, T., and R. Onofrio, 1995, Phys. Lett. A **198**, 279.
Caldeira, A. O., and A. J. Leggett, 1983a, Ann. Phys. (NY) **149**, 374.
Caldeira, A. O., and A. J. Leggett, 1983b, Physica A **121**, 587.
Carmichael, H. J., 1993, *An Open System Approach to Quantum Optics*, Lecture Notes in Physics Vol. 18 (Springer, Berlin).
Carmichael, H. J., S. Singh, R. Vyas, and P. R. Rice, 1989, Phys. Rev. A **39**, 1200.
Casati, G., and B. Chirikov, Eds., 1994, *Quantum Chaos: Between Order and Disorder* (Cambridge University Press, Cambridge).
Casati, G., and B. Chirikov, 1995, Physica D **86**, 220.
Caves, C. M., 1985, Phys. Rev. Lett. **54**, 2465.
Caves, C. M., 1986, Phys. Rev. D **33**, 1643.
Caves, C. M., 1987, Phys. Rev. D **35**, 1815.
Caves, C. M., 1989, in *Squeezed and Nonclassical Light*, edited by P. Tombesi and E. R. Pike (Plenum, New York), p. 29.
Caves, C. M., and P. D. Drummond, 1994, Rev. Mod. Phys. **66**, 481.
Caves, C. M., K. S. Thorne, R. W. P. Drever, V. D. Sandberg, and M. Zimmermann, 1980, Rev. Mod. Phys. **52**, 341.
Cinquegrana, C., E. Majorana, N. Pergola, P. Puppo, P. Rapagnani, and F. Ricci, 1994, Phys. Rev. D **50**, 3596.
Cinquegrana, C., E. Majorana, N. Pergola, P. Puppo, P. Rapagnani, and F. Ricci, 1995, Dipartimento di Fisica, Università di Roma ''La Sapienza'' Preprint No. 1032, March 1994.
Cinquegrana, C., E. Majorana, P. Rapagnani, and F. Ricci, 1993, Phys. Rev. D **48**, 448.
Collot, L., V. Lefèvre-Seguin, M. Brune, J. M. Raimond, and S. Haroche, 1993, Europhys. Lett. **23**, 327.
Davies, E. B., 1976, *Quantum Theory of Open Systems* (Academic, London).
Davis, K. B., M.-O. Mewes, M. R. Andrews, N. J. van Druten, D. S. Durfee, D. M. Kurn, and W. Ketterle, 1995, Phys. Rev. Lett. **75**, 3969.
Decroly, J. C., L. Laurent, J. C. Lienard, G. Marechal, and J. Vorsbeitchik, 1973, Parametric Amplifiers (MacMillan, London).
DiFilippo, F., V. Natarajan, K. R. Boyce, and D. E. Pritchard, 1992, Phys. Rev. Lett. **68**, 2859.
Diosi, L., 1988a, J. Phys. A **21**, 2885.
Diosi, L., 1988b, Phys. Rev. A **129**, 419.
Diosi, L., 1989, Phys. Rev. A **40**, 1165.
Dodonov, V. V., V. I. Man'ko, and V. N. Rudenko, 1980, Zh. Eksp. Teor. Fiz. **78**, 881 [Sov. Phys. JETP **51**, 443 (1980)].
Douglass, D. H., and V. B. Braginsky, 1979, in *General Relativity: An Einstein Centenary Survey*, edited by S. W. Hawking and W. Israel (Cambridge University, Cambridge), p. 90.
Drummond, P. D., R. M. Shelby, S. R. Friberg, and Y. Yamamoto, 1993, Nature **365**, 307.
Elsasser, W. M., 1937, Phys. Rev. **52**, 987.
Escobar, C. O., L. Ferreira dos Santos, and P. C. Marques F., 1994, Phys. Rev. A **50**, 1913.
Exner, P., 1985, *Open Quantum Systems and Feynman Integrals* (Reidel, Dordrecht).
Feynman, R. P., 1948, Rev. Mod. Phys. **20**, 367.
Feynman, R. P., 1986, Found. Phys. **16**, 507.
Feynman, R. P., and A. R. Hibbs, 1965, *Quantum Mechanics and Path Integrals* (McGraw-Hill, New York).
Feynman, R. P., and F. L. Vernon, 1963, Ann. Phys. **24**, 118.
Fisher, M. A., M. F. Bocko, L. E. Marchese, G. Zhang, and M. Karim, 1995, Rev. Sci. Instrum. **66**, 106.
Fock, V. A., 1962, Zh. Eksp. Teor. Fiz. **42**, 1135 [Sov. Phys. JETP **15**, 784 (1962)].
Fock, V. A., 1965, Usp. Fiz. Nauk. **86**, 363 [Sov. Phys. Usp. **8**, 628 (1966)].
Friberg, S. R., S. Machida, and Y. Yamamoto, 1992, Phys. Rev. Lett. **69**, 3165.
Fuligni, F., 1982, Internal Report IFSI-CNR, Frascati.
Fuligni, F., and V. Iafolla, 1983, in *Proceedings of the Third Marcell Grossmann Meeting on General Relativity*, edited by Hu Ning (Science Press, Beijing and North-Holland, Amsterdam), p. 1451.
Gagen, M. J., and G. J. Milburn, 1993, Phys. Rev. A **47**, 1467.
Gagen, M. J., H. M. Wiseman, and G. J. Milburn, 1993, Phys. Rev. A **48**, 132.
Ghirardi, G. C., A. Rimini, and T. Weber, 1986, Phys. Rev. D **34**, 470.
Giacobino, E., and C. Fabre, Eds., 1992, Appl. Phys. B **55** (Special issue on squeezed states and nonclassical light).
Giffard, R., 1976, Phys. Rev. D **14**, 2478.
Giovanardi, U., V. Iafolla, P. Napoleoni, B. Pavan, S. Ugazio, and F. Ricci, 1981, J. Phys. E **14**, 1067.
Gisin, N., 1984a, Phys. Rev. Lett. **52**, 1657.
Gisin, N., 1984b, Phys. Rev. Lett. **53**, 1776.
Gisin, N., and I. C. Percival, 1992a, J. Phys. A **25**, 5677.
Gisin, N., and I. C. Percival, 1992b, Phys. Lett. A **167**, 315.
Gorini, V., A. Kossakowski, and E. C. G. Sudarshan, 1976, J. Math. Phys. **17**, 821.
Grangier, P., J. M. Courty, and S. Reynaud, 1992, Opt. Commun. **89**, 99.
Grangier, P., J. F. Roch, and G. Roger, 1991, Phys. Rev. Lett. **66**, 1418.
Greywall, D. S., B. Yurke, P. A. Busch, A. N. Pargellis, and R. L. Willett, 1994, Phys. Rev. Lett. **72**, 2992.
Griffits, R. B., 1984, J. Stat. Phys. **36**, 219.
Grishchuk, L. P., and M. V. Sazhin, 1975, Zh. Eksp. Teor. Fiz. **68**, 1569 [Sov. Phys. JETP **41**, 787 (1975)].
Guerra, F., 1981, Phys. Rep. **77**, 121.
Haroche, S., 1992, in *Les Houches Summer School, Session LIII, Fundamental Systems in Quantum Optics*, edited by J. Dalibard, J. M. Raimond, and J. Zinn-Justin (Elsevier Science, Amsterdam), p. 26.
Haus, H. A., and J. A. Mullen, 1962, Phys. Rev. **128**, 2407.
Heffner, H., 1962, Proc. IRE **50**, 1604.

Helstrom, C. W., 1976, *Quantum Detection and Estimation Theory* (Academic, New York).
Holland, M. J., M. J. Collett, D. F. Walls, and M. D. Levenson, 1990, Phys. Rev. A **42**, 2995.
Hollenhorst, J. N., 1979, Phys. Rev. D **19**, 1669.
Ilchenko, V. S., and M. L. Gorodetsky, 1992, Laser Phys. **2**, 1004.
Ivanov, E. N., P. J. Turner, and D. G. Blair, 1993, Rev. Sci. Instrum. **64**, 3191.
Ivanov, E. N., P. J. Turner, M. E. Tobar, and D. G. Blair, 1993, Rev. Sci. Instrum. **64**, 1905.
Johnson, W. W., and M. F. Bocko, 1981, Phys. Rev. Lett. **47**, 1184.
Kaminsky, G., 1985, J. Vac. Sci. Technol. B **3**, 1015.
Kleiman, R. N., G. K. Kaminsky, J. D. Reppy, R. Pindak, and D. J. Bishop, 1985, Rev. Sci. Instrum. **56**, 208.
Lam, C. C., 1979, Ph.D. thesis, University of Rochester.
Landau, L. D., R. Peierls, 1931, Z. Phys. **69**, 56.
Lang, C. A., M. M. Dovek, C. F. Quate, 1989, Rev. Sci. Instrum. **60**, 3109.
La Porta, A., R. E. Slusher, and B. Yurke, 1989, Phys. Rev. Lett. **62**, 28.
Lavren'tev, G. Ya., 1969, Zh. Tekh. Fiz. **39**, 1316 [Sov. Phys.-Tech. Phys. **14**, 989 (1970)].
Leggett, A. J., 1986, in *New Techniques and Ideas in Quantum Measurement Theory*, edited by D. M. Greenberger, Annals of the New York Academy of Sciences Vol. 480 (New York Academy of Sciences, New York).
Leggett, A. J., and A. Garg, 1985, Phys. Rev. Lett. **54**, 857.
Lerner, P., and P. Tombesi, 1993, Phys. Rev. A **47**, 4436.
Levenson, M. D., R. M. Shelby, M. Reid, and D. F. Walls, 1986, Phys. Rev. Lett. **57**, 2473.
Li, Y. P., C. Tsui, J. J. Heremans, J. A. Simmons, and G. W. Weimann, 1990, Appl. Phys. Lett. **57**, 774.
Li, Y. P., A. Zaslasky, D. C. Tsui, M. Santos, and M. Shayegan, 1990, Phys. Rev. B **41**, 8388.
Lindblad, G., 1976, Commun. Math. Phys. **48**, 119.
Liu, H. C., J. Li, G. C. Aers, C. R. Leavens, M. Buchanan, and Z. R. Wasilewski, 1995, Phys. Rev. B. **51**, 5116.
Louisell, W. H., 1973, *Quantum Statistical Properties of Radiation* (Wiley, New York).
Louisell, W. H., A. Yariv, and A. E. Siegman, 1961, Phys. Rev. **124**, 1646.
Ludwig, G., 1985, *An Axiomatic Basis for Quantum Mechanics* (Springer, Berlin), Vol. 2.
Majorana, E., N. Pergola, P. Puppo, P. Rapagnani, and F. Ricci, 1993, Phys. Lett. A **180**, 43.
Marchese, L. E., M. F. Bocko, and R. Onofrio, 1992, Phys. Rev. D **45**, 1869.
Marzoli I., and P. Tombesi, 1993, Europhys. Lett. **24**, 515.
Mensky, M. B., 1979, Phys. Rev. D **20**, 384.
Mensky, M. B., 1993, *Continuous Measurements and Path Integrals* (Institute of Physics, Bristol-Philadelphia).
Mensky, M. B., 1994, Phys. Lett. A **196**, 159.
Mensky, M. B., R. Onofrio, and C. Presilla, 1991, Phys. Lett. A **161**, 236.
Mensky, M. B., R. Onofrio, and C. Presilla, 1993, Phys. Rev. Lett. **70**, 2825.
Misner, C. W., K. S. Thorne, and J. J. Wheeler, 1973, *Gravitation* (Freeman, San Francisco).
Mitrofanov, V. P., and V. N. Yakinov, 1989, Vestn. Mosk. Univ. Fiz. **44**, No. 4, p. 36.
Natarajan, V., F. DiFilippo, and D. E. Pritchard, 1995, Phys. Rev. Lett. **74**, 2855.
Nelson, E., 1980, *Dynamical Theories of Brownian Motion* (Princeton University, Princeton).
Nelson, E., 1985, *Quantum Fluctuations* (Princeton University, Princeton).
Niksch, M., and G. Binnig, 1988, J. Vac. Technol. A **6**, 470.
Oelfke, W. C., and W. O. Hamilton, 1978, Acta Astron. **5**, 87.
Oelfke, W. C., and W. O. Hamilton, 1983, Rev. Sci. Instrum. **54**, 410.
Onofrio, R., 1987, Phys. Lett. A **120**, 1.
Onofrio, R., 1990, Europhys. Lett. **11**, 695.
Onofrio, R., and F. Bordoni, 1991, Phys. Rev. A **43**, 2113.
Onofrio, R., and T. Calarco, 1995, Phys. Lett. A **208**, 40.
Onofrio, R., and C. Presilla, 1992, Phys. Lett. A **166**, 24.
Onofrio, R., and C. Presilla, 1993, Europhys. Lett. **22**, 333.
Onofrio, R., and A. Rioli, 1993, Phys. Rev. D **47**, 2176.
Ozawa, M., 1988, Phys. Rev. Lett. **60**, 385.
Ozawa, M., 1989, in *Squeezed and Nonclassical Light*, edited by P. Tombesi and E. R. Pike (Plenum, New York/London), p. 263.
Paik, H. J., 1976, J. Appl. Phys. **47**, 21.
Panov, V. I., and F. Ya. Khalili, 1980, in *Abstract of Contributed Papers for the discussion groups: 9th International Conference on General Relativity and Gravitation (GR9), July 14–19, 1980, Friedrich Schiller University, Jena, German Democratic Republic*. (International Society on General Relativity and Gravitation, Jena), p. 2 and p. 397.
Papoulis, A., 1977, *Signal Analysis* (McGraw-Hill, New York).
Pearle, P., 1986, Phys. Rev. D **33**, 2240.
Percival, I. C., 1994, Proc. R. Soc. London A **447**, 189.
Poizat, J.-Ph., J.-F. Roch, and P. Grangier, 1994, Ann. Phys. (Paris) **19**, 265.
Presilla, C., R. Onofrio, and M. F. Bocko, 1992, Phys. Rev. B **45**, 3735.
Presilla, C., R. Onofrio, and U. Tambini, 1996, Ann. Phys. (N.Y.) **248**, 94.
Przibram, K., Ed. 1967, *Letters on Wave Mechanics: Schrödinger, Planck, Einstein, Lorentz* (Philosophical Library, New York), p. 35.
Rapagnani, P., 1982, Nuovo Cimento C **5**, 385.
Richard, J. P., 1982, in *Proceedings of the Second Marcell Grossmann Meeting on General Relativity*, edited by R. Ruffini (North-Holland, Amsterdam), p. 1239.
Richard, J. P., 1984, Phys. Rev. Lett. **52**, 165.
Richard, J. P., 1986, J. Appl. Phys. **60**, 3807.
Roch, J. F., G. Roger, P. Grangier, J.-M. Courty, and S. Reynaud, 1992, Appl. Phys. B **55**, 291.
Rugar, D., and P. Grutter, 1991, Phys. Rev. Lett. **67**, 699.
Ruggiero, P., and M. Zannetti, 1985, Riv. Nuovo Cimento **5**, 8.
Schiller, S., and R. L. Byer, 1991, Opt. Lett. **16**, 130.
Schrödinger, E., 1935, Naturwissenschaften **23**, 807; **23**, 823; **23**, 844 [English translation by J. P. Trimmer, in Proc. Am. Philos. Soc. **124**, 323 (1980)].
Schumaker, B. L., 1985, J. Opt. Soc. Am. A **2**, 92.
Schumaker, B. L., 1986, Phys. Rep. **125**, 318.
Schumaker, B. L., S. H. Permutter, R. M. Shelby, and M. D. Levenson, 1987, Phys. Rev. Lett. **58**, 357.
Slusher, R. E., P. Grangier, A. La Porta, B. Yurke, and M. J. Potasek, 1987, Phys. Rev. Lett. **59**, 2566.
Smith, D. P. E., and G. Binnig, 1986, Rev. Sci. Instrum. **57**, 1688.

Smithey, D. T., M. Beek, M. G. Raymer, and A. Faridani, 1993, Phys. Rev. Lett. **70**, 1244.
Spetz, G. W., A. G. Mann, W. O. Hamilton, W. C. Oelfke, 1984, Phys. Lett. A **104**, 335.
Stephenson, K. A., M. F. Bocko, and R. H. Koch, 1989, Phys. Rev. A **40**, 6615.
Tesche, C. D., 1990, Phys. Rev. Lett. **64**, 2358.
Thomas, J. E., and L. J. Wang, 1995, Phys. Rep. **262**, 311.
Thorne, K. S., 1980, Rev. Mod. Phys. **52**, 299.
Thorne, K. S., C. M. Caves, V. D. Sandberg, M. Zimmermann, and R. W. P. Drever, 1979, in *Sources of Gravitational Radiation*, edited by L. Smarr (Cambridge University, Cambridge), p. 49.
Thorne, K. S., R. W. P. Drever, C. M. Caves, M. Zimmermann, and V. D. Sandberg, 1978, Phys. Rev. Lett. **40**, 667.
Tobar, M. E., and D. G. Blair, 1993, J. Phys. D **26**, 2276.
Tobar, M. E., and D. G. Blair, 1995, Rev. Sci. Instrum. **66**, 2751.
Toda, M., S. Adachi, and K. Ikeda, 1989, Prog. Theor. Phys. Suppl. **98**, 323.
Unruh, W. G., 1978, Phys. Rev. D **18**, 1764.
Unruh, W. G., 1979, Phys. Rev. D **19**, 2888.
Unruh, W. G., and W. H. Zurek, 1989, Phys. Rev. D **40**, 1071.
van Bentum, P. J. M., H. van Kempen, L. E. C. van de Leemput, and P. A. A. Teussinen, 1988, Phys. Rev. Lett. **60**, 369.
van der Roer, T. G., H. C. Heyker, J. J. Kwaspen, H. P. Joosten, and M. Henini, 1991, Electron. Lett. **27**, 2158.
Vogel, K., and H. Risken, 1989, Phys. Rev. A **40**, 2847.
Vorontsov, Yu. Y., 1981, Usp. Fiz. Nauk. **133**, 351 [Sov. Phys. Usp. **24**, 150 (1981)].
Vourdas, A., 1990, Opt. Commun. **76**, 164.
Wajid, A., 1984, Ph.D. thesis, University of Rochester.
Wallis, H., 1995, Phys. Rep. **255**, 203.
Walls, D. F., 1983, Nature **306**, 141.
Weigert, S., 1991, Phys. Rev. A **43**, 6597.
Weiss, D. S., V. Sandoghdar, J. Hare, V. LeFèvre-Seguin, J.-M. Raimond, and S. Haroche, 1995, Opt. Lett. **20**, 1835.
Wengler, M. J., and M. F. Bocko, 1989, IEEE Trans. Magn. **25**, 1376.
Wheeler, J. A., and W. H. Zurek, Eds., 1983, *Quantum Theory and Measurements* (Princeton University, Princeton).
Wineland, D. J., J. J. Bollinger, W. M. Itano, F. L. Moore, and D. J. Heinzen, 1992, Phys. Rev. A **46**, R 6797.
Yuen, H. P., 1983, Phys. Rev. Lett. **51**, 719.
Yurke, B., 1991, Science **252**, 528.
Yurke, B., L. R. Corruccini, P. G. Kaminsky, L. W. Rupp, A. D. Smith, A. H. Silver, R. W. Simon, and E. A. Whittaker, 1989, Phys. Rev. A **39**, 2519.
Yurke, B., P. Grangier, R. E. Slusher, and M. Potasek, 1987, Phys. Rev. A **35**, 3586.
Yurke, B., P. G. Kaminsky, R. E. Miller, E. A. Whittaker, A. D. Smith, A. H. Silver, and R. W. Simon, 1988, Phys. Rev. Lett. **60**, 764.
Yurke, B., and G. P. Kochanski, 1990, Phys. Rev. B **41**, 8184.
Zhang, Z., M. F. Bocko, and M. J. Wengler, 1989, IEEE Trans. Magn. **25**, 1042.
Zoller, P., M. Marte, and D. F. Walls, 1987, Phys. Rev. A **35**, 198.
Zurek, W. H., 1981, Phys. Rev. D **24**, 1516.
Zurek, W. H., 1982, Phys. Rev. D **26**, 1862.
Zurek, W. H., Ed., 1990, *Complexity, Entropy and the Physics of Information* (Addison-Ewsley, Reading).
Zurek, W. H., S. Habib, and J. P. Paz, 1993, Phys. Rev. Lett. **70**, 1187.
Zurek, W. H., and J. P. Paz, 1995, Physica D **83**, 300.